Interaction of Particles with Matter

Werner Riegler, CERN, werner.riegler@cern.ch

Danube School on Instrumentation in Elementary Particle & Nuclear Physics
University of Novi Sad, Serbia, September 8th-13th, 2014.

On Tools and Instrumentation

“New directions in science are launched by new tools much more often than by new concepts.

The effect of a concept-driven revolution is to explain old things in new ways.

The effect of a tool-driven revolution is to discover new things that have to be explained”

Freeman Dyson, Imagined Worlds

→ New tools and technologies will be extremely important to go beyond LHC

Physics Nobel Prices for Instrumentation

1927: C.T.R. Wilson, Cloud Chamber
1939: E. O. Lawrence, Cyclotron & Discoveries
1948: P.M.S. Blacket, Cloud Chamber & Discoveries
1950: C. Powell, Photographic Method & Discoveries
1954: Walter Bothe, Coincidence method & Discoveries
1960: Donald Glaser, Bubble Chamber
1968: L. Alvarez, Hydrogen Bubble Chamber & Discoveries
1992: Georges Charpak, Multi Wire Proportional Chamber

All Nobel Price Winners related to the Standard Model: 87 !
(personal statistics by W. Riegler)

31 for Standard Model Experiments
13 for Standard Model Instrumentation and Experiments
3 for Standard Model Instrumentation
21 for Standard Model Theory
9 for Quantum Mechanics Theory
9 for Quantum Mechanics Experiments
1 for Relativity

56 for Experiments and instrumentation
31 for Theory

The ‘Real’ World of Particles

E. Wigner:

“A particle is an irreducible representation of the inhomogeneous Lorentz group”

Spin=0,1/2,1,3/2 … Mass>0

ANNALS OF MATHEMATICS
Vol. 40, No. 1, January, 1939

ON UNITARY REPRESENTATIONS OF THE INHOMOGENEOUS LORENTZ GROUP*

BY E. WIGNER

(Received December 22, 1937)

1. ORIGIN AND CHARACTERIZATION OF THE PROBLEM

It is perhaps the most fundamental principle of Quantum Mechanics that the system of states forms a *linear manifold*,[1] in which a unitary *scalar product* is defined.[2] The states are generally represented by wave functions[3] in such a way that φ and constant multiples of φ represent the same physical state. It is possible, therefore, to normalize the wave function, i.e., to multiply it by a constant factor such that its scalar product with itself becomes 1. Then, only a constant factor of modulus 1, the so-called phase, will be left undetermined in the wave function. The linear character of the wave function is called the superposition principle. The square of the modulus of the unitary scalar product (ψ, φ) of two normalized wave functions ψ and φ is called the transition probability from the state ψ into φ, or conversely. This is supposed to give the probability that an experiment performed on a system in the state φ, to see whether or not the state is ψ, gives the result that it is ψ. If there are two or more different experiments to decide this (e.g., essentially the same experiment,

E.g. in Steven Weinberg, The Quantum Theory of Fields, Vol1

The ‘Real’ World of Particles

W. Riegler:

“…a particle is an object that interacts with your detector such that you can follow it’s track,

it interacts also in your readout electronics and will break it after some time,

and if you a silly enough to stand in an intense particle beam for some time you will be dead …”

Particle Detector Systems

W. Riegler/CERN

Cloud Chamber

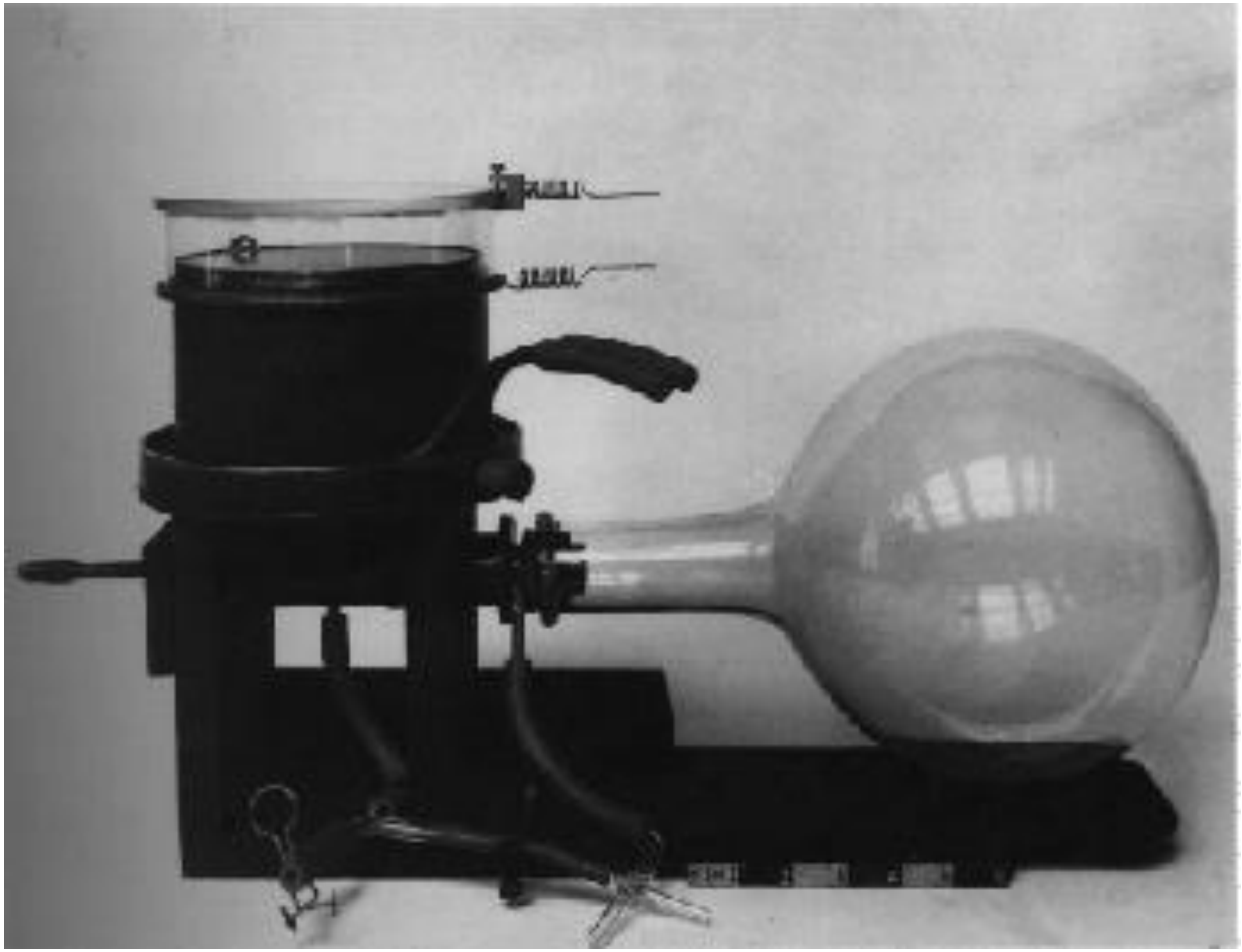

Wilson Cloud Chamber 1911

Cloud Chamber

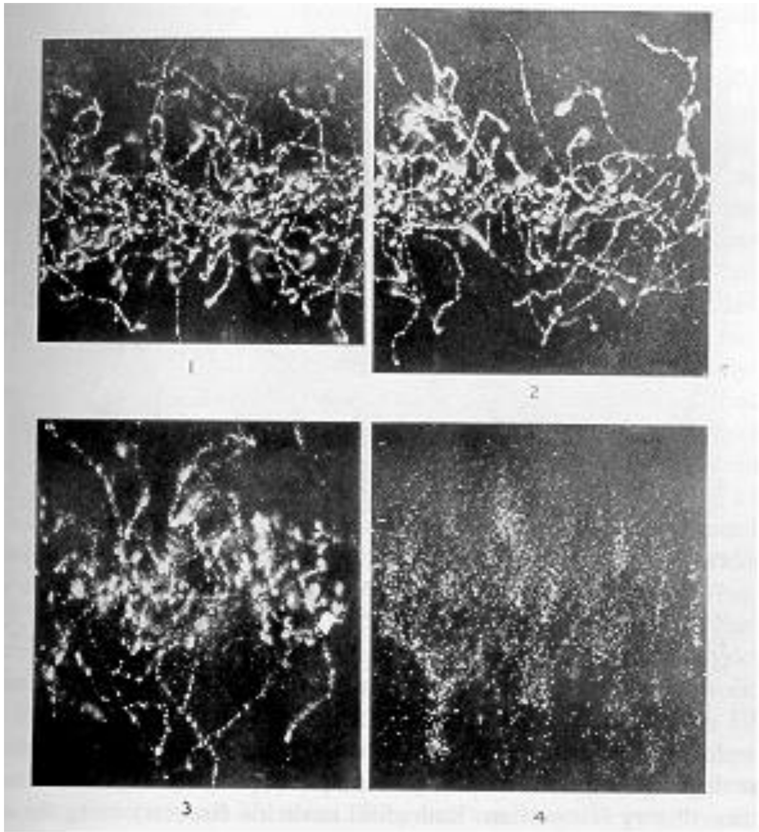

X-rays, Wilson 1912

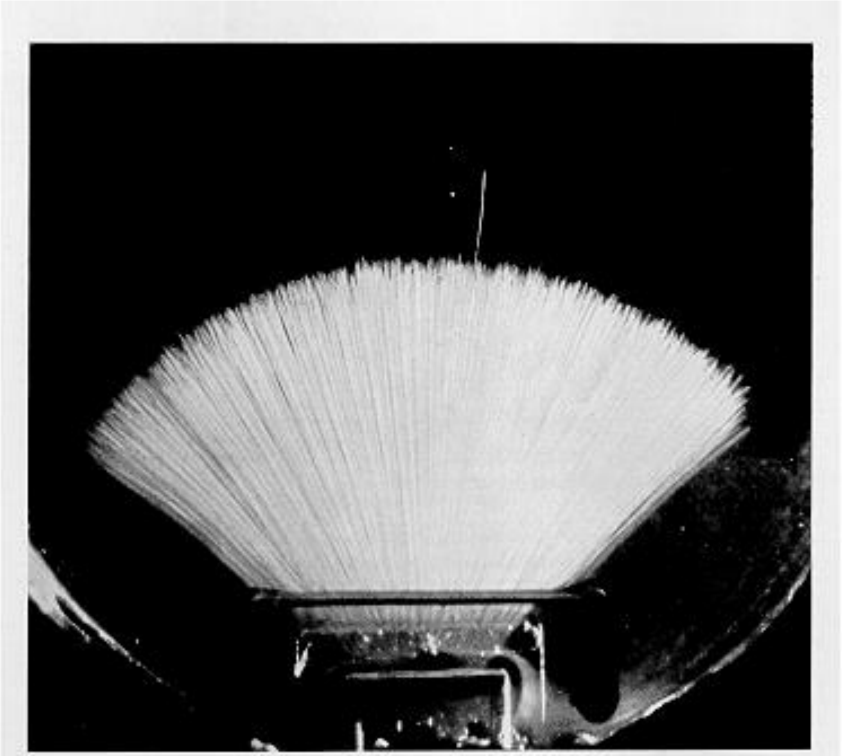

Fig. 13. K. Philipp, Naturwiss. 14, 1203 (1926).

Alphas, Philipp 1926

Cloud Chamber

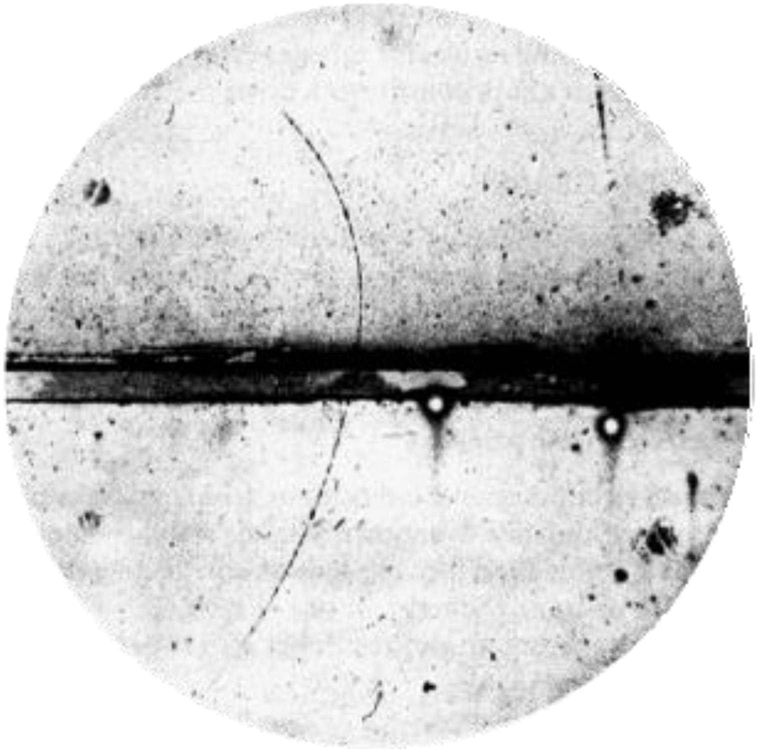

Magnetic field 15000 Gauss, chamber diameter 15cm. A 63 MeV positron passes through a 6mm lead plate, leaving the plate with energy 23MeV.

The ionization of the particle, and its behaviour in passing through the foil are the same as those of an electron.

Positron discovery, Carl Andersen 1933

Cloud Chamber

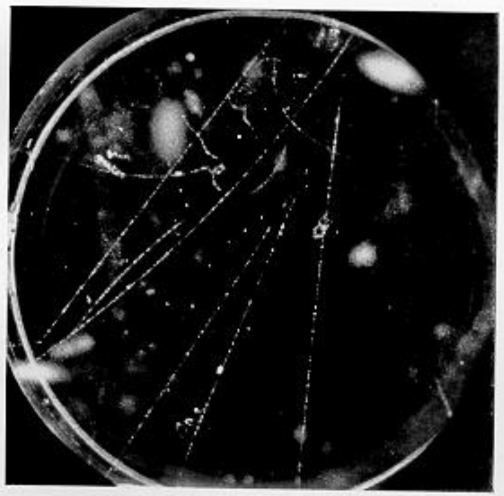

Plate 115

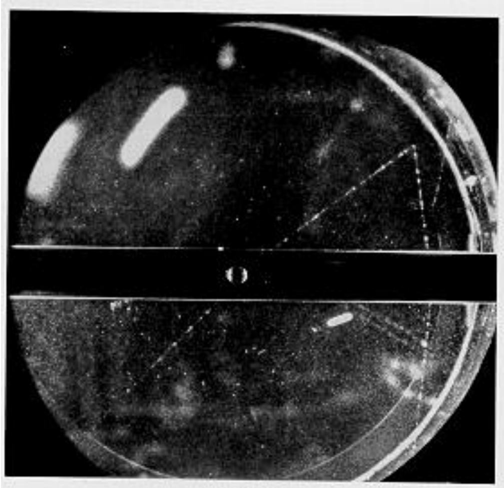

Plate 116

Rochester and Wilson

Particle momenta are measured by the bending in the magnetic field.

' … The V0 particle originates in a nuclear Interaction outside the chamber and decays after traversing about one third of the chamber. The momenta of the secondary particles are 1.6+-0.3 BeV/c and the angle between them is 12 degrees … '

By looking at the specific ionization one can try to identify the particles and by assuming a two body decay on can find the mass of the V0.

'… if the negative particle is a negative proton, the mass of the V0 particle is 2200 m, if it is a Pi or Mu Meson the V0 particle mass becomes about 1000m …'

Nuclear Emulsion

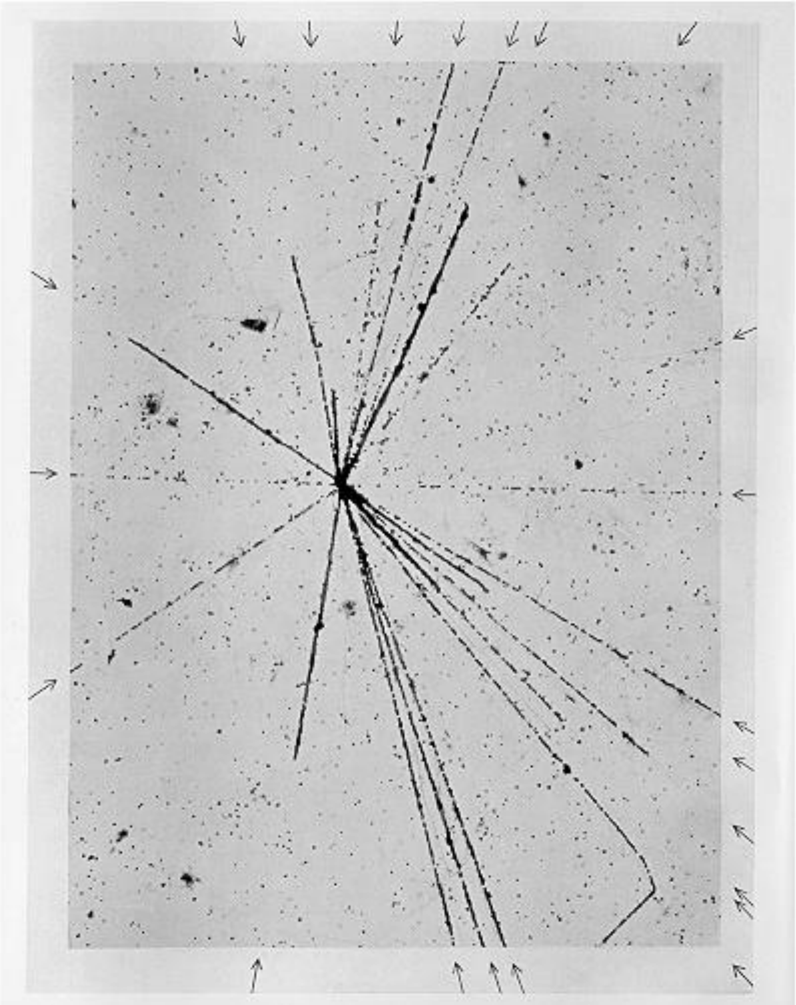

'EXPLOSIVE' DISINTEGRATION OF A NUCLEUS

Film played an important role in the discovery of radioactivity but was first seen as a means of studying radioactivity rather than photographing individual particles.

Between 1923 and 1938 Marietta Blau pioneered the nuclear emulsion technique.

E.g.
Emulsions were exposed to cosmic rays at high altitude for a long time (months) and then analyzed under the microscope.
In 1937, nuclear disintegrations from cosmic rays were observed in emulsions.

The high density of film compared to the cloud chamber 'gas' made it easier to see energy loss and disintegrations.

Nuclear Emulsion

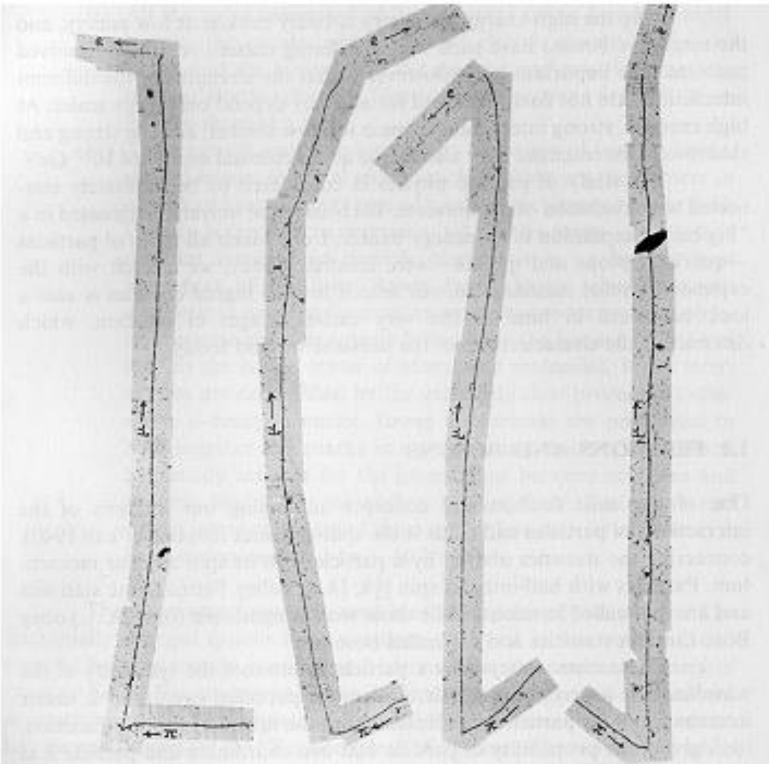

Discovery of muon and pion

Discovery of the Pion:

The muon was discovered in the 1930ies and was first believed to be Yukawa's meson that mediates the strong force.

The long range of the muon was however causing contradictions with this hypothesis.

In 1947, Powell et. al. discovered the Pion in Nuclear emulsions exposed to cosmic rays, and they showed that it decays to a muon and an unseen partner.

The constant range of the decay muon indicated a two body decay of the pion.

Bubble Chamber

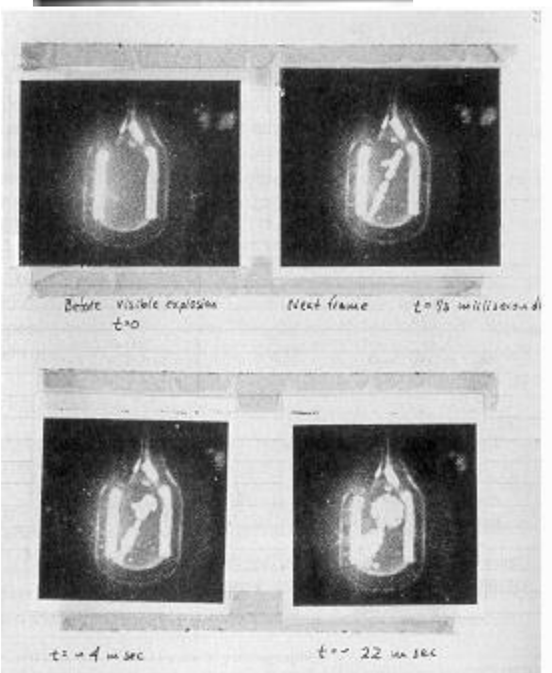

Figure 5.5 Bubble chamber movies (1952). Glaser first filmed distinct track

In the early 1950ies Donald Glaser tried to build on the cloud chamber analogy:

Instead of supersaturating a gas with a vapor one would superheat a liquid. A particle depositing energy along it's path would then make the liquid boil and form bubbles along the track.

In 1952 Glaser photographed first Bubble chamber tracks. Luis Alvarez was one of the main proponents of the bubble chamber.

The size of the chambers grew quickly

1954: 2.5'' (6.4cm)
1954: 4'' (10cm)
1956: 10'' (25cm)
1959: 72'' (183cm)
1963: 80'' (203cm)
1973: 370cm

Bubble Chamber

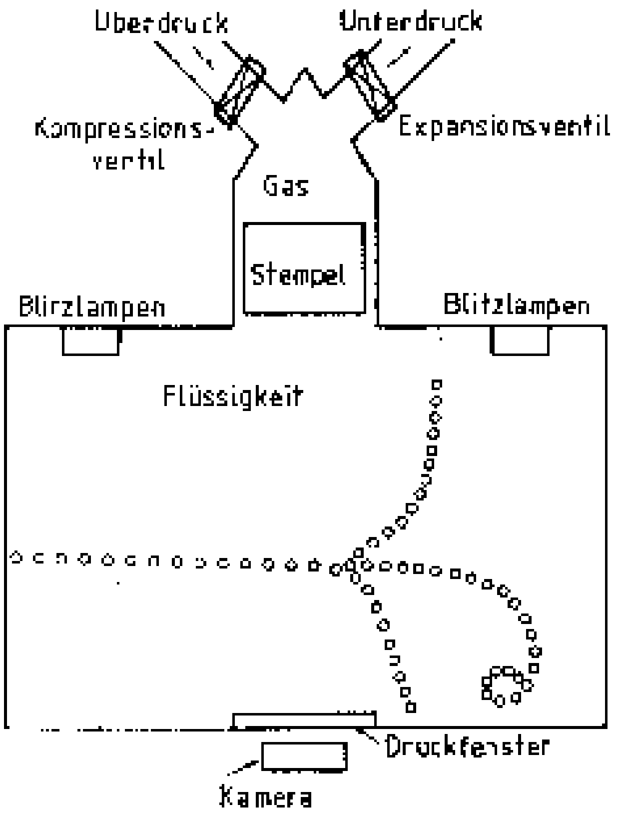

‘old bubbles’

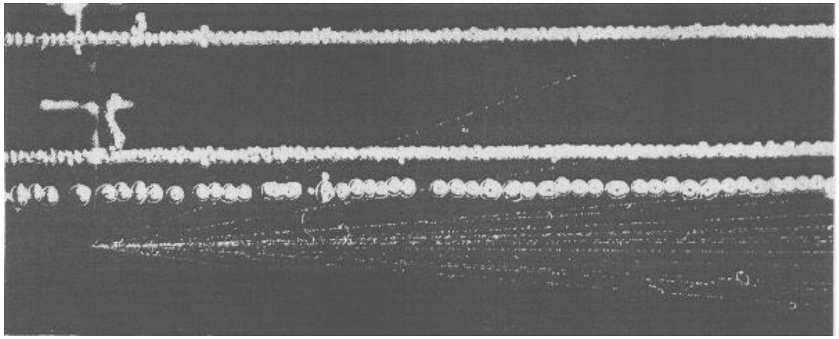

‘new bubbles’

Unlike the Cloud Chamber, the Bubble Chamber could not be triggered, i.e. the bubble chamber had to be already in the superheated state when the particle was entering. It was therefore not useful for Cosmic Ray Physics, but as in the 50ies particle physics moved to accelerators it was possible to synchronize the chamber compression with the arrival of the beam.

For data analysis one had to look through millions of pictures.

Bubble Chamber

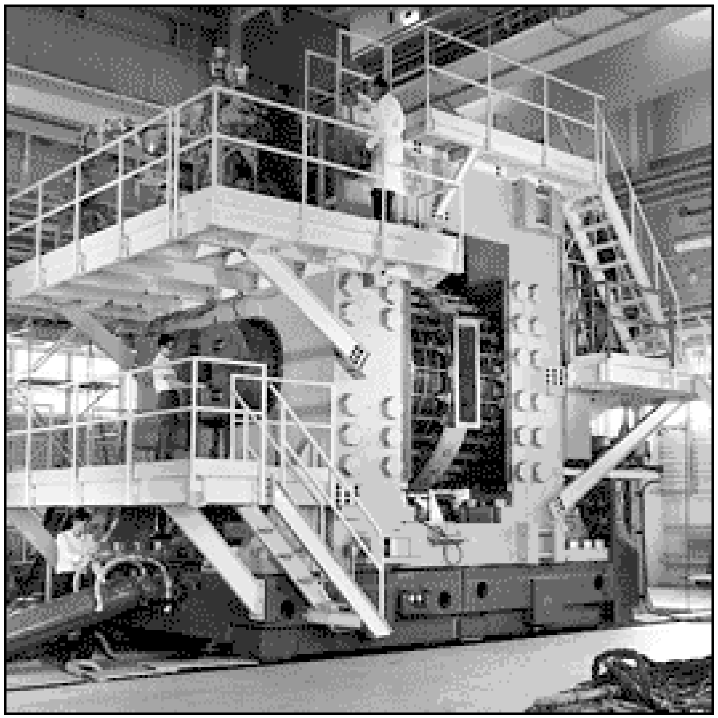

The 80-inch Bubble Chamber

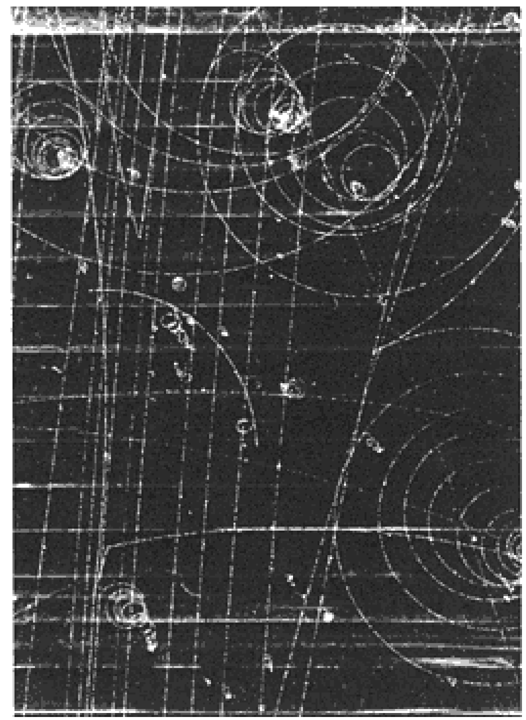

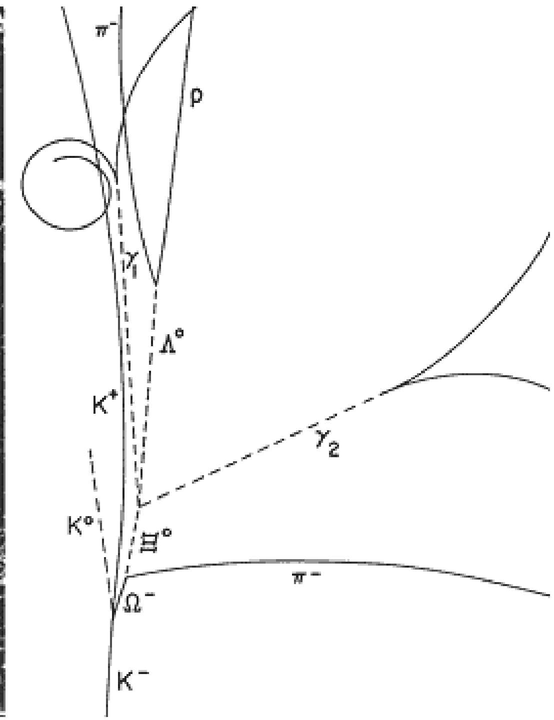

BNL, First Pictures 1963, 0.03s cycle

Discovery of the Ω^- in 1964

Geiger Rutherford

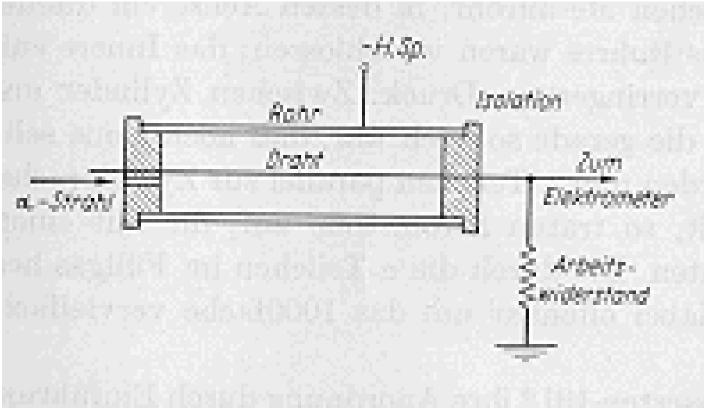

Rutherford and Geiger 1908

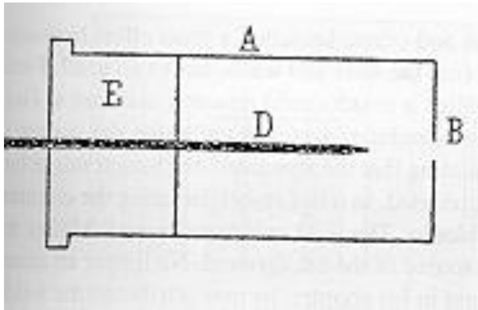

Tip counter, Geiger 1913

In 1908, Rutherford and Geiger developed an electric device to measure alpha particles.

The alpha particles ionize the gas, the electrons drift to the wire in the electric field and they multiply there, causing a large discharge which can be measured by an electroscope.

The ‘random discharges’ in absence of alphas were interpreted as ‘instability’, so the device wasn’t used much.

As an alternative, Geiger developed the tip counter, that became standard for radioactive experiments for a number of years.

Detector + Electronics 1929

In 1928 Walther Müller started to study the sponteneous discharges systematically and found that they were actually caused by cosmic rays discovered by Victor Hess in 1911.

By realizing that the wild discharges were not a problem of the counter, but were caused by cosmic rays, the Geiger-Müller counter went, without altering a single screw from a device with 'fundametal limits' to the most sensitive intrument for cosmic rays physics.

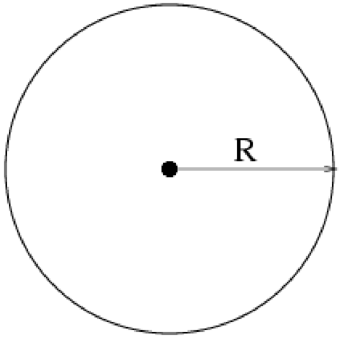

'Zur Vereinfachung von Koinzidenzzählungen'
W. Bothe, November 1929

Coincidence circuit for 2 tubes

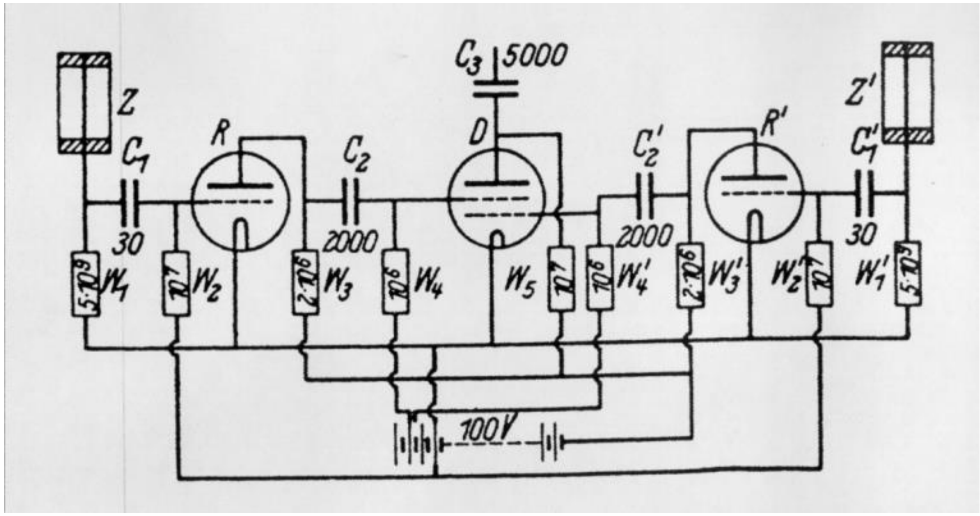

1930 - 1934

Cosmic ray telescope 1934

Rossi 1930: Coincidence circuit for n tubes

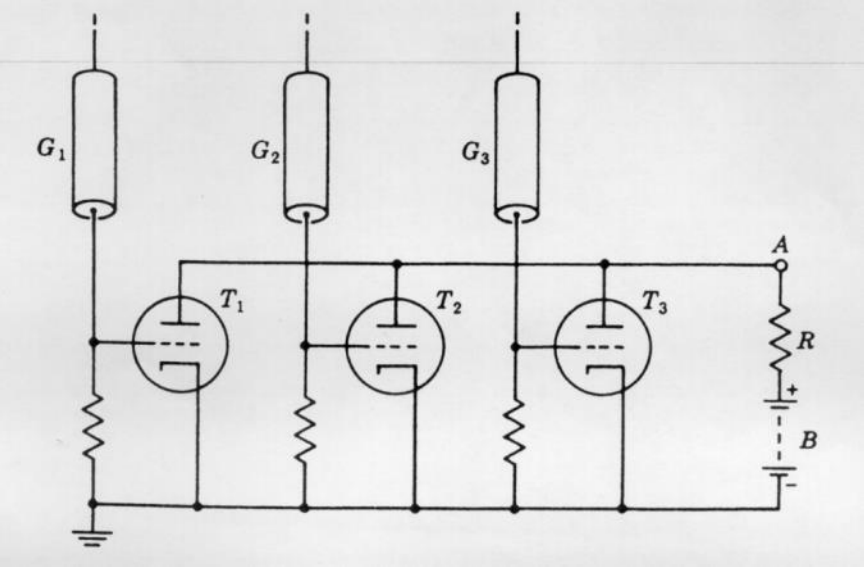

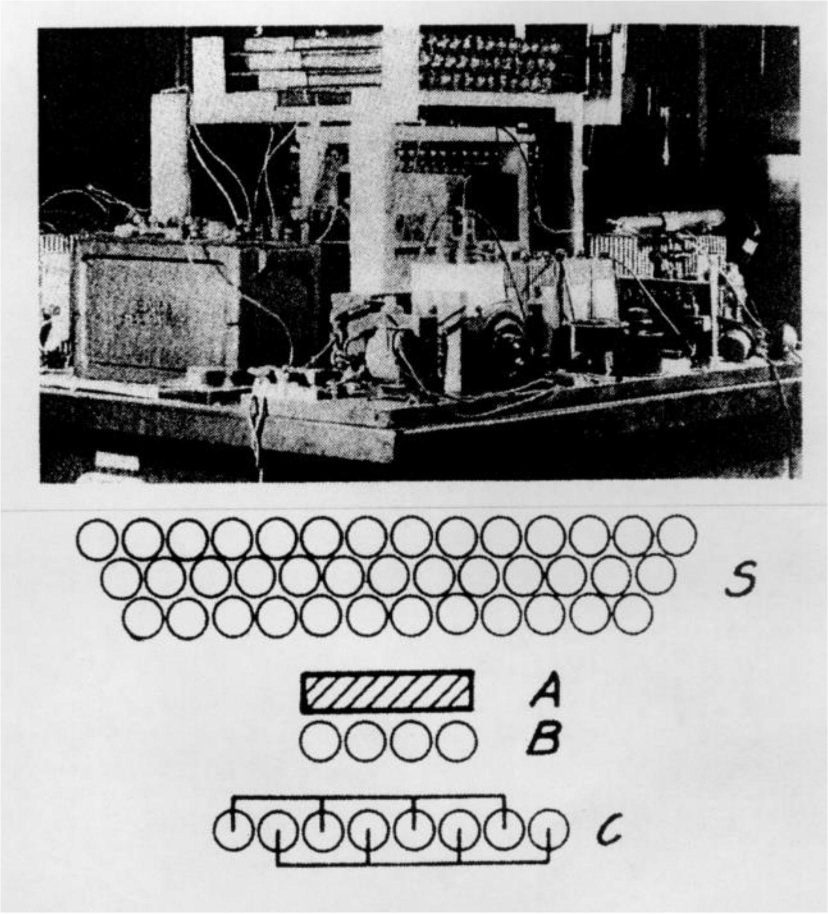

Scintillators, Cerenkov light, Photomultipliers

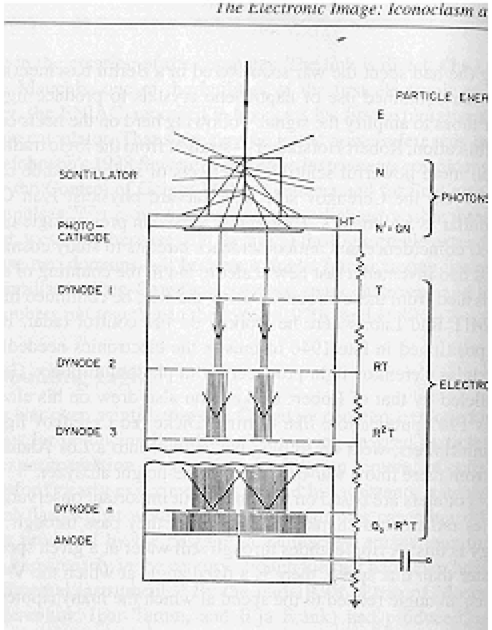

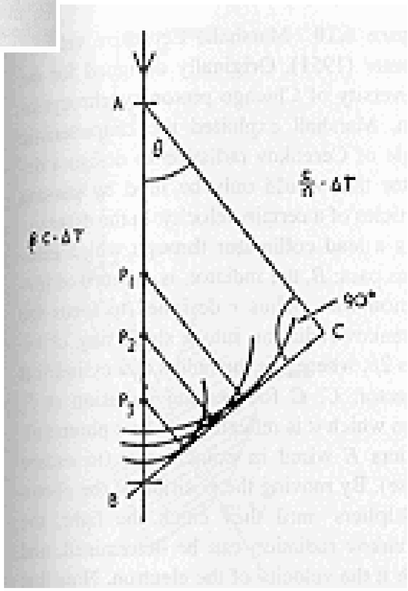

In the late 1940ies, scintillation counters and Cerenkov counters exploded into use.

Scintillation of materials on passage of particles was long known.

By mid 1930 the bluish glow that accompanied the passage of radioactive particles through liquids was analyzed and largely explained (Cerenkov Radiation).

Mainly the electronics revolution begun during the war initiated this development.

High-gain photomultiplier tubes, amplifiers, scalers, pulse-height analyzers.

Anti Neutrino Discovery 1959

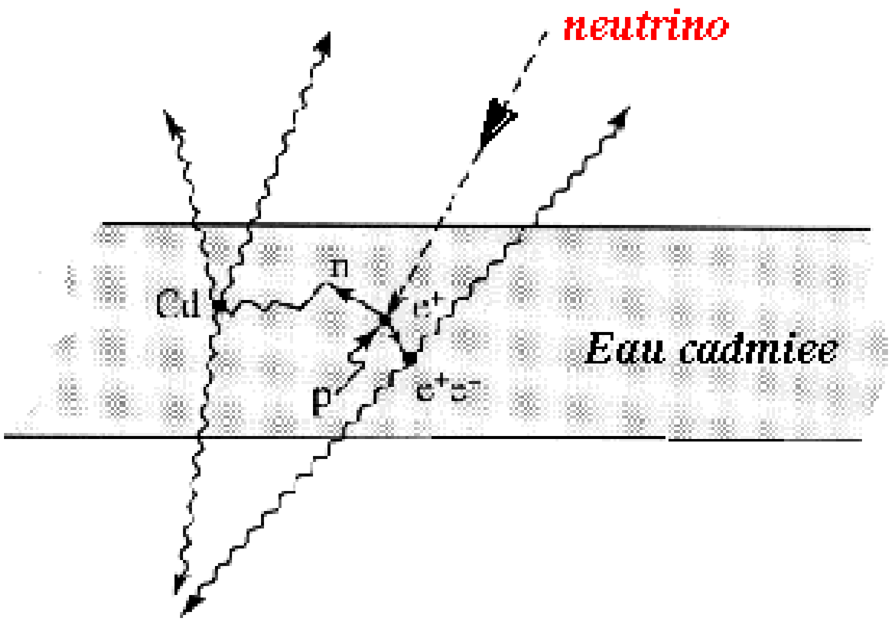

$\bar{\nu} + p \rightarrow n + e^{+}$

Reines and Cowan experiment principle consisted in using a target made of around 400 liters of a mixture of water and cadmium chloride.

The anti-neutrino coming from the nuclear reactor interacts with a proton of the target matter, giving a positron and a neutron.

The positron annihilates with an electron of the surrounding material, giving two simultaneous photons and the neutron slows down until it is eventually captured by a cadmium nucleus, implying the emission of photons some 15 microseconds after those of the positron annihilation.

Multi Wire Proportional Chamber

Tube, Geiger- Müller, 1928

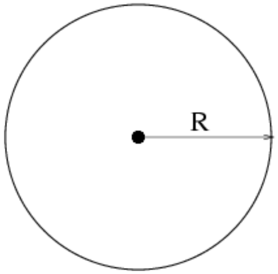

Multi Wire Geometry, in H. Friedmann 1949

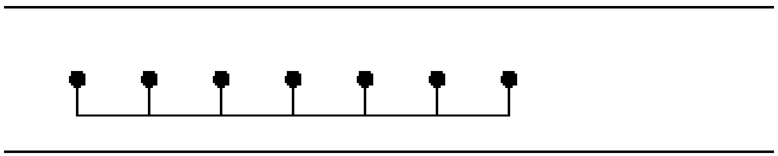

G. Charpak 1968, Multi Wire Proportional Chamber, readout of individual wires and proportional mode working point.

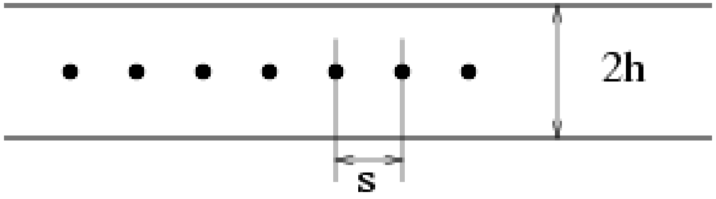

MWPC

Individual wire readout: A charged particle traversing the detector leaves a trail of electrons and ions. The wires are on positive HV. The electrons drift to the wires in the electric field and start to form an avalanche in the high electric field close to the wire. This induces a signal on the wire which can be read out by an amplifier.

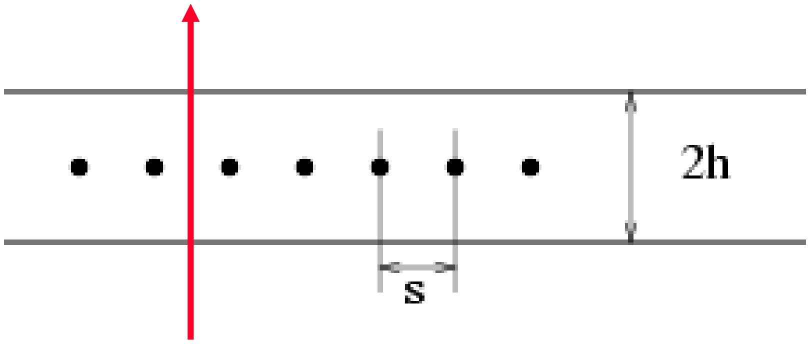

Measuring this drift time, i.e. the time between passage of the particle and the arrival time of the electrons at the wires, made this detector a precision positioning device.

W, Z-Discovery 1983/84

UA1 used a very large wire chamber.

Can now be seen in the CERN Microcosm Exhibition

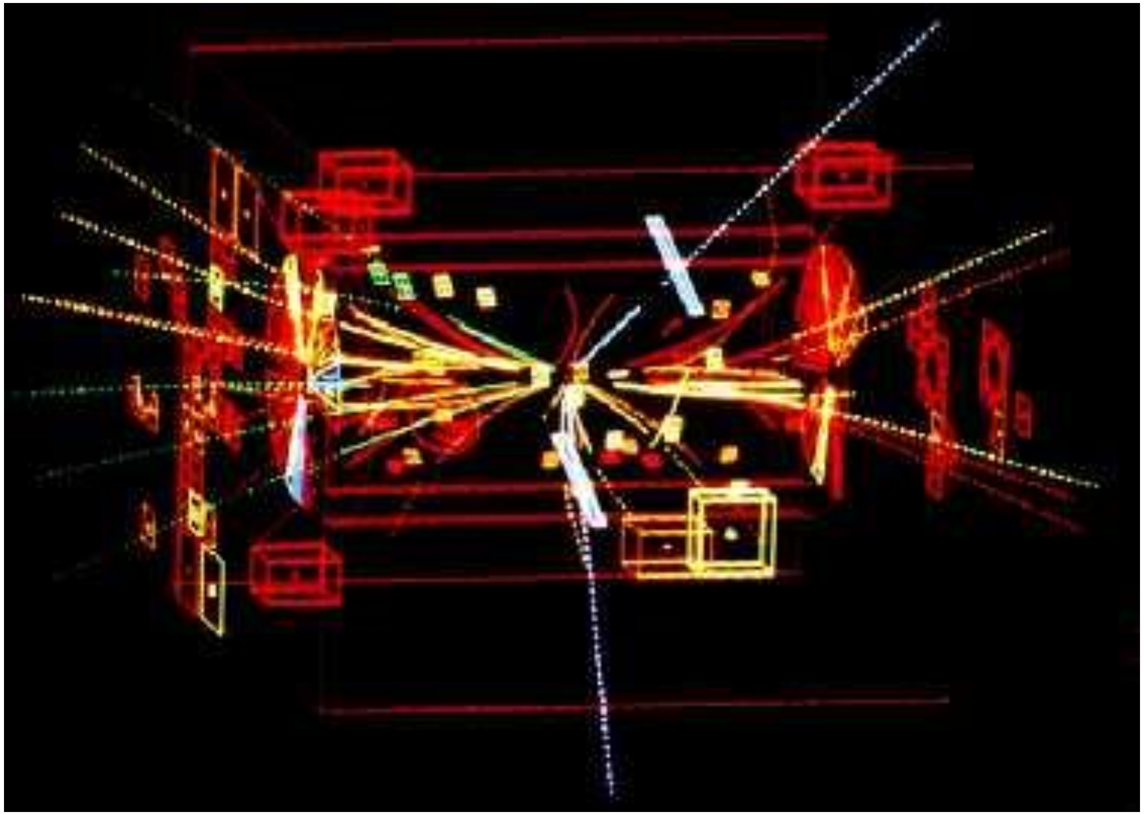

This computer reconstruction shows the tracks of charged particles from the proton-antiproton collision. The two white tracks reveal the Z's decay. They are the tracks of a high-energy electron and positron.

LEP 1988-2000

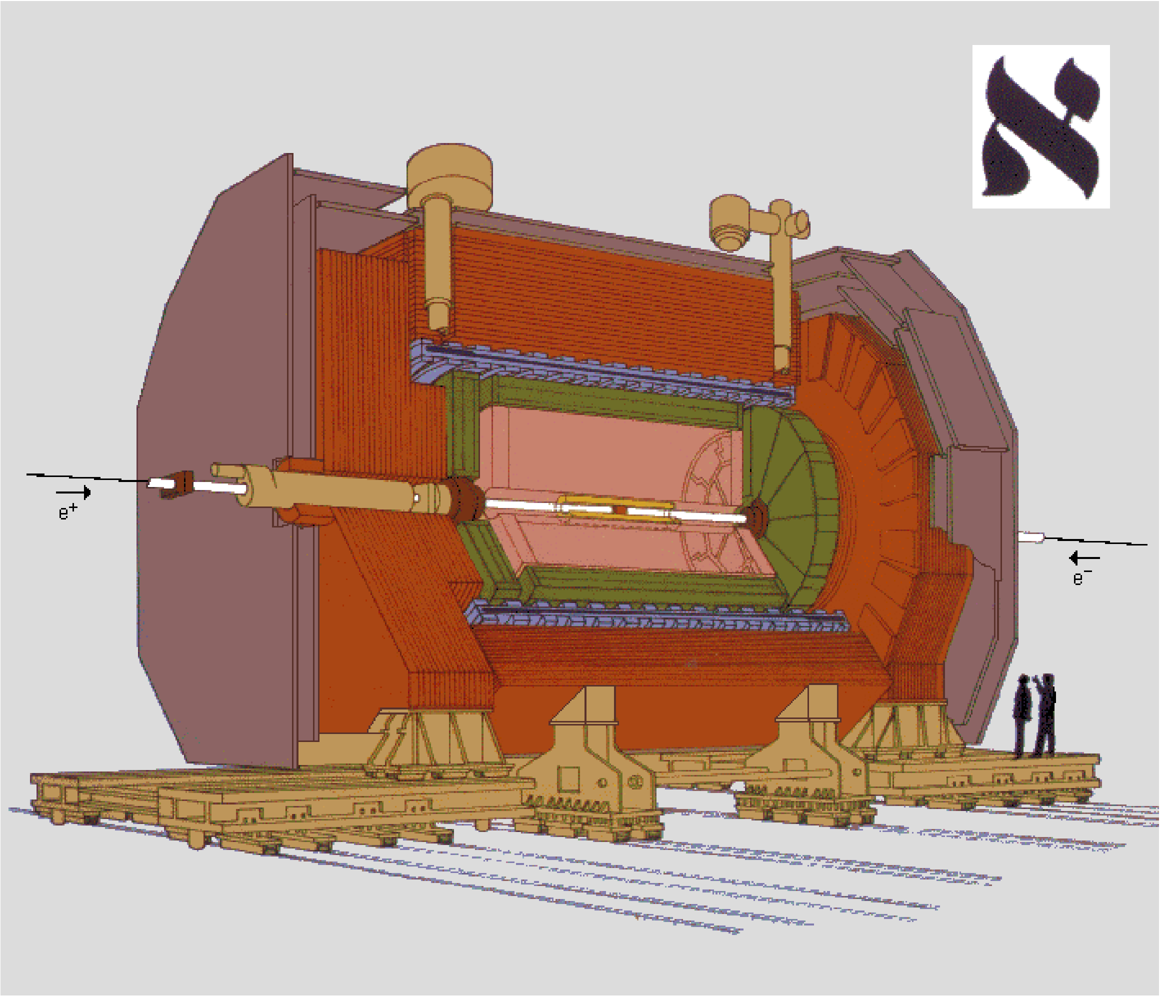

- Vertex Detector
- Inner Tracking Chamber
- Time Projection Chamber
- Electromagnetic Calorimeter
- Superconducting Magnet Coil
- Hadron Calorimeter
- Muon Chambers
- Luminosity Monitors

The ALEPH Detector

All Gas Detectors

LEP 1988-2000

Aleph Higgs Candidate Event: $e^+ e^- \rightarrow HZ \rightarrow b\bar{b} + jj$

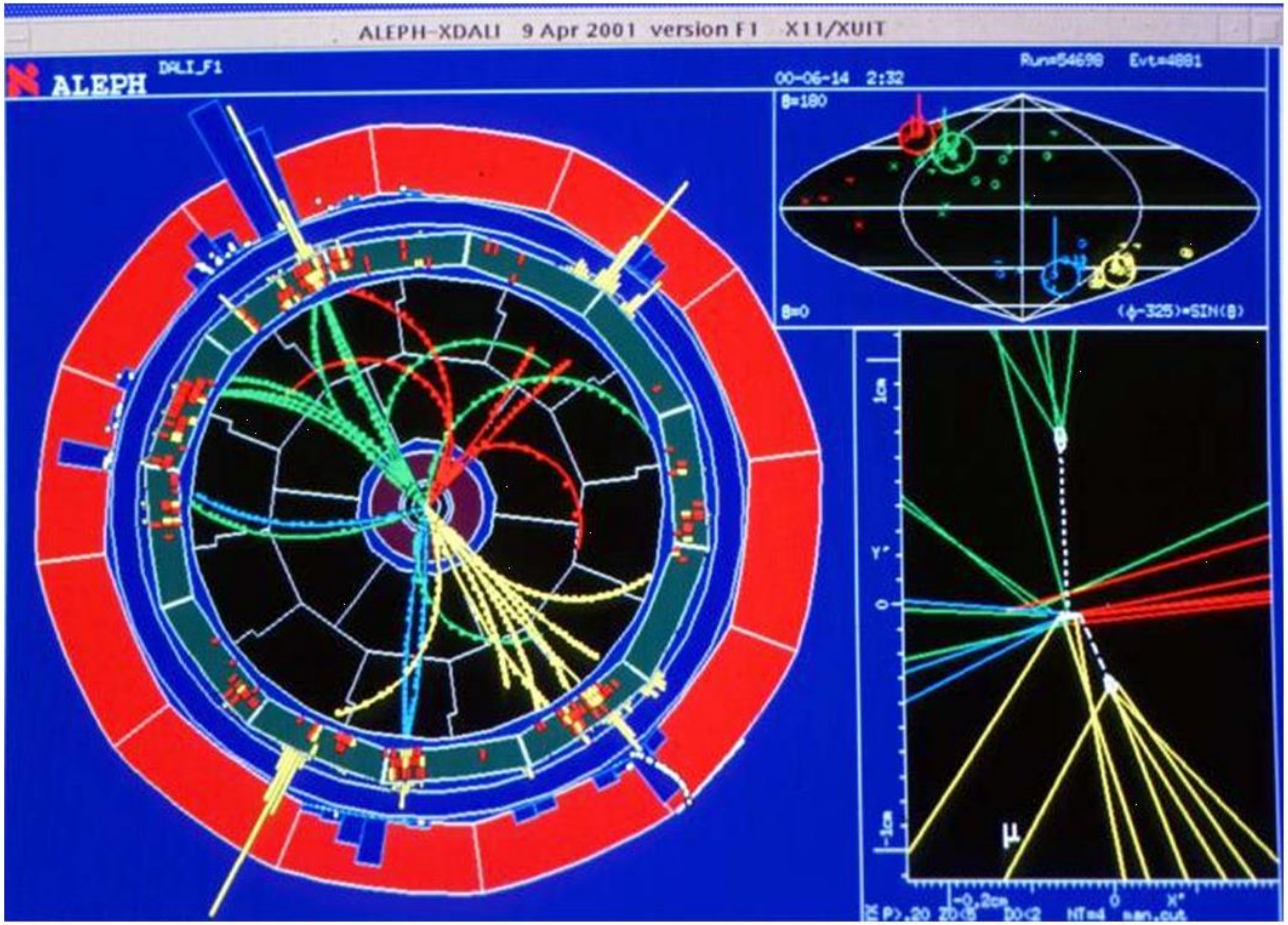

Increasing Multiplicities in Heavy Ion Collisions

e+ e- collision in the ALEPH Experiment/LEP.

Au+ Au+ collision in the STAR Experiment/RHIC
Up to 2000 tracks

Pb+ Pb+ collision in the ALICE Experiment/LHC
Up to 10 000 tracks/collision

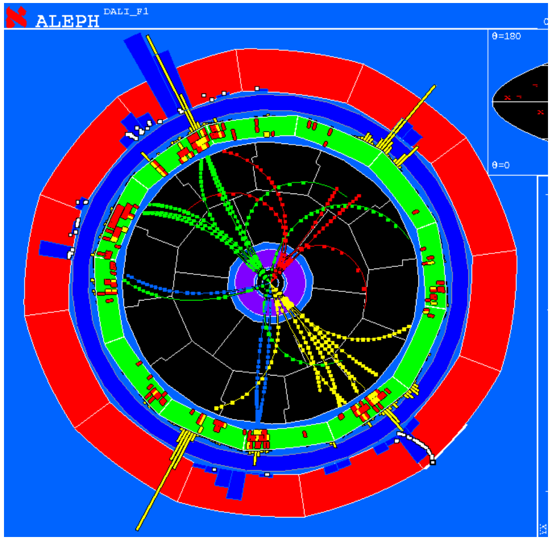

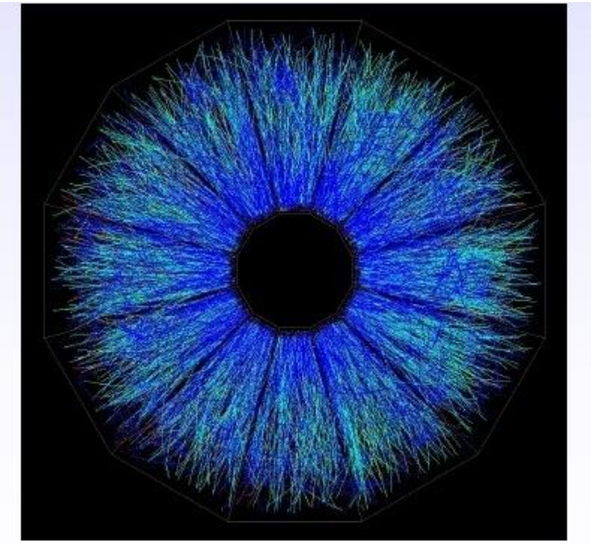

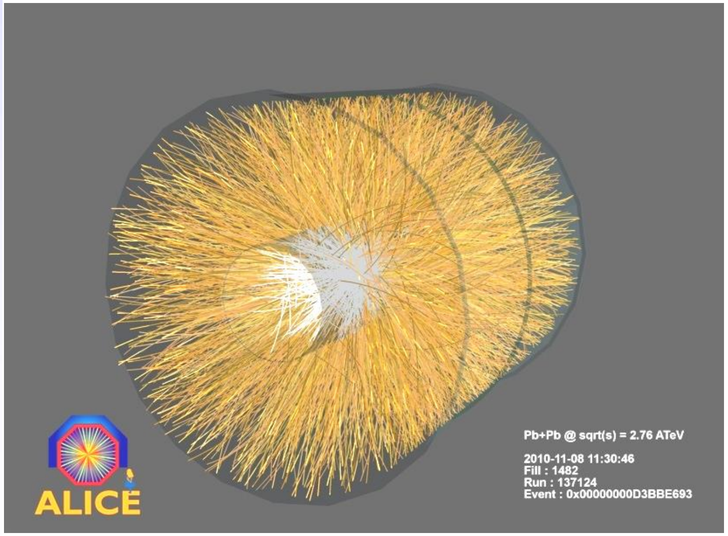

ATLAS at LHC

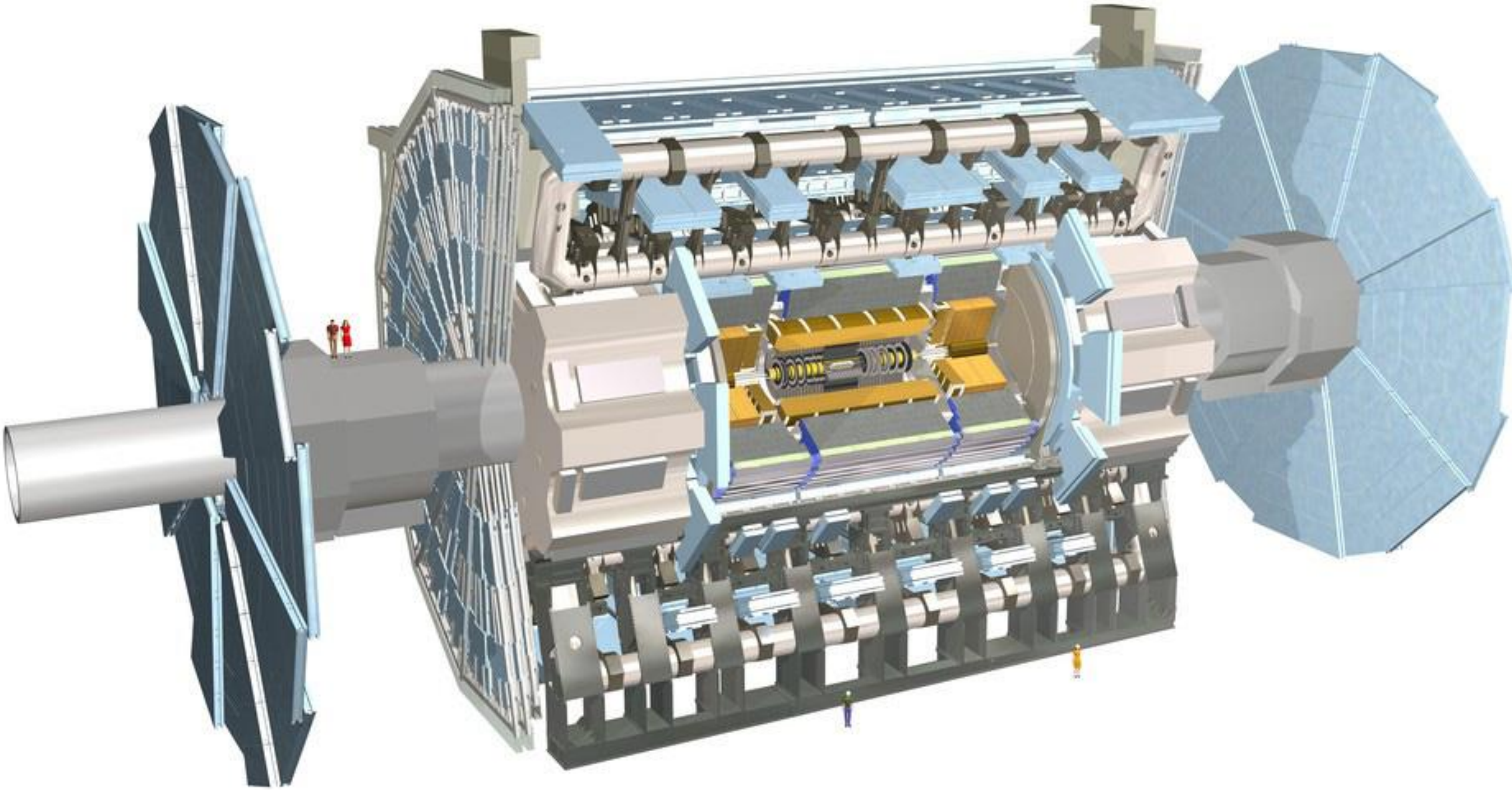

Large Hadron Collider at CERN.

The ATLAS detector uses more than 100 million detector channels.

AMANDA

Antarctic **M**uon **A**nd **N**eutrino **D**etector **A**rray

AMANDA

South Pole

AMANDA

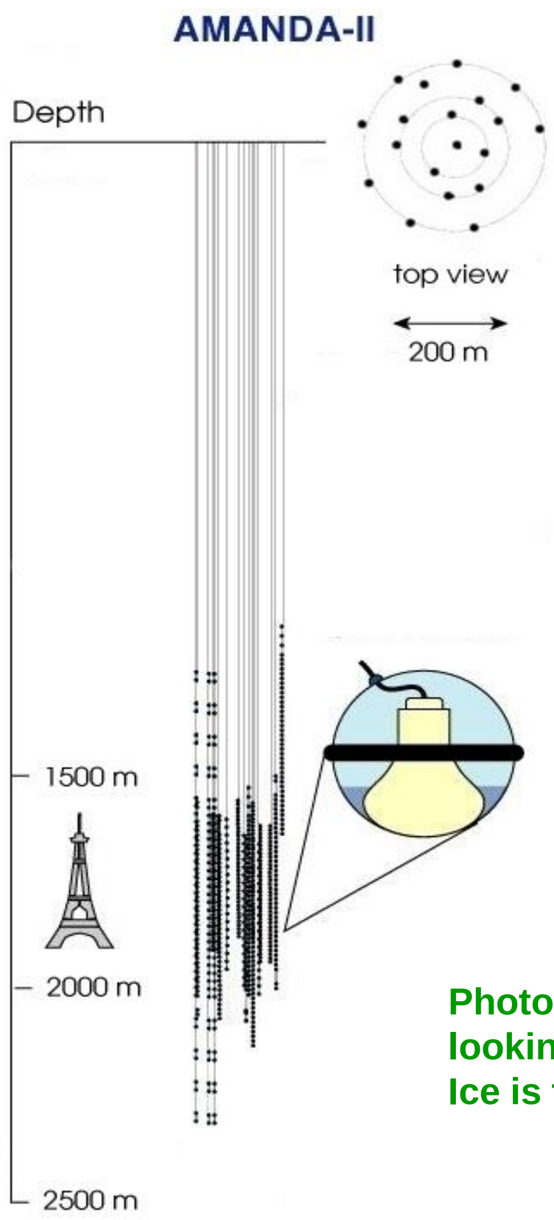

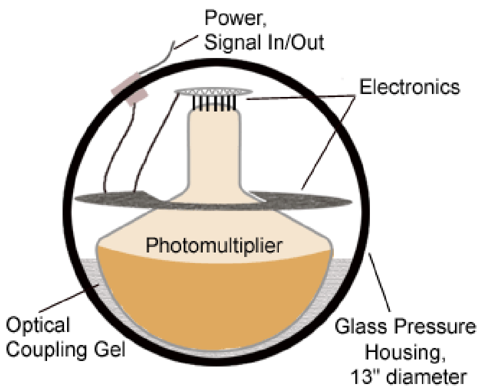

Photomultipliers in the Ice,
looking downwards.
Ice is the detecting medium.

AMANDA

Look for upwards going Muons from Neutrino Interactions.
Cherekov Light propagating through the ice.

→ Find neutrino point sources in the universe !

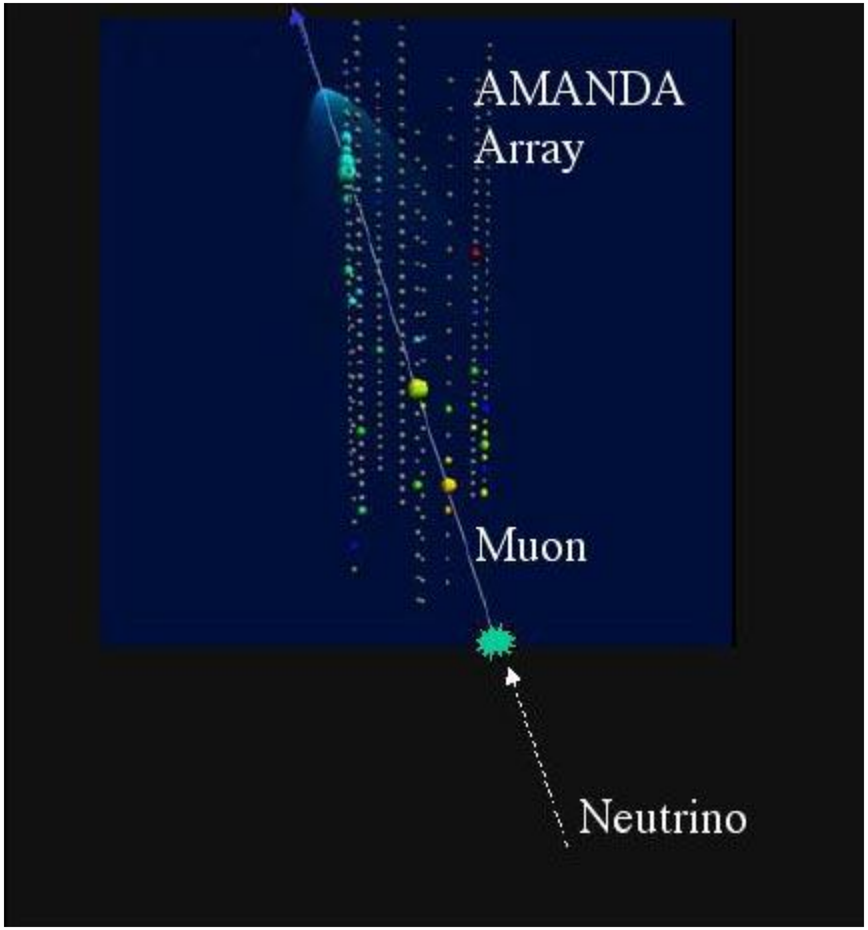

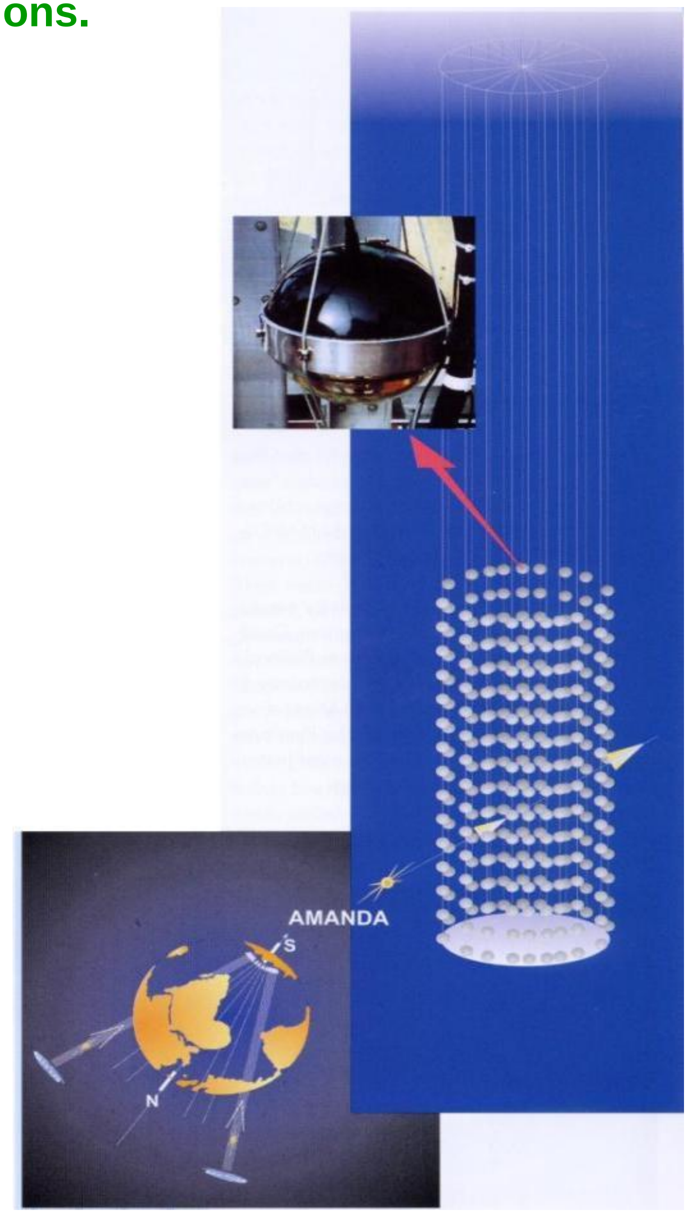

AMANDA

Event Display

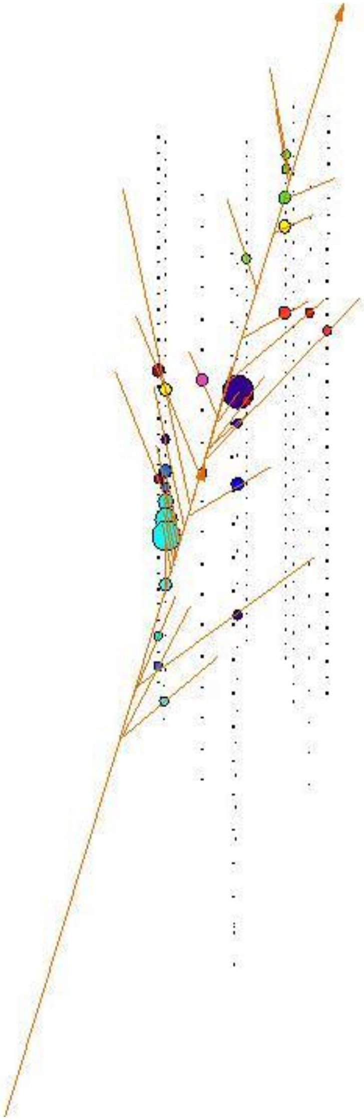

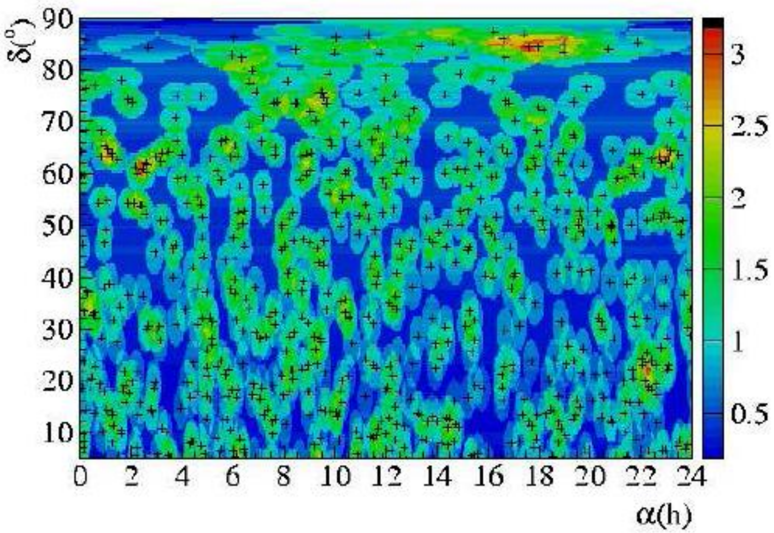

Up to now: No significant point sources but just neutrinos from cosmic ray interactions in the atmosphere were found .

The Ice Cube neutrino observatory is designed so that 5,160 optical sensors view a cubic kilometer of clear South Polar ice.

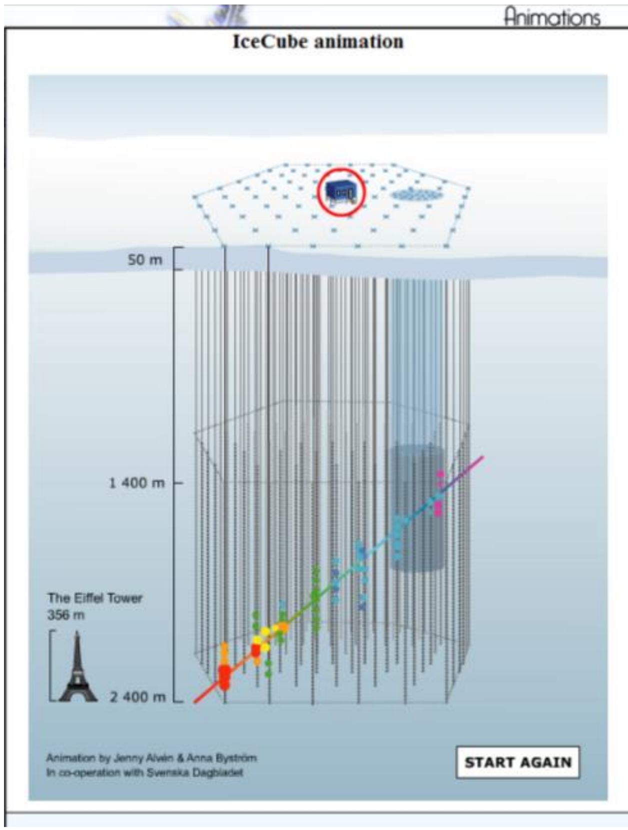

CERN Neutrino Gran Sasso

(CNGS)

Tau Candidate seen!

Hypothesis:

τ (parent) → hadron (daughter) + π_0 (decaying instantly to γ_1, γ_2)+ ν_τ (invisible)

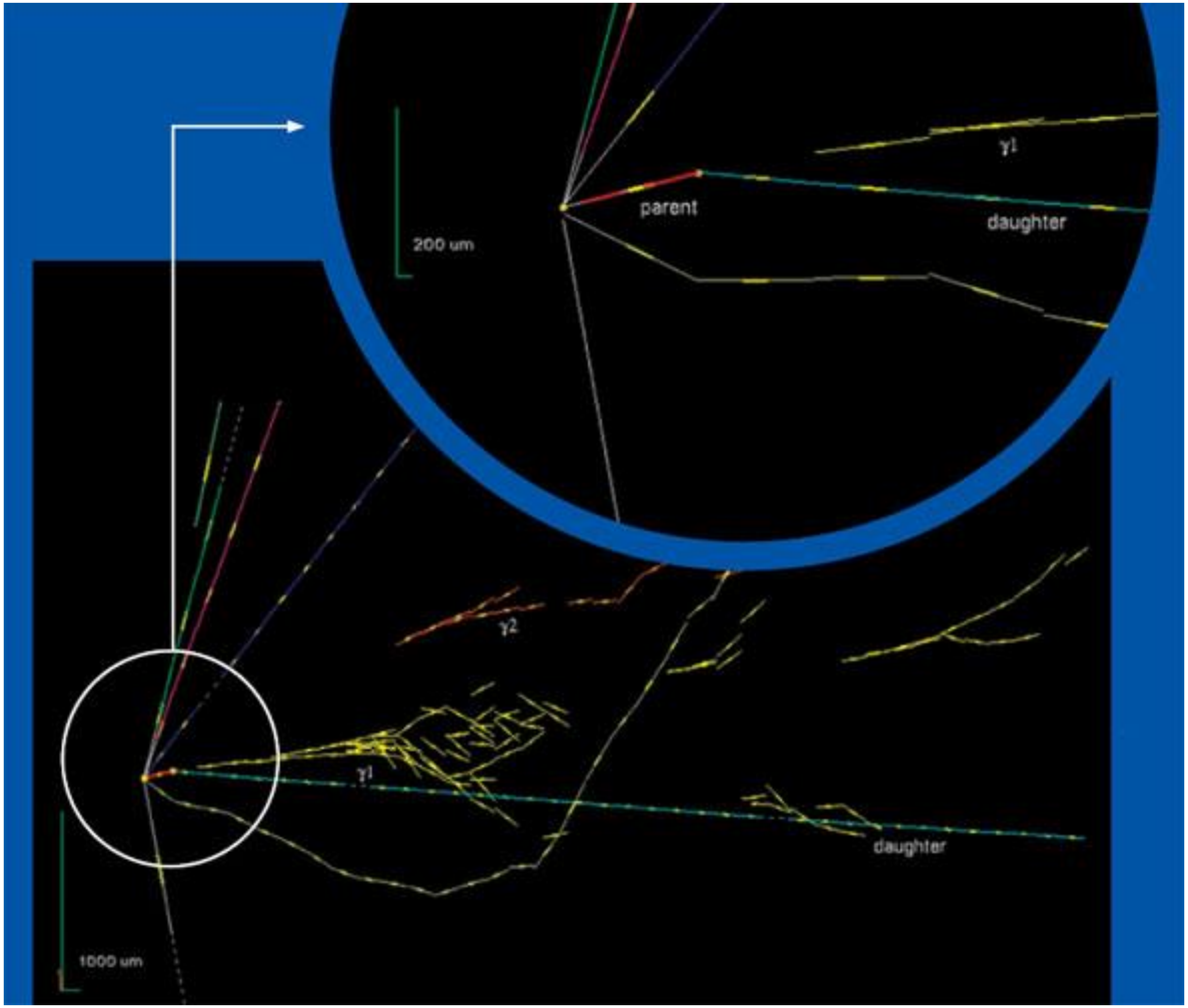

AMS

Alpha Magnetic Spectrometer

Try to find Antimatter in the primary cosmic rays.
Study cosmic ray composition etc. etc.

Was launched into space on STS-134 on 16 May 2011.

AMS Installed on the space station.

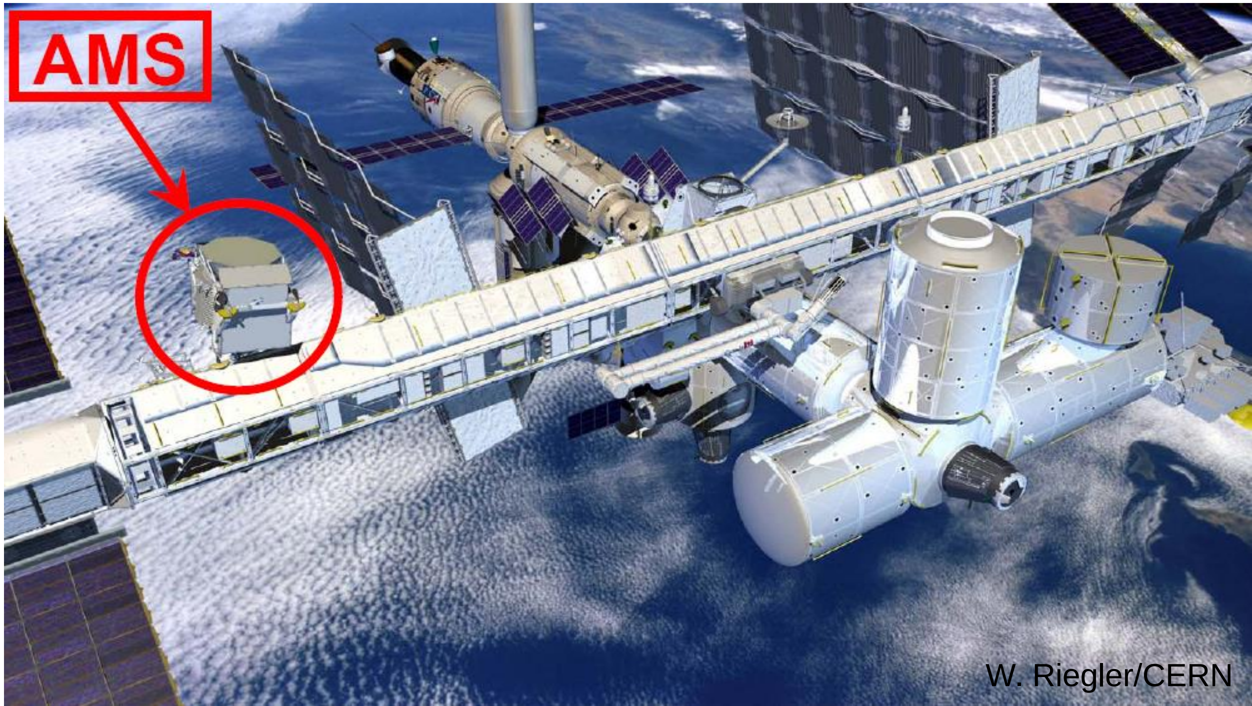

AMS

A state of the art particle detector with many 'earth bound' techniques going to space !

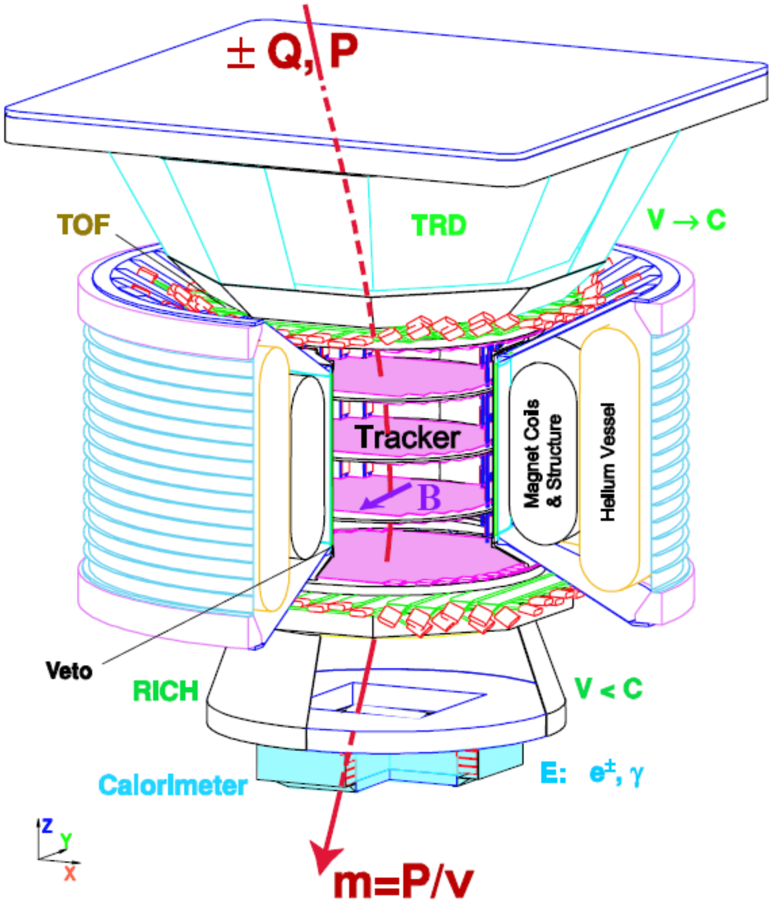

AMS

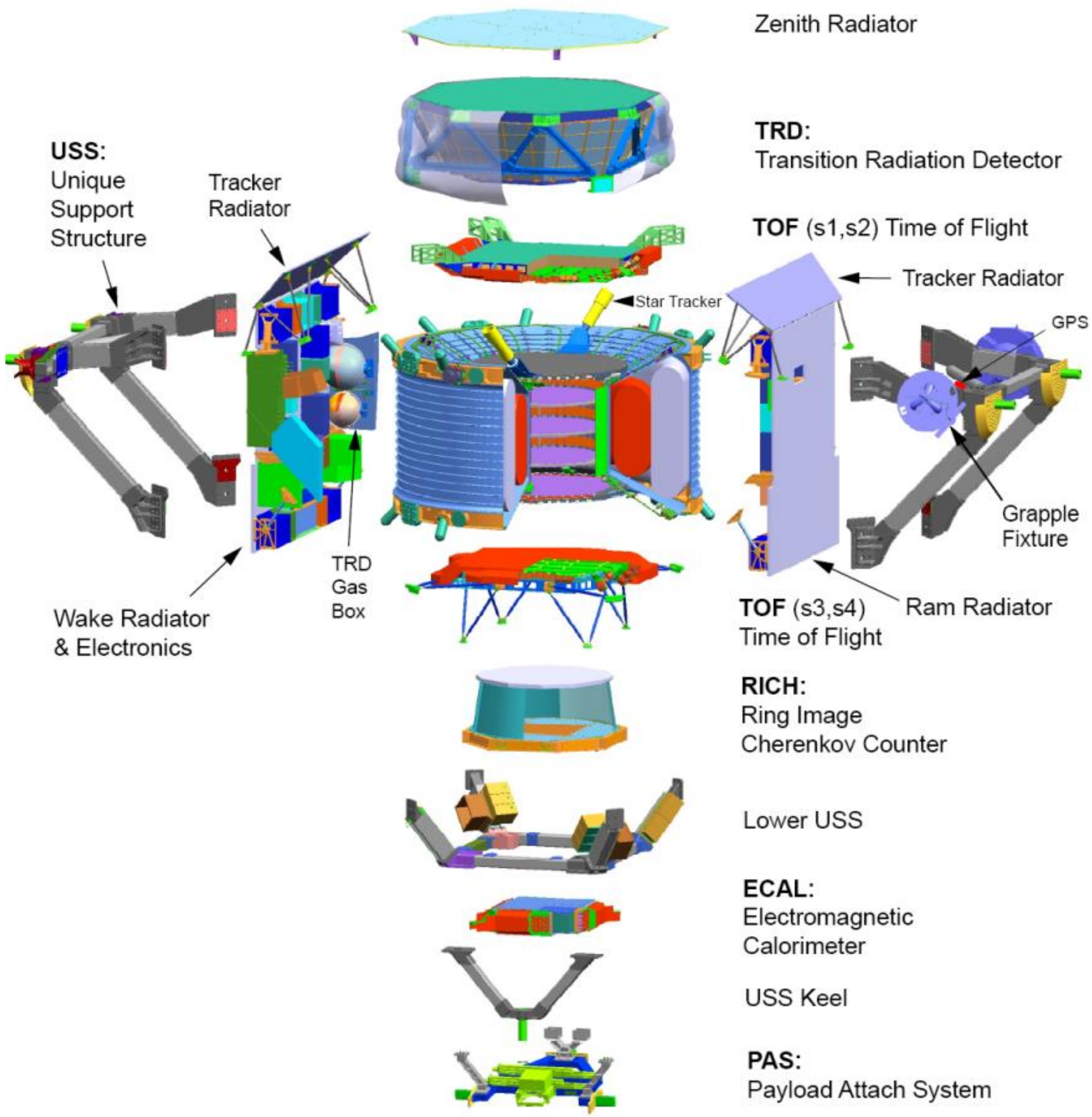
Zenith Radiator
TRD:
Transition Radiation Detector
USS:
Unique
Support
Structure
Tracker
Radiator
TOF (s1,s2) Time of Flight
Tracker Radiator
Star Tracker
GPS
Grapple
Fixture
TRD
Gas
Box
Wake Radiator
& Electronics
TOF (s3,s4)
Time of Flight
Ram Radiator
RICH:
Ring Image
Cherenkov Counter
Lower USS
ECAL:
Electromagnetic
Calorimeter
USS Keel
PAS:
Payload Attach System

Detector Physics

Precise knowledge of the processes leading to signals in particle detectors is necessary.

The detectors are nowadays working close to the limits of theoretically achievable measurement accuracy – even in large systems.

Due to available computing power, detectors can be simulated to within 5-10% of reality, based on the fundamental microphysics processes (atomic and nuclear crossections)

e.g. GEANT, FLUKA, MAGBOTLZ, HEED, GARFIELD

Particle Detector Simulation

Electric Fields in a Micromega Detector

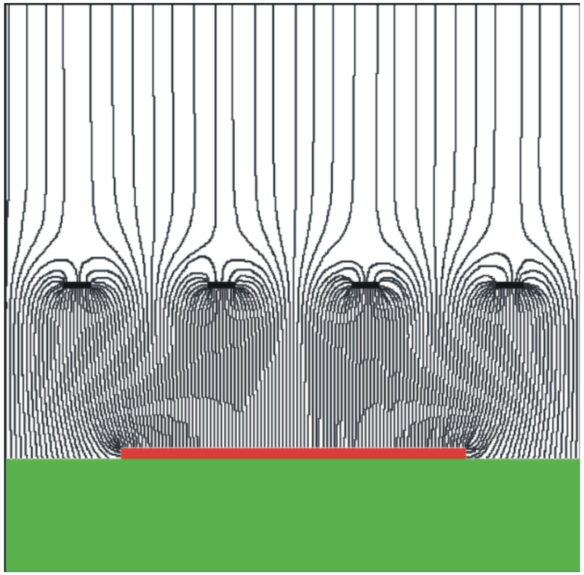

Very accurate simulations of particle detectors are possible due to availability of Finite Element simulation programs and computing power.

Follow every single electron by applying first principle laws of physics.

For Gaseous Detectors: GARFIELD by R. Veenhof

Electric Fields in a Micromega Detector

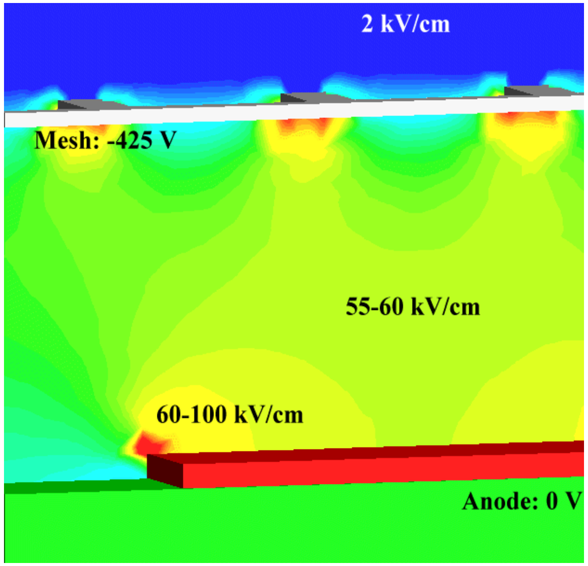

Electrons avalanche multiplication

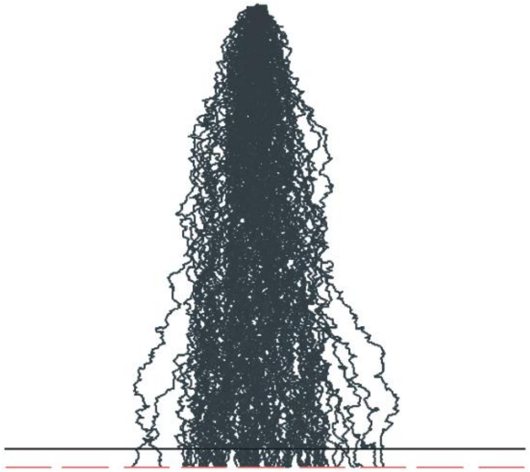

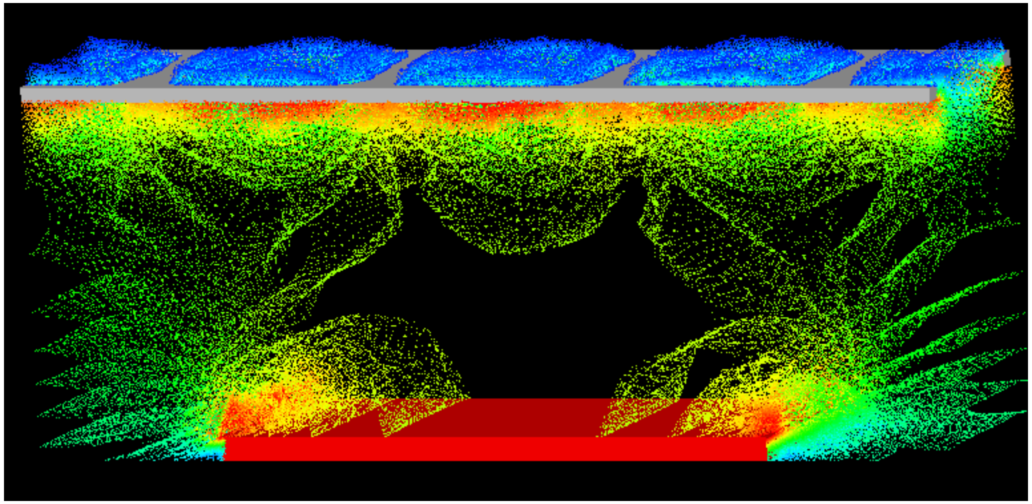

Particle Detector Simulation

I) C. Moore's Law:
Computing power doubles 18 months.

II) W. Riegler's Law:
The use of brain for solving a problem is inversely proportional to the available computing power.

→ I) + II) = ...

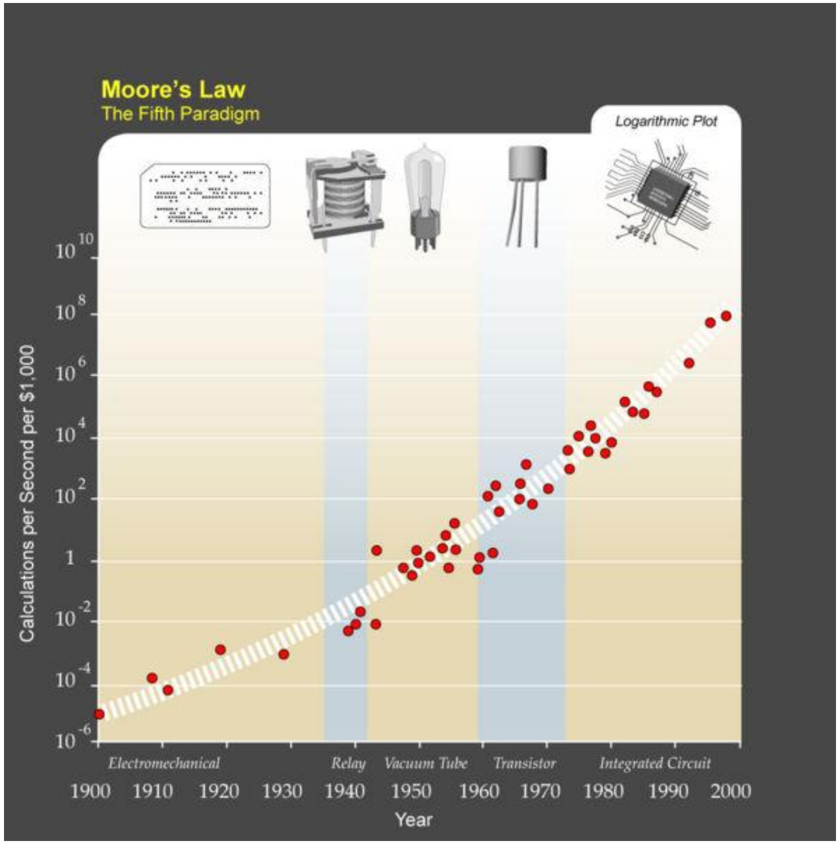

Knowing the basics of particle detectors is essential …

Interaction of Particles with Matter

Any device that is to detect a particle must interact with it in some way → almost …

In many experiments neutrinos are measured by missing transverse momentum.

E.g. e^+e^- collider. $P_{tot}=0$,
If the $\Sigma\, p_i$ of all collision products is $\neq 0$ → neutrino escaped.

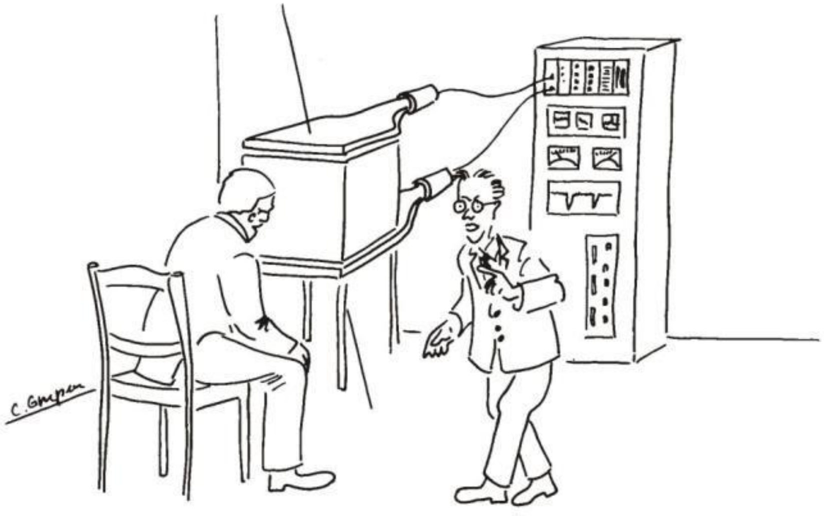

"Did you see it?"
"No nothing."
"Then it was a neutrino!"

Claus Grupen, Particle Detectors, Cambridge University Press, Cambridge 1996 (455 pp. ISBN 0-521-55216-8)

Interaction of Particles with Matter

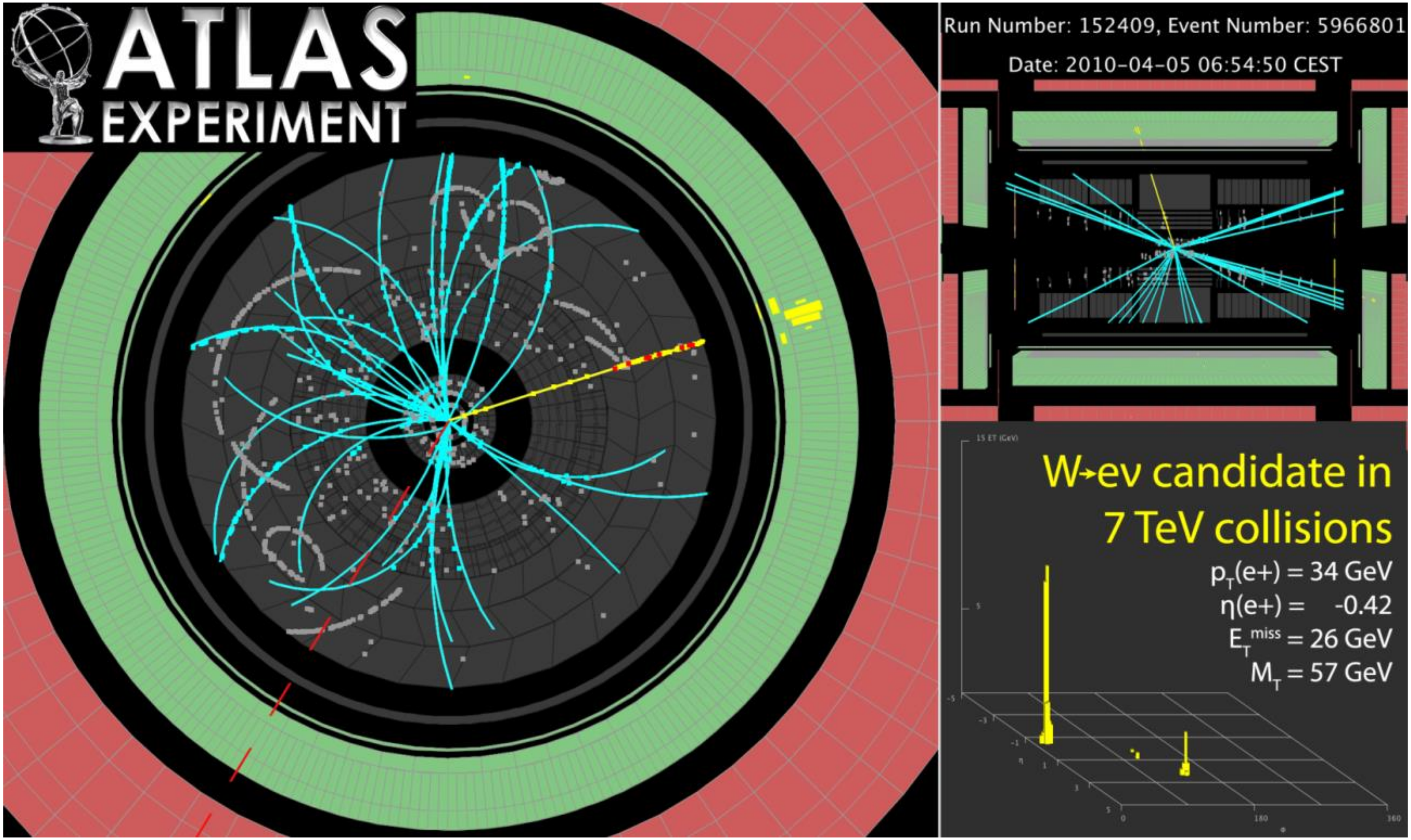

How can a particle detector distinguish the hundreds of particles that we know by now ?

http://pdg.lbl.gov ~ 180 Selected Particles

$\gamma, W^\pm, Z^0, g, e, \mu, \tau, \nu_e, \nu_\mu, \nu_\tau, \pi^\pm, \pi^0, \eta, f_0(600), \rho(770),$
$\omega(782), \eta'(958), f_0(980), a_0(980), \phi(1020), h_1(1170), b_1(1235),$
$a_1(1260), f_2(1270), f_1(1285), \eta(1295), \pi(1300), a_2(1320),$
$f_0(1370), f_1(1420), \omega(1420), \eta(1440), a_0(1450), \rho(1450),$
$f_0(1500), f_2'(1525), \omega(1650), \omega_3(1670), \pi_2(1670), \phi(1680),$
$\rho_3(1690), \rho(1700), f_0(1710), \pi(1800), \phi_3(1850), f_2(2010),$
$a_4(2040), f_4(2050), f_2(2300), f_2(2340), K^\pm, K^0, K^0_S, K^0_L, K^*(892),$
$K_1(1270), K_1(1400), K^*(1410), K_0^*(1430), K_2^*(1430), K^*(1680),$
$K_2(1770), K_3^*(1780), K_2(1820), K_4^*(2045), D^\pm, D^0, D^*(2007)^0,$
$D^*(2010)^\pm, D_1(2420)^0, D_2^*(2460)^0, D_2^*(2460)^\pm, D_s^\pm, D_s^{*\pm},$
$D_{s1}(2536)^\pm, D_{sJ}(2573)^\pm, B^\pm, B^0, B^*, B_s^0, B_c^\pm, \eta_c(1S), J/\psi(1S),$
$\chi_{c0}(1P), \chi_{c1}(1P), \chi_{c2}(1P), \psi(2S), \psi(3770), \psi(4040), \psi(4160),$
$\psi(4415), \Upsilon(1S), \chi_{b0}(1P), \chi_{b1}(1P), \chi_{b2}(1P), \Upsilon(2S), \chi_{b0}(2P),$
$\chi_{b2}(2P), \Upsilon(3S), \Upsilon(4S), \Upsilon(10860), \Upsilon(11020), p, n, N(1440),$
$N(1520), N(1535), N(1650), N(1675), N(1680), N(1700), N(1710),$
$N(1720), N(2190), N(2220), N(2250), N(2600), \Delta(1232), \Delta(1600),$
$\Delta(1620), \Delta(1700), \Delta(1905), \Delta(1910), \Delta(1920), \Delta(1930), \Delta(1950),$
$\Delta(2420), \Lambda, \Lambda(1405), \Lambda(1520), \Lambda(1600), \Lambda(1670), \Lambda(1690),$
$\Lambda(1800), \Lambda(1810), \Lambda(1820), \Lambda(1830), \Lambda(1890), \Lambda(2100),$
$\Lambda(2110), \Lambda(2350), \Sigma^+, \Sigma^0, \Sigma^-, \Sigma(1385), \Sigma(1660), \Sigma(1670),$
$\Sigma(1750), \Sigma(1775), \Sigma(1915), \Sigma(1940), \Sigma(2030), \Sigma(2250), \Xi^0, \Xi^-,$
$\Xi(1530), \Xi(1690), \Xi(1820), \Xi(1950), \Xi(2030), \Omega^-, \Omega(2250)^-,$
$\Lambda_c^+, \Lambda_c^+, \Sigma_c(2455), \Sigma_c(2520), \Xi_c^+, \Xi_c^0, \Xi_c'^+, \Xi_c'^0, \Xi(2645)$
$\Xi_c(2790), \Xi_c(2815), \Omega_c^0, \Lambda_b^0, \Xi_b^0, \Xi_b^-, t\bar{t}$

There are many more

These are all the known 27 particles with a lifetime that is long enough such that at GeV energies they travel more than 1 micrometer.

All Particles with $c\tau > 1\mu m$ @ GeV Level

Particle	Mass (MeV)	Lifetime τ (s)	$c\tau$
γ	0	∞	∞
$\pi^\pm$ $(u\bar{d}, d\bar{u})$	140	$2.6 \cdot 10^{-8}$	7.8 m
$K^\pm$ $(u\bar{s}, \bar{u}s)$	494	$1.2 \cdot 10^{-8}$	3.7 m
K^0 $(d\bar{s}, \bar{d}s)$	497	$5.1 \cdot 10^{-8}$ $8.9 \cdot 10^{-11}$	15.5 m 2.7 cm
$D^\pm$ $(c\bar{d}, \bar{c}d)$	1869	$1.0 \cdot 10^{-12}$	315 μm
D^0 $(c\bar{u}, u\bar{c})$	1864	$4.1 \cdot 10^{-13}$	123 μm
$D_s^\pm$ $(c\bar{s}, \bar{c}s)$	1969	$4.9 \cdot 10^{-13}$	147 μm
$B^\pm$ $(u\bar{b}, \bar{b}u)$	5279	$1.7 \cdot 10^{-12}$	502 μm
B^0 $(b\bar{d}, d\bar{b})$	5279	$1.5 \cdot 10^{-12}$	462 μm
B_s^0 $(s\bar{b}, \bar{s}b)$	5370	$1.5 \cdot 10^{-12}$	438 μm
$B_c^\pm$ $(c\bar{b}, \bar{c}b)$	~6400	$\sim 5 \cdot 10^{-13}$	150 μm
p (uud)	938.3	$> 10^{33}$ y	∞
n (udd)	939.6	885.7 s	$2.655 \cdot 10^{8}$ km
Λ^0 (uds)	1115.7	$2.6 \cdot 10^{-10}$	7.89 cm
Σ^+ (uus)	1189.4	$8.0 \cdot 10^{-11}$	2.404 cm
Σ^- (dds)	1197.4	$1.5 \cdot 10^{-10}$	4.434 cm
Ξ^0 (uss)	1315	$2.9 \cdot 10^{-10}$	8.71 cm
Ξ^- (dss)	1321	$1.6 \cdot 10^{-10}$	4.91 cm
Ω^- (sss)	1672	$8.2 \cdot 10^{-11}$	2.461 cm
Λ_c^+ (udc)	2285	$\sim 2 \cdot 10^{-13}$	60 μm
Ξ_c^+ (usc)	2466	$4.4 \cdot 10^{-13}$	132 μm
Ξ_c^0 (dcs)	2472	$\sim 1 \cdot 10^{-13}$	29 μm
Ω_c^0 (ssc)	2698	$6.0 \cdot 10^{-14}$	19 μm
Λ_b (udb)	5620	$1.2 \cdot 10^{-12}$	368 μm

"Secondary Vertices"

W. Riegler/CERN

From the 'hundreds' of Particles listed by the PDG there are only ~27 with a life time $c\tau > \sim 1\mu m$ i.e. they can be seen as 'tracks' in a Detector.

~13 of the 27 have $c\tau < 500\mu m$ i.e. only ~mm range at GeV Energies.
→ "short" tracks measured with Emulsions or Vertex Detectors.

From the ~14 remaining particles

$$e^\pm, \mu^\pm, \gamma, \pi^\pm, K^\pm, K^0, p^\pm, n$$

are by far the most frequent ones

A particle Detector must be able to identify and measure Energy and Momenta of these 8 particles.

The 8 Particles a Detector must be able to Measure and Identify

$e^{\pm}$ $m_e = 0.511$ MeV
$\mu^{\pm}$ $m_\mu = 105.7$ MeV $\sim 200\, m_e$
γ $m_\gamma = 0$, $Q = 0$

EM

$\pi^{\pm}$ $m_\pi = 139.6$ MeV $\sim 270\, m_e$
$K^{\pm}$ $m_K = 493.7$ MeV $\sim 1000\, m_e$
$p^{\pm}$ $m_p = 938.3$ MeV $\sim 2000\, m_e$

EM, Strong

$\sim 3.5\, m_\pi$

K^0 $m_{K^0} = 497.7$ MeV $Q = 0$
n $m_n = 939.6$ MeV $Q = 0$

Strong

The Difference in

Mass, Charge, Interaction

is the key to the Identification

The 8 Particles a Detector must be able to Measure and Identify

- Electrons ionize and show Bremsstrahlung due to the small mass
- Photons don't ionize but show Pair Production in high Z Material. From then on equal to $e^\pm$
- Charged Hadrons ionize and show Hadron Shower in dense material.
- Neutral Hadrons don't ionize and show Hadron Shower in dense Material
- Myons ionize and don't shower

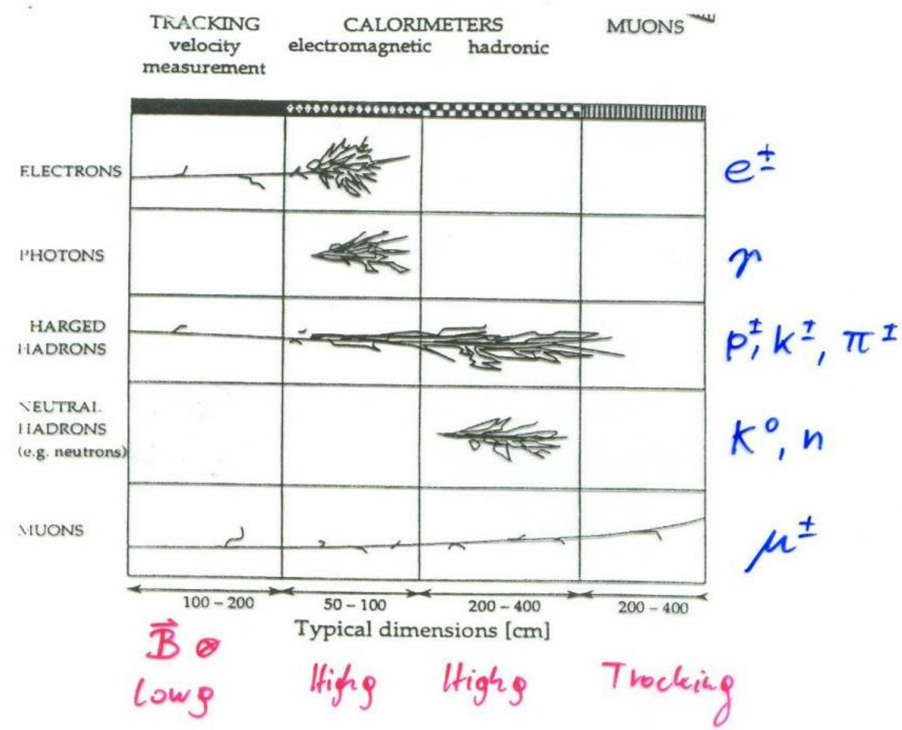

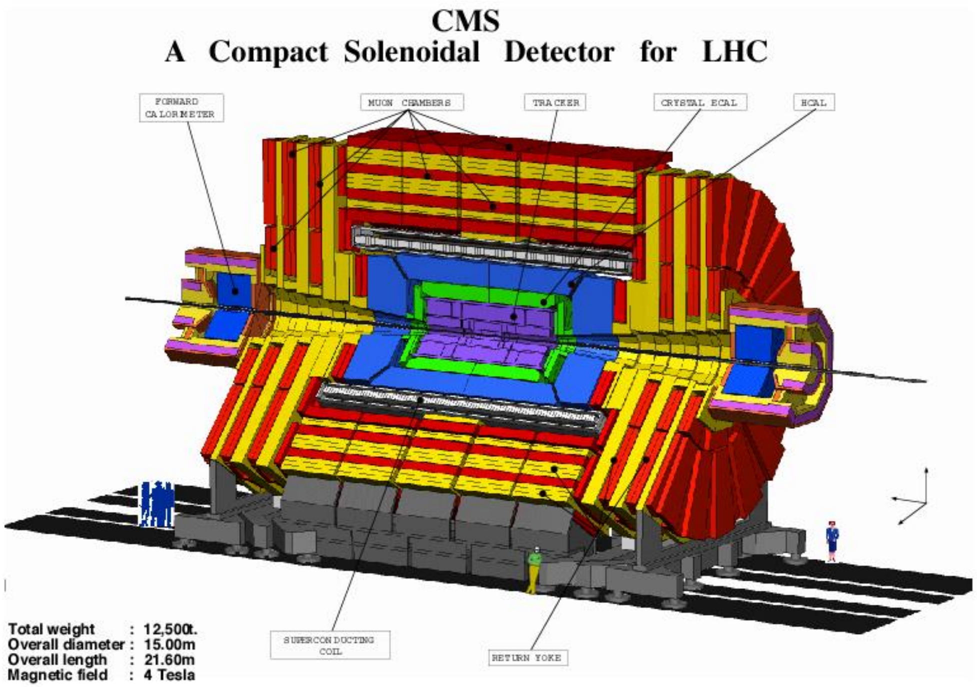

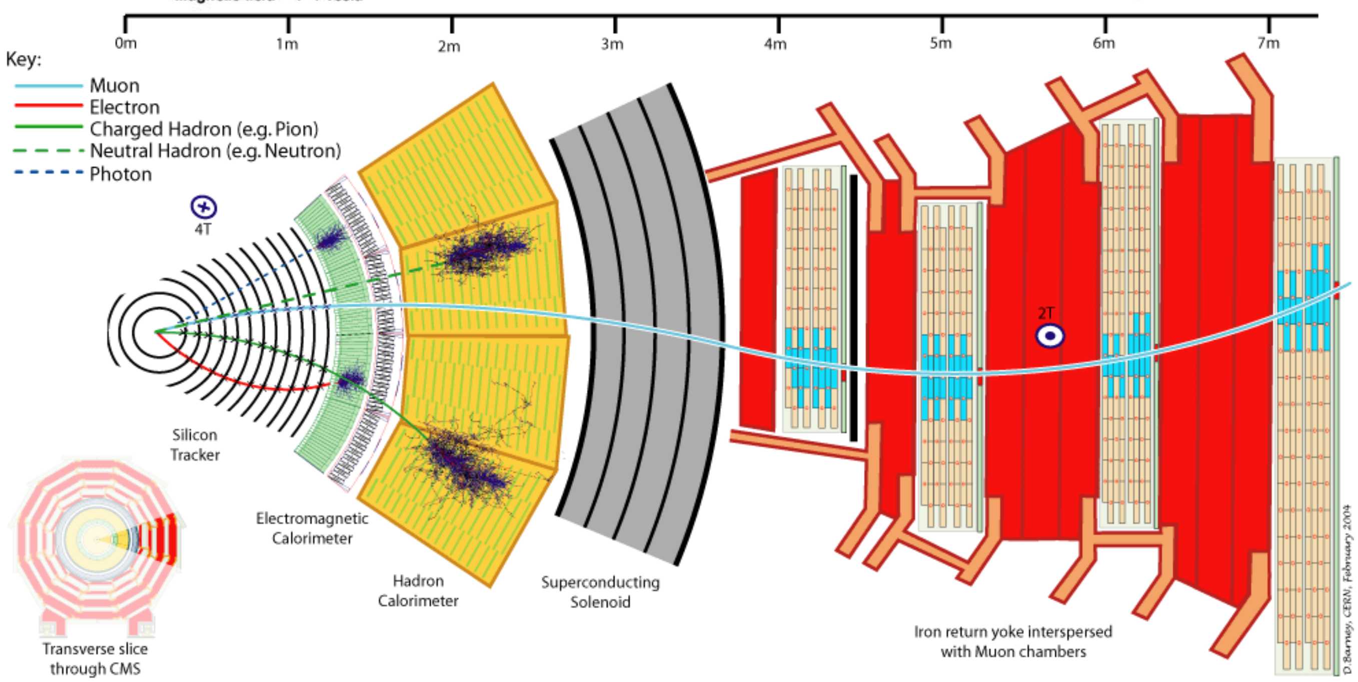

W. Riegler/CERN

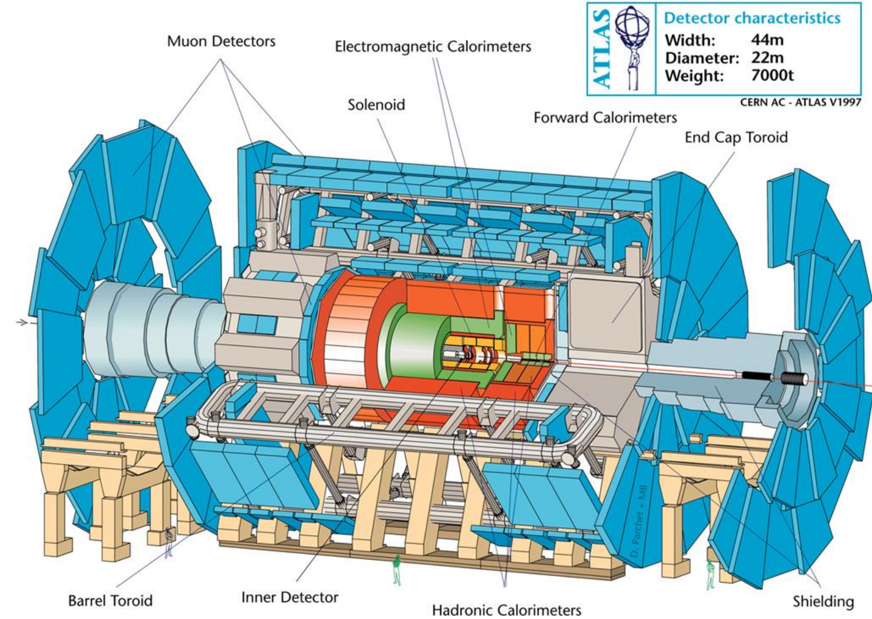

Detector characteristics
ATLAS
Width: 44m
Diameter: 22m
Weight: 7000t
CERN AC - ATLAS V1997
Muon Detectors
Electromagnetic Calorimeters
Solenoid
Forward Calorimeters
End Cap Toroid
Barrel Toroid
Inner Detector
Hadronic Calorimeters
Shielding

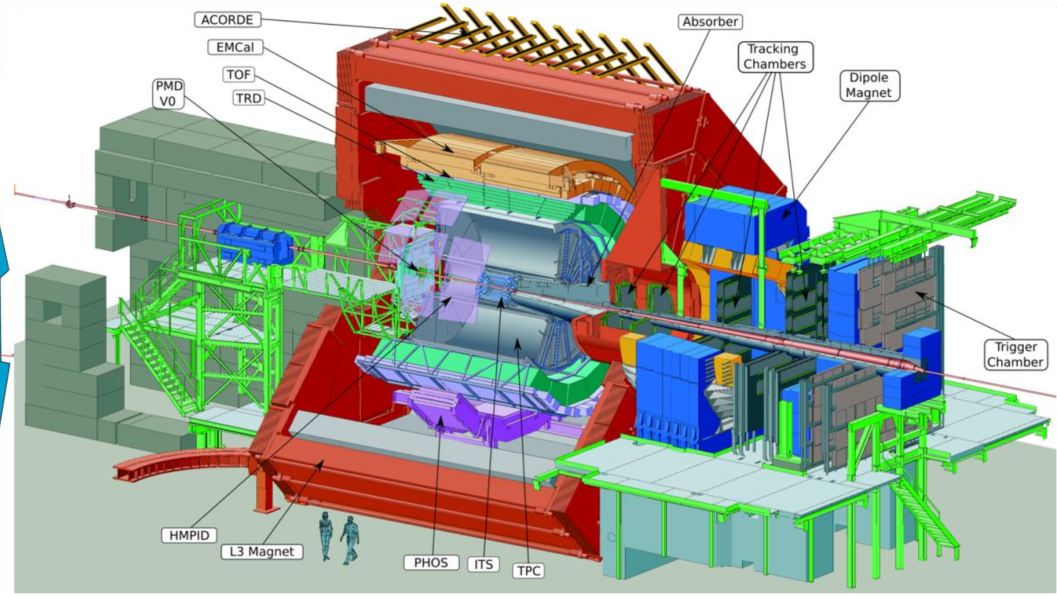

ACORDE
EMCal
TOF
TRD
PMD
V0
Absorber
Tracking Chambers
Dipole Magnet
Trigger Chamber
HMPID
L3 Magnet
PHOS
ITS
TPC

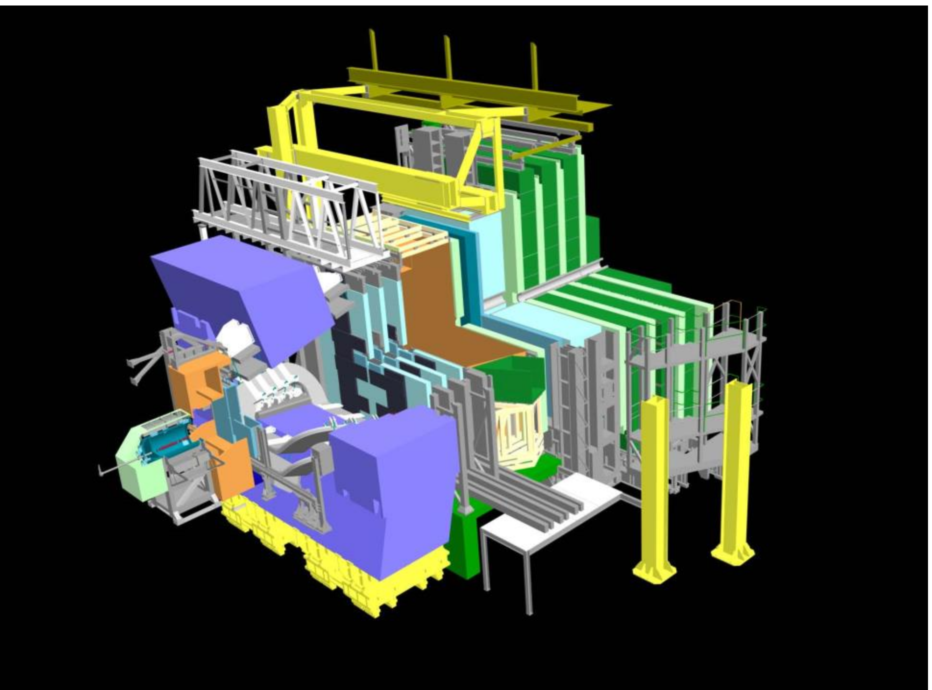

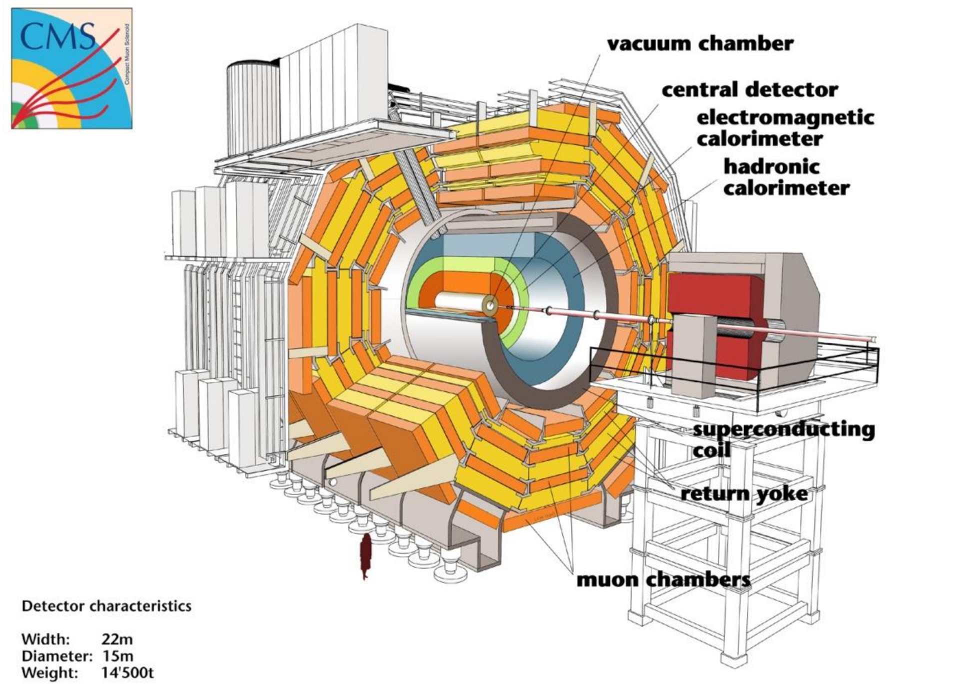

CMS
vacuum chamber
central detector
electromagnetic calorimeter
hadronic calorimeter
superconducting coil
return yoke
muon chambers
Detector characteristics
Width: 22m
Diameter: 15m
Weight: 14'500t

Creation of the Signal

Detectors based on Registration of Ionization: Tracking in Gas and Solid State Detectors

Charged particles leave a trail of ionization (and excited atoms) along their path: Electron-Ion pairs in gases and liquids, electron hole pairs in solids.

The produced charges can be registered → Position measurement → Tracking Detectors.

Cloud Chamber: Charges create drops → photography.
Bubble Chamber: Charges create bubbles → photography.
Emulsion: Charges 'blacked' the film.

Gas and Solid State Detectors: Moving Charges (electric fields) induce electronic signals on metallic electrons that can be read by dedicated electronics.

→In solid state detectors the charge created by the incoming particle is sufficient.

→In gas detectors (e.g. wire chamber) the charges are internally multiplied in order to provide a measurable signal.

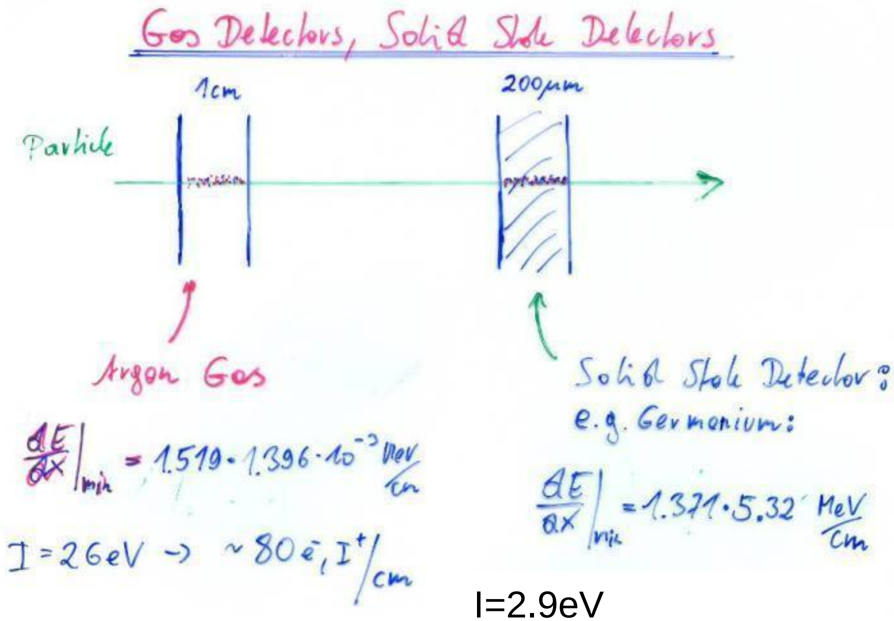

I=2.9eV
2.5 x 10^6 e/h pairs/cm

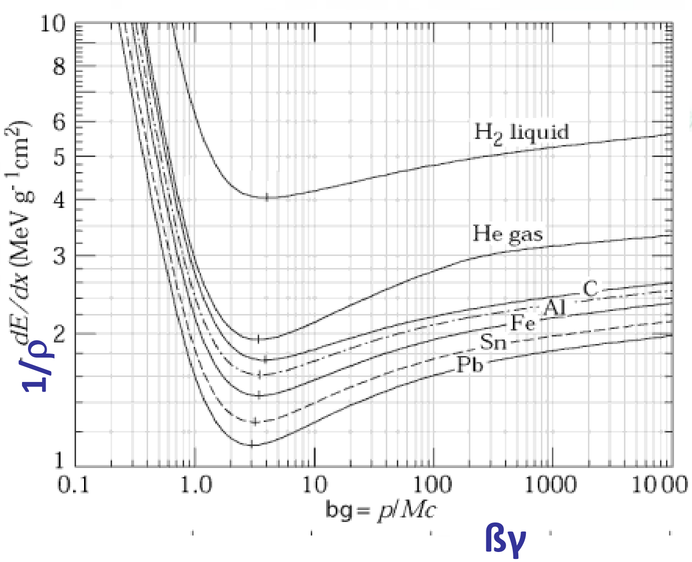

The induced signals are readout out by dedicated electronics.

The noise of an amplifier determines whether the signal can be registered. Signal/Noise >>1

The noise is characterized by the 'Equivalent Noise Charge (ENC)' = Charge signal at the input that produced an output signal equal to the noise.

ENC of very good amplifiers can be as low as 50e-, typical numbers are ~ 1000e-.

In order to register a signal, the registered charge must be q >> ENC i.e. typically q>>1000e-.

Gas Detector: q=80e- /cm → too small.

Solid state detectors have 1000x more density and factor 5-10 less ionization energy.
→Primary charge is 10^4-10^5 times larger than is gases.

Gas detectors need internal amplification in order to be sensitive to single particle tracks.

Without internal amplification they can only be used for a large number of particles that arrive at the same time (ionization chamber).

W. Riegler/CERN

Principle of Signal Induction by Moving Charges

A point charge q at a distance z_0

Above a grounded metal plate 'induces' a surface charge.

The total induced charge on the surface is –q.

Different positions of the charge result in different charge distributions.

The total induced charge stays –q.

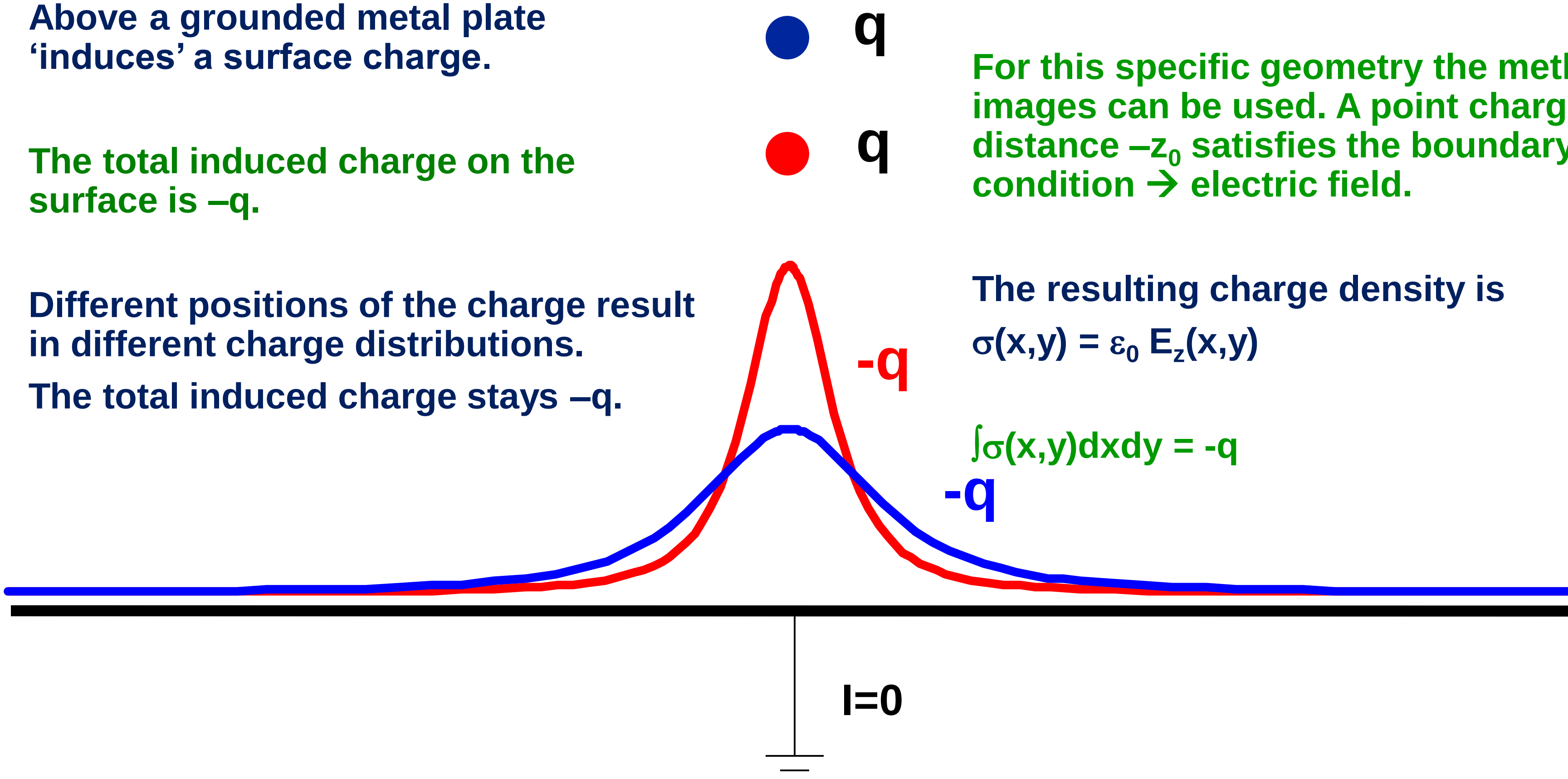

The electric field of the charge must be calculated with the boundary condition that the potential φ=0 at z=0.

For this specific geometry the method of images can be used. A point charge –q at distance $-z_0$ satisfies the boundary condition → electric field.

The resulting charge density is

$\sigma(x,y) = \varepsilon_0 E_z(x,y)$

$\int \sigma(x,y)dxdy = -q$

$$E_z(x,y) = -\frac{q z_0}{2\pi\varepsilon_0 (x^2+y^2+z_0^2)^{\frac{3}{2}}} \qquad E_x = E_y = 0 \qquad \sigma(x,y) = \varepsilon_0 E_z(x,y) \qquad Q = \int_{-\infty}^{\infty}\int_{-\infty}^{\infty} \sigma(x,y)dxdy = -q$$

W. Riegler/CERN

Principle of Signal Induction by Moving Charges

If we segment the grounded metal plate and if we ground the individual strips the surface charge density doesn't change with respect to the continuous metal plate.

The charge induced on the individual strips is now depending on the position z_0 of the charge.

If the charge is moving there are currents flowing between the strips and ground.

→ The movement of the charge induces a current.

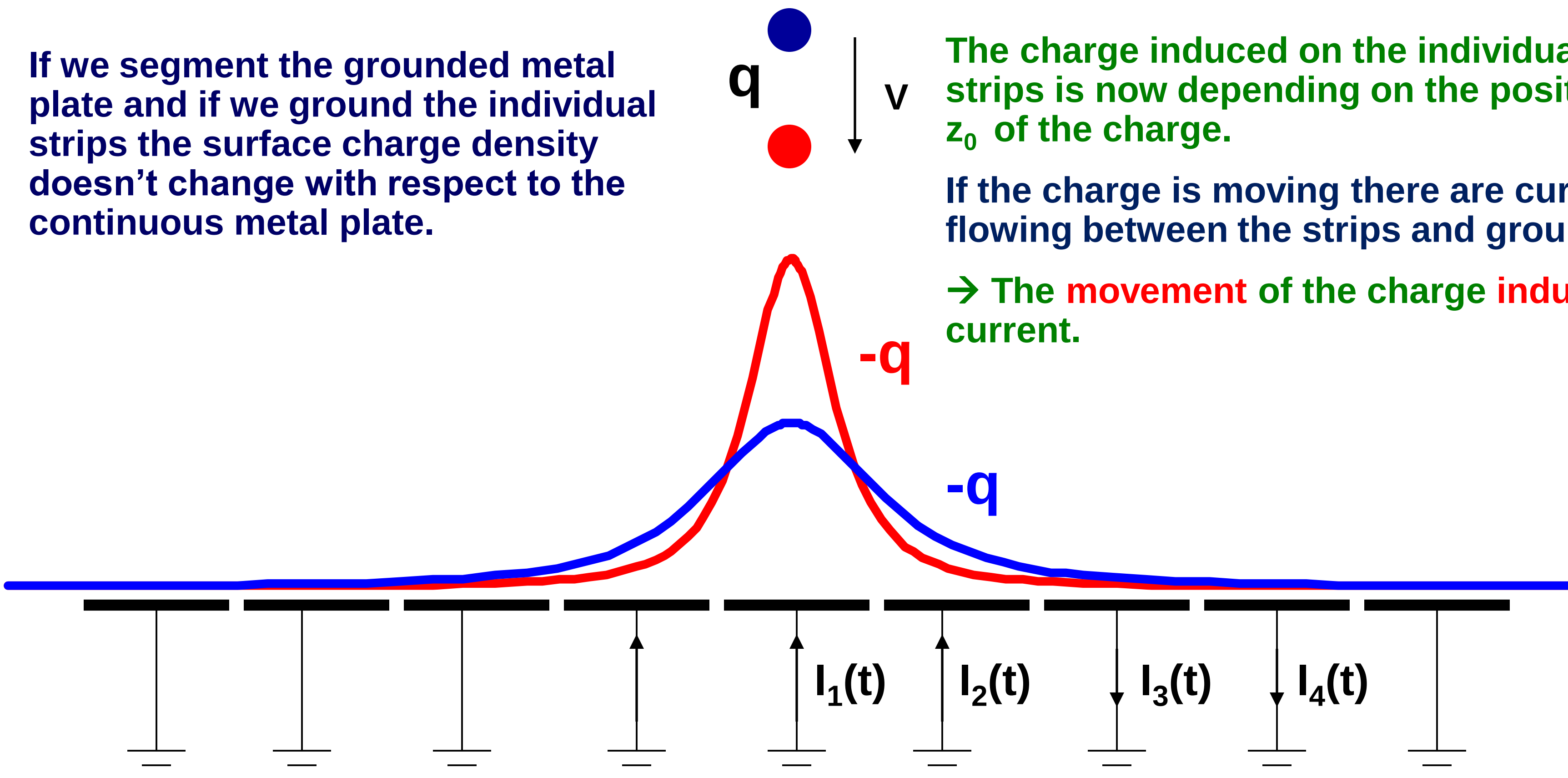

$$Q_1(z_0) = \int_{-\infty}^{\infty}\int_{-w/2}^{w/2} \sigma(x,y)\,dx\,dy = -\frac{2q}{\pi}\arctan\left(\frac{w}{2z_0}\right)$$

$$z_0(t) = z_0 - vt$$

$$I_1^{ind}(t) = -\frac{d}{dt}Q_1[z_0(t)] = -\frac{\partial Q_1[z_0(t)]}{\partial z_0}\frac{dz_0(t)}{dt} = \frac{4qw}{\pi[4z_0(t)^2 + w^2]}\,v$$

W. Riegler/CERN

Signal Theorems

What are the charges induced by a moving charge on electrodes that are connected with arbitrary linear impedance elements ?

One first removes all the impedance elements, connects the electrodes to ground and calculates the currents induced by the moving charge on the grounded electrodes.

The current induced on a grounded electrode by a charge q moving along a trajectory x(t) is calculated the following way (Ramo Theorem):

One removes the charge q from the setup, puts the electrode to voltage V_0 while keeping all other electrodes grounded. This results in an electric field $E_n(x)$, the Weighting Field, in the volume between the electrodes, from which the current is calculated by

$$I_n(t) = -\frac{q}{V_0}\vec{E_n}[\vec{x}(t)]\frac{d\vec{x}(t)}{dt} = -\frac{q}{V_0}\vec{E_n}[\vec{x}(t)]\vec{v}(t)$$

These currents are then placed as ideal current sources on a circuit where the electrodes are 'shrunk' to simple nodes and the mutual electrode capacitances are added between the nodes. These capacitances are calculated from the weighting fields by

$$c_{nm} = \frac{\varepsilon_0}{V_w}\oint_{\boldsymbol{A}_n}\boldsymbol{E}_m(\boldsymbol{x})dA \qquad C_{nn} = \sum_m c_{nm} \qquad C_{nm} = -c_{nm} \quad n \neq m$$

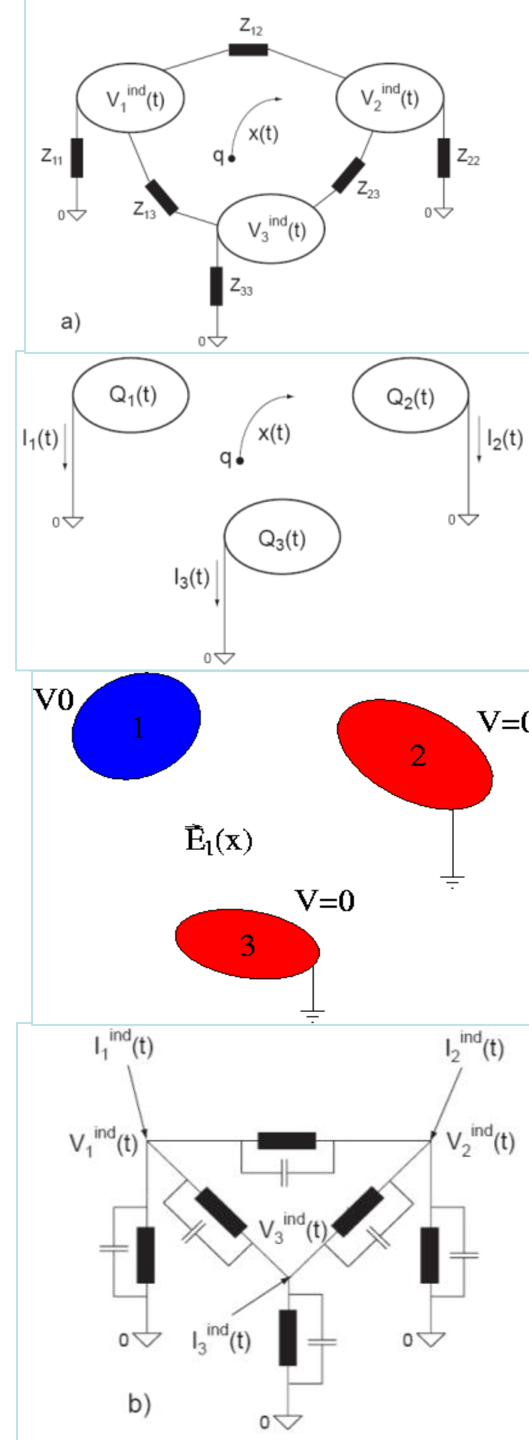

More on signal theorems, readout electronics etc. can be found in this book →

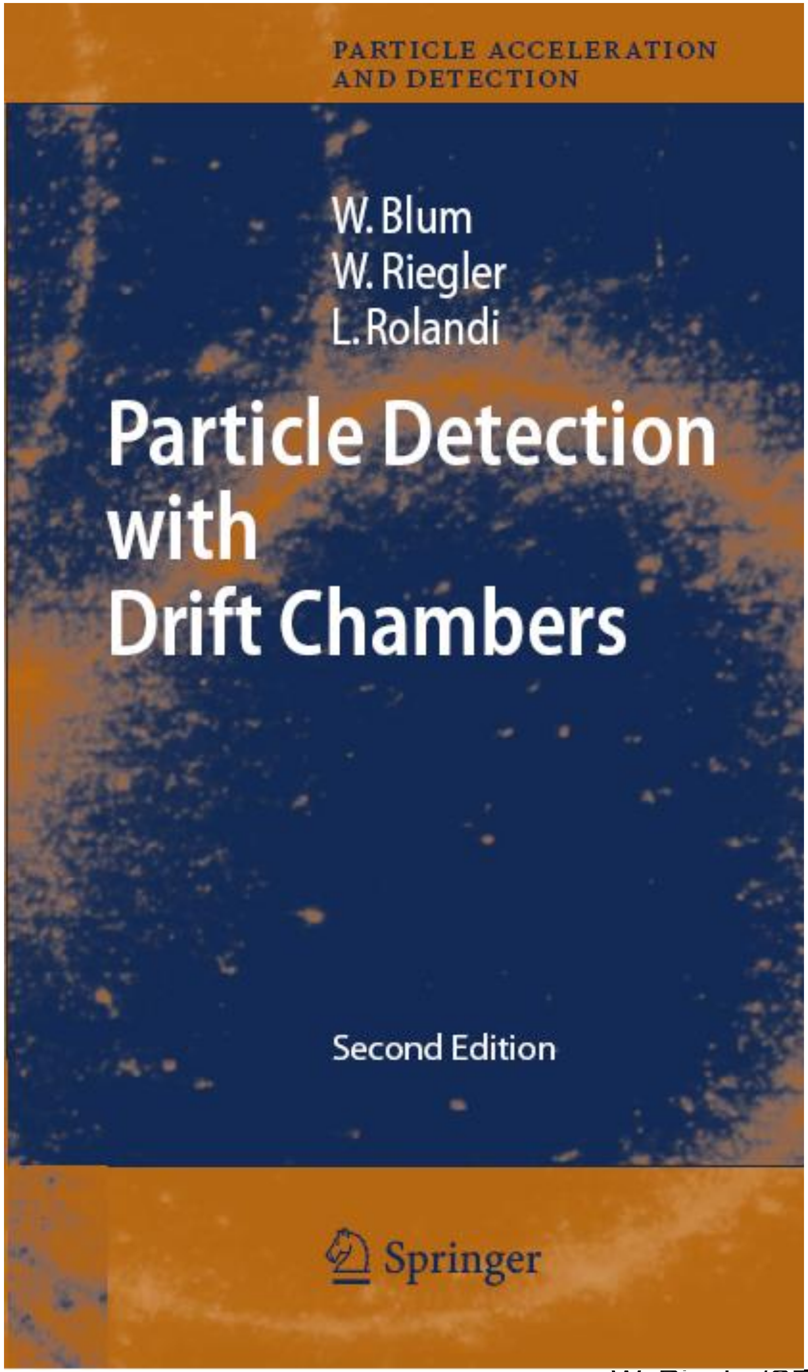

Electromagnetic Interaction of Particles with Matter

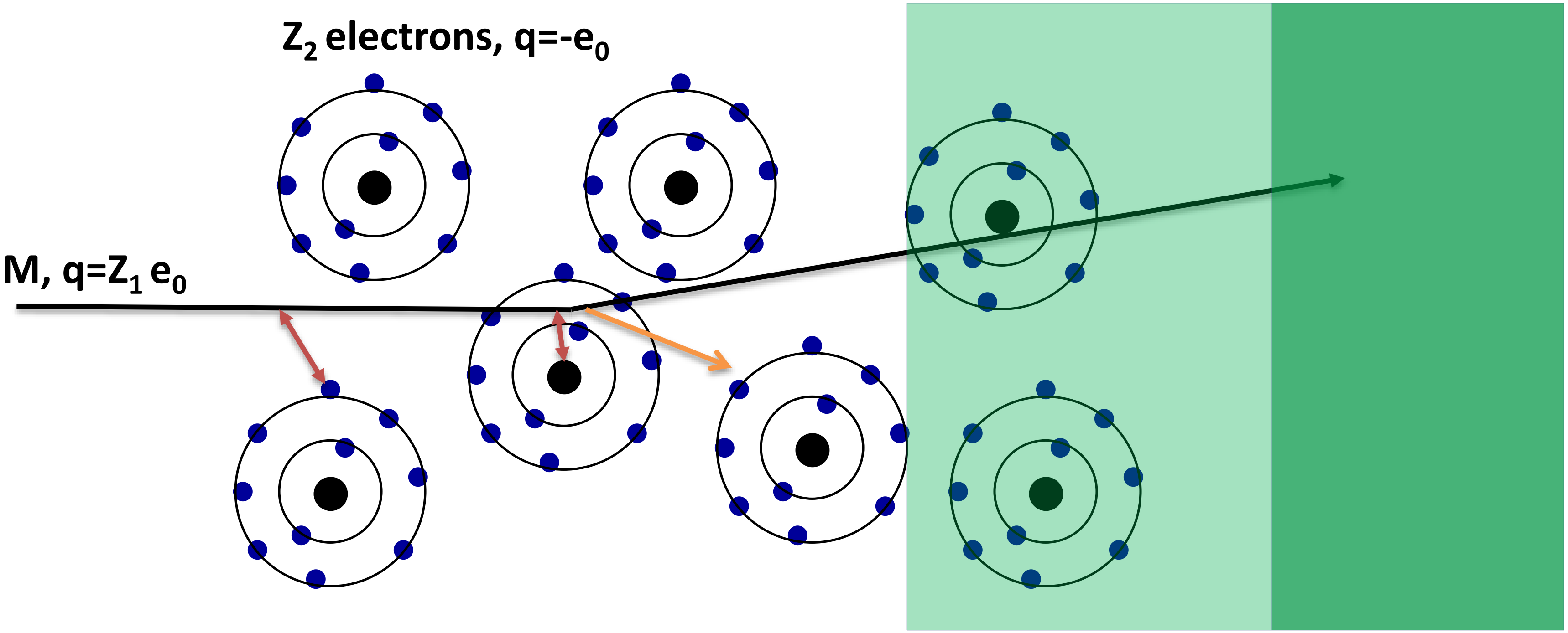

Interaction with the atomic electrons. The incoming particle loses energy and the atoms are excited or ionized.

Interaction with the atomic nucleus. The particle is deflected (scattered) causing multiple scattering of the particle in the material. During this scattering a Bremsstrahlung photon can be emitted.

In case the particle's velocity is larger than the velocity of light in the medium, the resulting EM shockwave manifests itself as Cherenkov Radiation. When the particle crosses the boundary between two media, there is a probability of the order of 1% to produced and X ray photon, called Transition radiation.

Ionization and Excitation

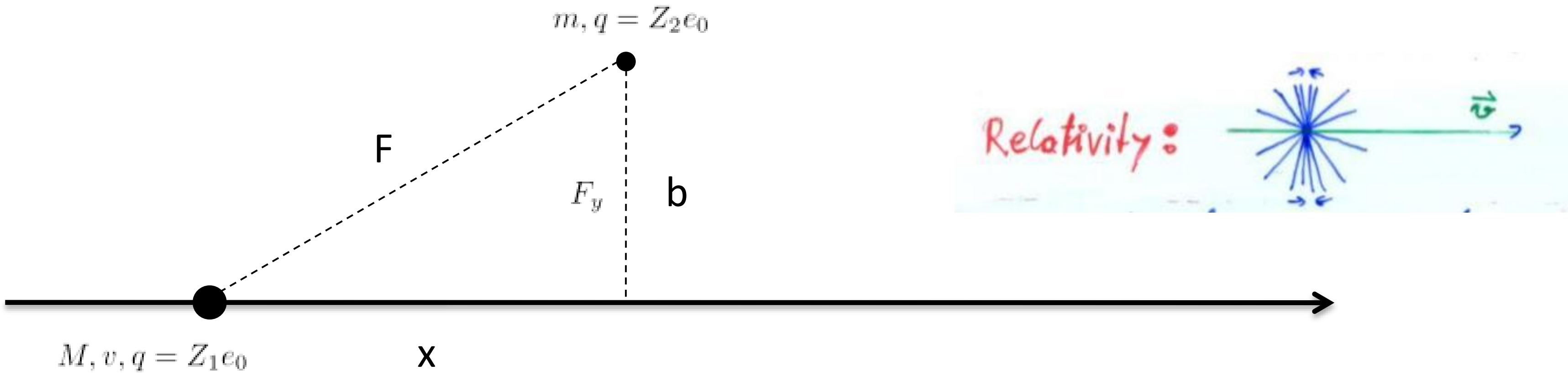

While the charged particle is passing another charged particle, the Coulomb Force is acting, resulting in momentum transfer

$$F_y = \frac{Z_1 Z_2 e_0^2}{4\pi\varepsilon_0 (b^2 + v^2 t^2)} \frac{b}{\sqrt{b^2 + v^2 t^2}} \qquad \Delta p = \int_{-\infty}^{\infty} F_y(t) dt = \frac{2 Z_1 Z_2 e_0^2}{4\pi\varepsilon_0 v b}$$

The relativistic form of the transverse electric field doesn't change the momentum transfer. The transverse field is stronger, but the time of action is shorter

$$F_y = \frac{\gamma Z_1 Z_2 e_0^2 b}{4\pi\varepsilon_0 (b^2 + \gamma^2 v^2 t^2)^{3/2}} \qquad \Delta p = \int_{-\infty}^{\infty} F_y(t) dt = \frac{2 Z_1 Z_2 e_0^2}{4\pi\varepsilon_0 v b}$$

The transferred energy is then $\quad \Delta E = \frac{(\Delta p)^2}{2m} = \frac{Z_2^2}{m} \frac{2 Z_1^2 e_0^4}{(4\pi\varepsilon_0)^2 v^2 b^2}$

$$\Delta E(electrons) = Z_2 \frac{1}{m_e} \frac{2 Z_1^2 e_0^4}{(4\pi\varepsilon_0)^2 v^2 b^2} \qquad \Delta E(nucleus) = \frac{Z_2^2}{2 Z_2 m_p} \frac{2 Z_1^2 e_0^4}{(4\pi\varepsilon_0)^2 v^2 b^2} \qquad \frac{\Delta E(electrons)}{\Delta E(nucleus)} = \frac{2 m_p}{m_e} \approx 4000$$

→ The incoming particle transfer energy only (mostly) to the atomic electrons !

Ionization and Excitation

Target material: mass A, Z_2, density ρ [g/cm^3], Avogadro number N_A

A gramm → N_A Atoms: **Number of atoms/cm^3** $n_a = N_A \rho / A$ [1/cm^3]

Number of electrons/cm^3 $n_e = N_A \rho Z_2 / A$ [1/cm^3]

$$\Delta E(electrons) = \frac{2 Z_2 Z_1^2 m_e c^2}{\beta^2 b^2} \frac{e_0^4}{(4\pi\varepsilon_0 m_e c^2)^2} = \frac{2 Z_2 Z_1^2 m_e c^2}{\beta^2 b^2} r_e^2$$

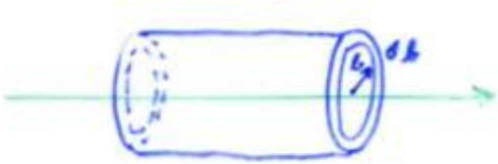

$$dE = -\int_{b_{min}}^{b_{max}} n_e \Delta E dx 2b\pi db = -\frac{4\pi Z_2 Z_1^2 m_e c^2 r_e^2}{\beta^2} \frac{N_A \rho}{A} \int_{b_{min}}^{b_{max}} \frac{db}{b}$$

With $\Delta E(b)$ → $db/b = -1/2\, dE/E$ → $E_{max} = \Delta E(b_{min})$ $E_{min} = \Delta E(b_{max})$

$$\frac{dE}{dx} = -2\pi r_e^2 m_e^2 c^2 \frac{Z_1^2}{\beta^2} \frac{N_A Z_2 \rho}{A} \int_{E_{min}}^{E_{max}} \frac{dE}{E} \quad = \quad -2\pi r_e^2 m_e^2 c^2 \frac{Z_1^2}{\beta^2} \frac{N_A Z_2 \rho}{A} \ln \frac{E_{max}}{E_{min}}$$

$E_{min} \approx I$ (Ionization Energy)

Relativistic Collision Kinematics, E_{max}

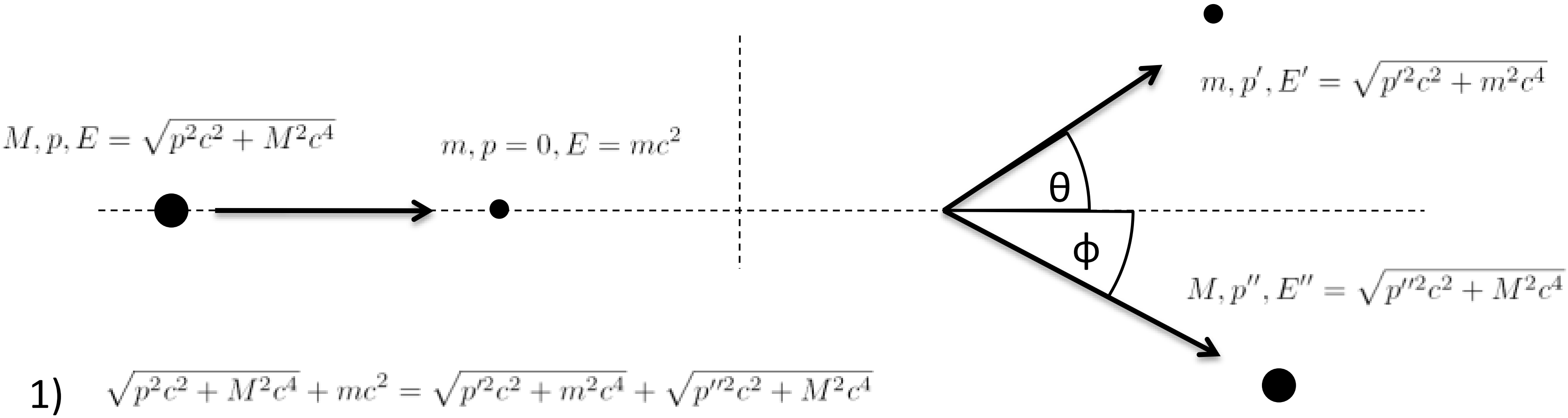

1) $\sqrt{p^2c^2 + M^2c^4} + mc^2 = \sqrt{p'^2c^2 + m^2c^4} + \sqrt{p''^2c^2 + M^2c^4}$

2) $p = p' \cos\theta + p'' \cos\phi$ $\qquad p''^2 = p'^2 + p^2 - 2pp' \cos\theta$

$0 = p' \sin\theta + p'' \sin\phi$

1+2) $E^{k'} = \sqrt{p'^2c^2 + m^2c^4} - mc^2 = \dfrac{2mc^2\, p^2c^2 \cos^2\theta}{\left[mc^2 + \sqrt{p^2c^2 + M^2c^4}\right]^2 - p^2c^2\cos^2\theta}$

$$E^{k'}{}_{max} = \frac{2mc^2p^2c^2}{(m^2 + M^2)c^4 + 2m\sqrt{p^2c^2 + M^2c^4}} = 2mc^2\beta^2\gamma^2 F \qquad F = \left(1 + \frac{2m}{M}\sqrt{1 + \beta^2\gamma^2} + \frac{m^2}{M^2}\right)^{-1}$$

Classical Scattering on Free Electrons

$$\frac{1}{\rho}\frac{dE}{dx} = -2\pi r_e^2\, m_e c^2\, \frac{Z_1^2}{\beta^2}\, N_A \frac{Z}{A} \ln \frac{2m_e c^2 \beta^2 \gamma^2 F}{I}$$

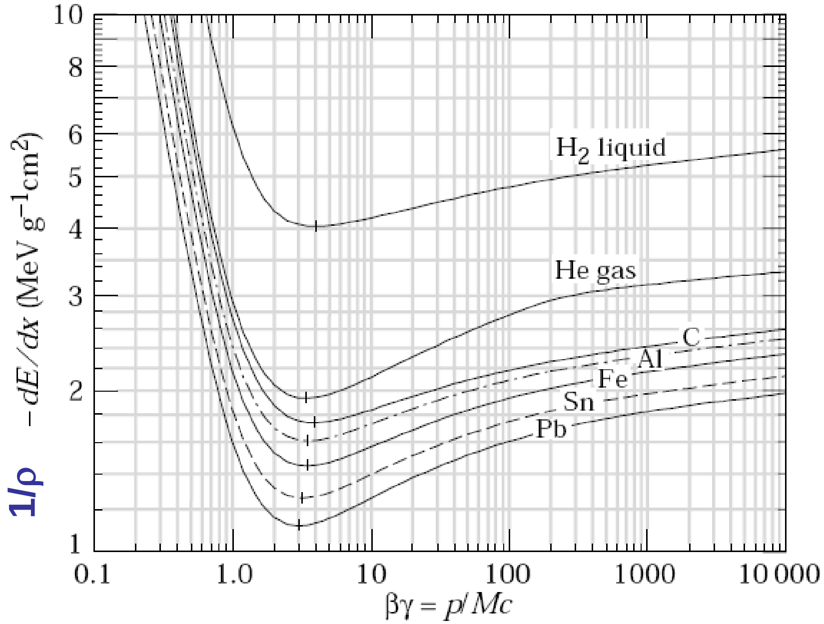

This formula is up to a factor 2 and the density effect identical to the precise QM derivation →

Bethe Bloch Formula

$$\frac{1}{\rho}\frac{dE}{dx} = \underline{-4}\pi r_e^2\, m_e c^2\, \frac{Z_1^2}{\beta^2}\, N_A \frac{Z}{A} \left[\ln \frac{2m_e c^2 \beta^2 \gamma^2 F}{I} - \beta^2 - \underline{\frac{\delta(\beta\gamma)}{2}}\right]$$

$$\delta(\beta\gamma) = \ln h\omega_p / I + \ln \beta\gamma - \frac{1}{2}$$

Electron Spin

Density effect. Medium is polarized Which reduces the log. rise.

Bethe Bloch Formula

$$\frac{1}{\rho}\frac{dE}{dx} = -4\pi r_e^2\, m_e c^2\, \frac{Z_1^2}{\beta^2}\, N_A \frac{Z}{A}\left[\ln\frac{2m_e c^2\beta^2\gamma^2 F}{I} - \beta^2 - \frac{\delta(\beta\gamma)}{2}\right]$$

Für Z>1, $I \approx 16Z^{0.9}$ eV

For Large $\beta\gamma$ the medium is being polarized by the strong transverse fields, which reduces the rise of the energy loss → density effect

At large Energy Transfers (delta electrons) the liberated electrons can leave the material.
In reality, E_{max} must be replaced by E_{cut} and the energy loss reaches a plateau (Fermi plateau).

Characteristics of the energy loss as a function of the particle velocity ($\beta\gamma$)

The specific Energy Loss $1/\rho\ dE/dx$

- first decreases as $1/\beta^2$
- increases with $\ln\gamma$ for $\beta = 1$
- is $\approx$ independent of M ($M \gg m_e$)
- is proportional to Z_1^2 of the incoming particle.
- is $\approx$ independent of the material ($Z/A \approx$ const)
- shows a plateau at large $\beta\gamma$ (>>100)
- $dE/dx \approx 1\text{-}2 \times \rho\ [g/cm^3]$ MeV/cm

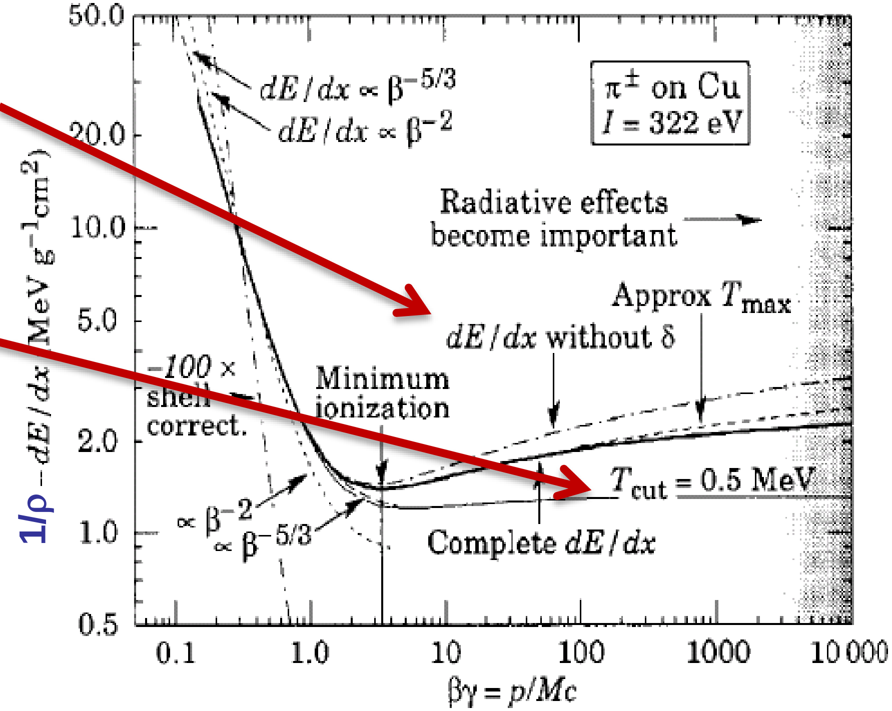

Small energy loss
→ Fast Particle

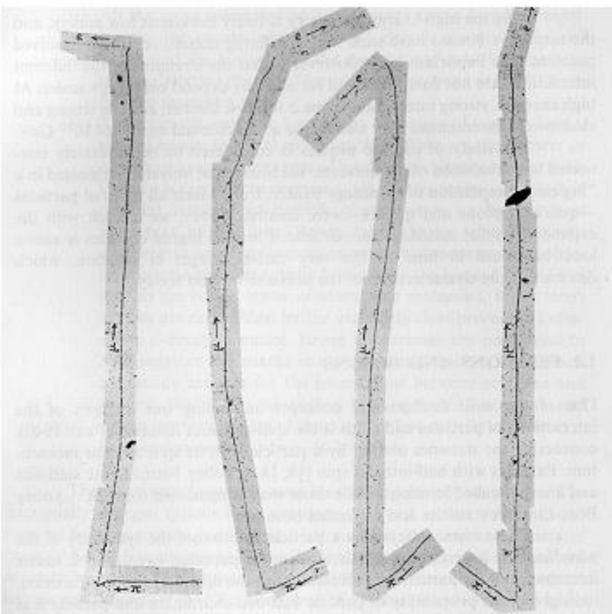

Discovery of muon and pion

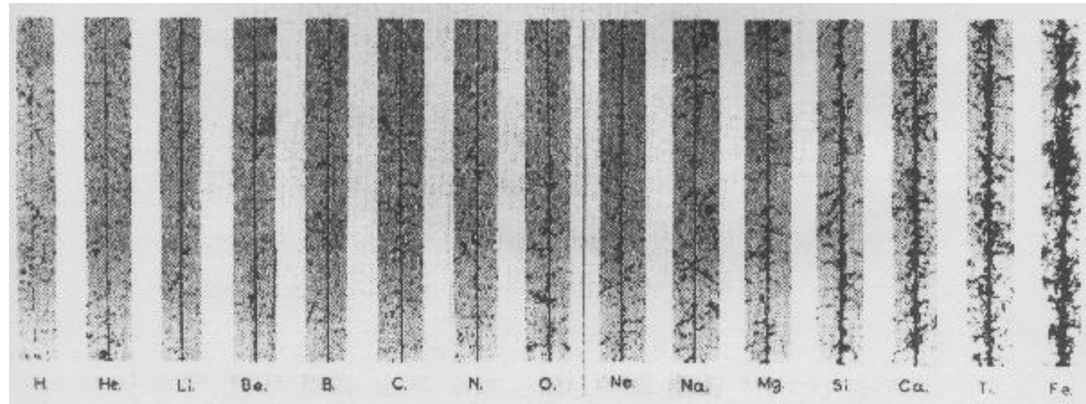

Cosmis rays: dE/dx α Z^2

Small energy loss
→ Fast particle

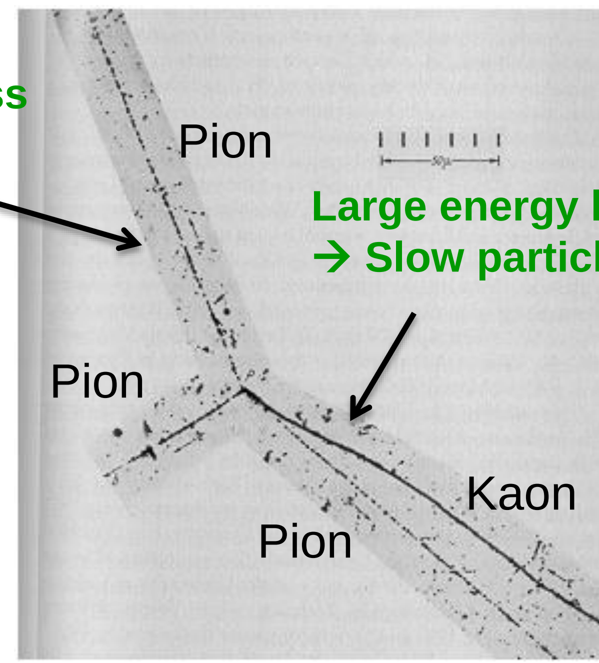

Bethe Bloch Formula

Bethe Bloch Formula, a few Numbers:

For $Z \approx 0.5\,A$
$1/\rho\; dE/dx \approx 1.4$ MeV cm^2/g for $\beta\gamma \approx 3$

Example :
Iron: Thickness = 100 cm; $\rho = 7.87$ g/cm^3
$dE \approx 1.4 * 100 * 7.87 = 1102$ MeV

→ A 1 GeV Muon can traverse 1m of Iron

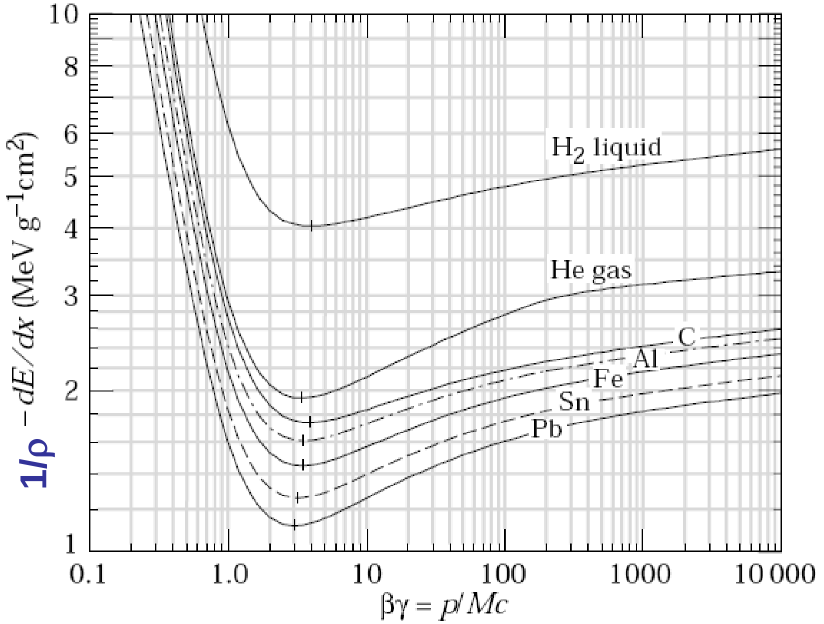

This number must be multiplied with ρ [g/cm^3] of the Material → dE/dx [MeV/cm]

Energy Loss as a Function of the Momentum

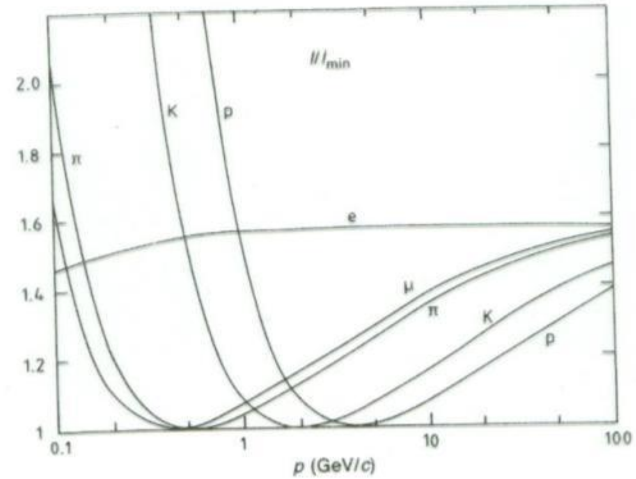

Energy loss depends on the particle velocity and is ≈ independent of the particle's mass M.

The energy loss as a function of particle Momentum P= Mcβγ IS however depending on the particle's mass

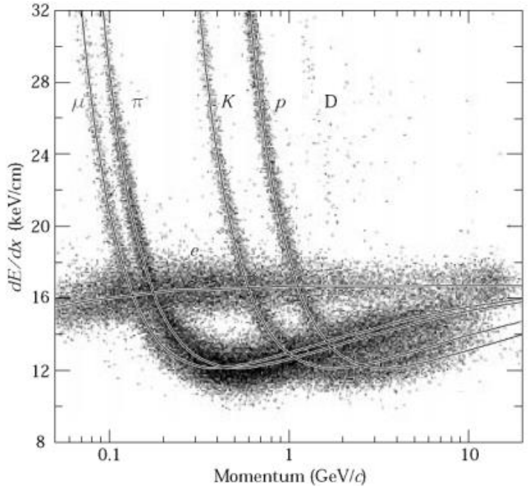

By measuring the particle momentum (deflection in the magnetic field) and measurement of the energy loss on can measure the particle mass

→ Particle Identification !

$$\frac{1}{\rho}\frac{dE}{dx} = -4\pi r_e^2\, m_e c^2\, Z_1^2 \frac{p^2 + M^2c^2}{p^2}\, N_A \frac{Z}{A}\left[\ln\frac{2m_ec^2F}{I}\frac{p^2}{M^2c^2} - \frac{p^2}{p^2+M^2c^2}\right]$$

Energy Loss as a Function of the Momentum

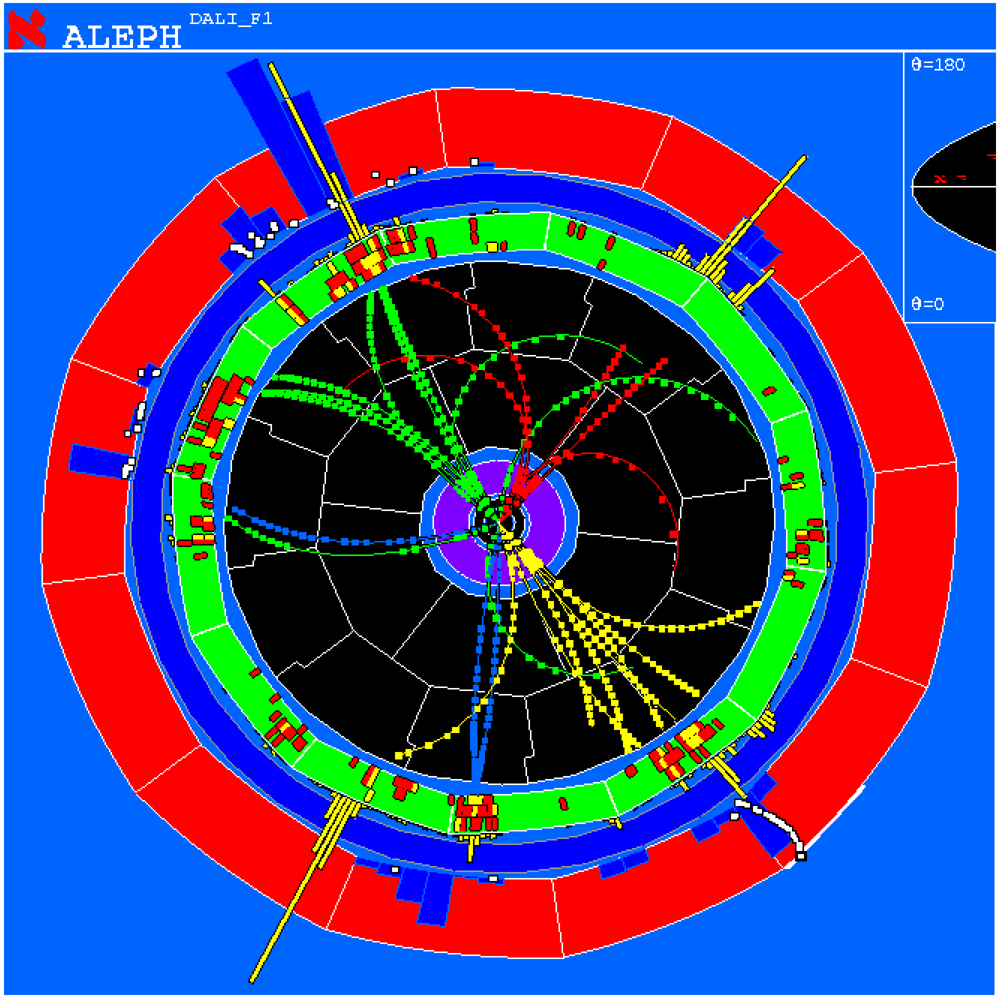

Measure momentum by curvature of the particle track.

Find dE/dx by measuring the deposited charge along the track.

→Particle ID

Range of Particles in Matter

Particle of mass M and kinetic Energy E_0 enters matter and looses energy until it comes to rest at distance R.

$$R(E_0) = \int_{E_0}^{0} \frac{-1}{dE/dx} dE$$

$$R(\beta_0\gamma_0) = \frac{Mc^2}{\rho} \frac{1}{Z_1^2} \frac{A}{Z} f(\beta_0\gamma_0)$$

$$\frac{\rho}{Mc^2} R(\beta_0\gamma_0) = \frac{1}{Z_1^2} \frac{A}{Z} f(\beta_0\gamma_0)$$

≈Independent of the material

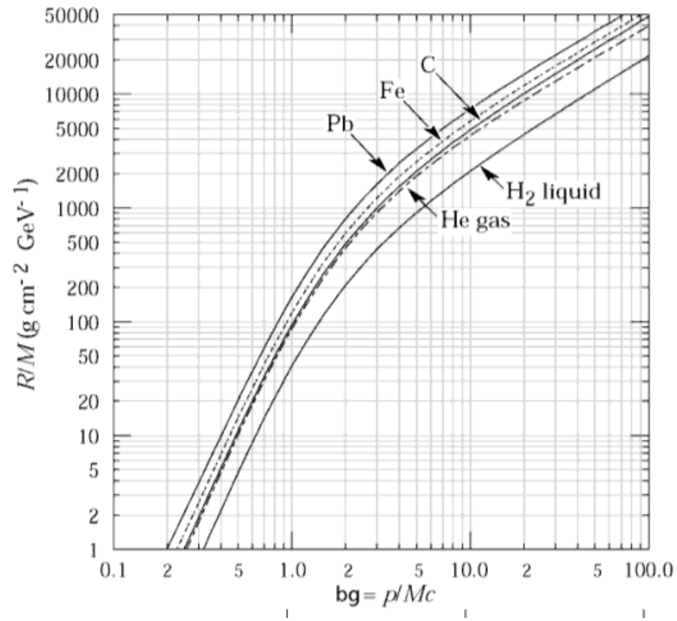

Bragg Peak:

For βγ>3 the energy loss is ≈ constant (Fermi Plateau)

If the energy of the particle falls below βγ=3 the energy loss rises as $1/\beta^2$

Towards the end of the track the energy loss is largest → Cancer Therapy.

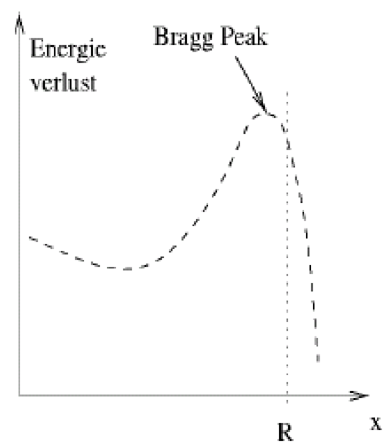

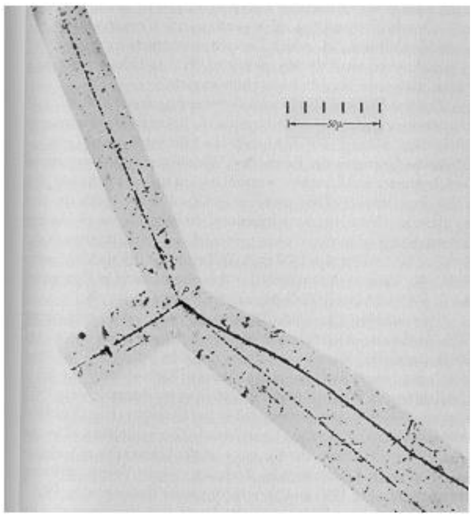

Range of Particles in Matter

Average Range:

Towards the end of the track the energy loss is largest → Bragg Peak → Cancer Therapy

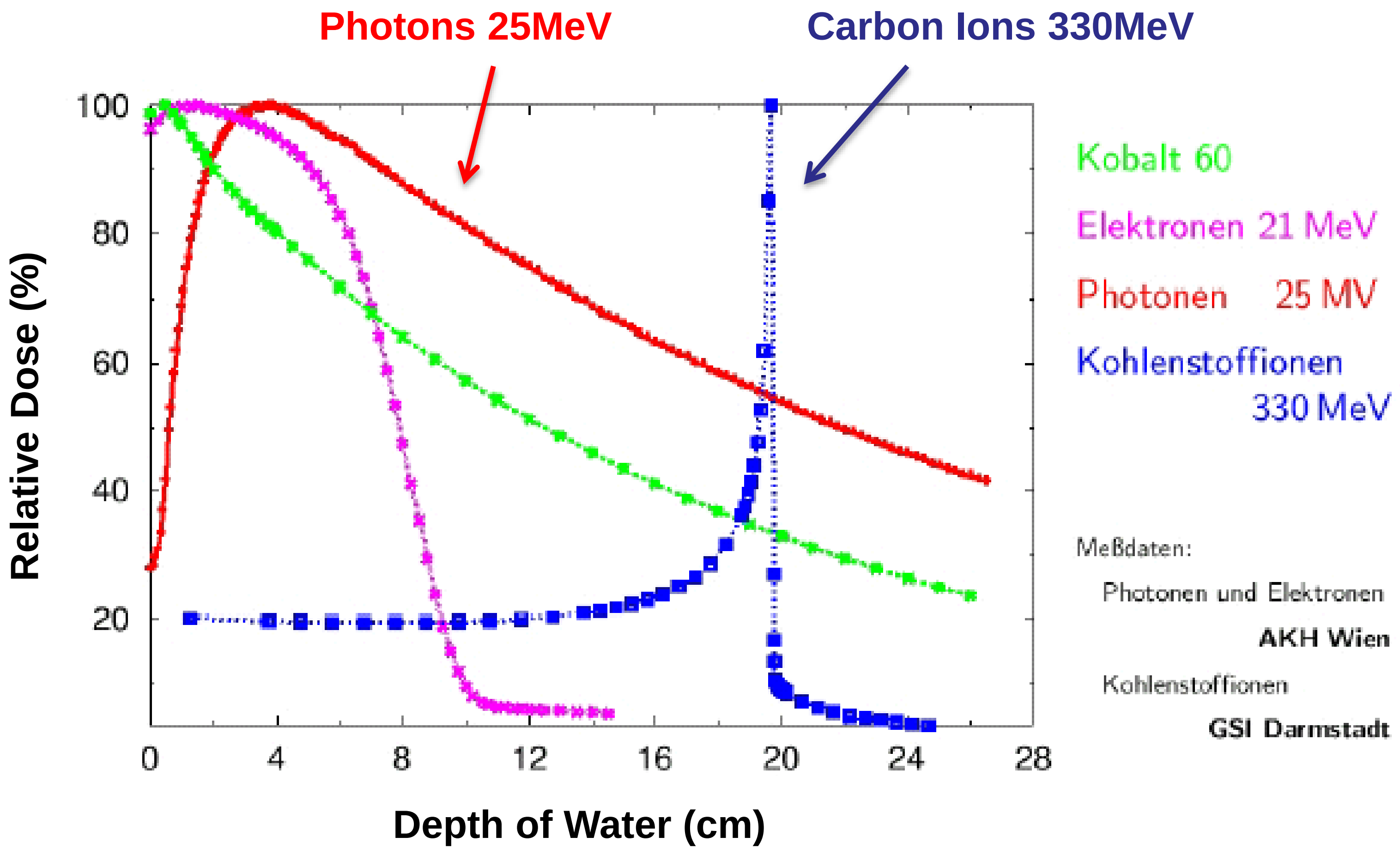

Search for Hidden Chambers in the Pyramids

The structure of the Second Pyramid of Giza is determined by cosmic-ray absorption.

Luis W. Alvarez, Jared A. Anderson, F. El Bedwei, James Burkhard, Ahmed Fakhry, Adib Girgis, Amr Goneid, Fikhry Hassan, Dennis Iverson, Gerald Lynch, Zenab Miligy, Ali Hilmy Moussa, Mohammed-Sharkawi, Lauren Yazolino

Fig. 2 (bottom right). Cross sections of (a) the Great Pyramid of Cheops and (b) the Pyramid of Chephren, showing the known chambers: (A) Smooth limestone cap, (B) the Belzoni Chamber, (C) Belzoni's entrance, (D) Howard-Vyse's entrance, un descending passageway, (F) ascending passageway, (G) underground chamber, (/-1) Grand Gallery, (I) King's Chamber, (J) Queen's Chamber, (K) center line of the pyramid.

6 FEBRUARY 1970

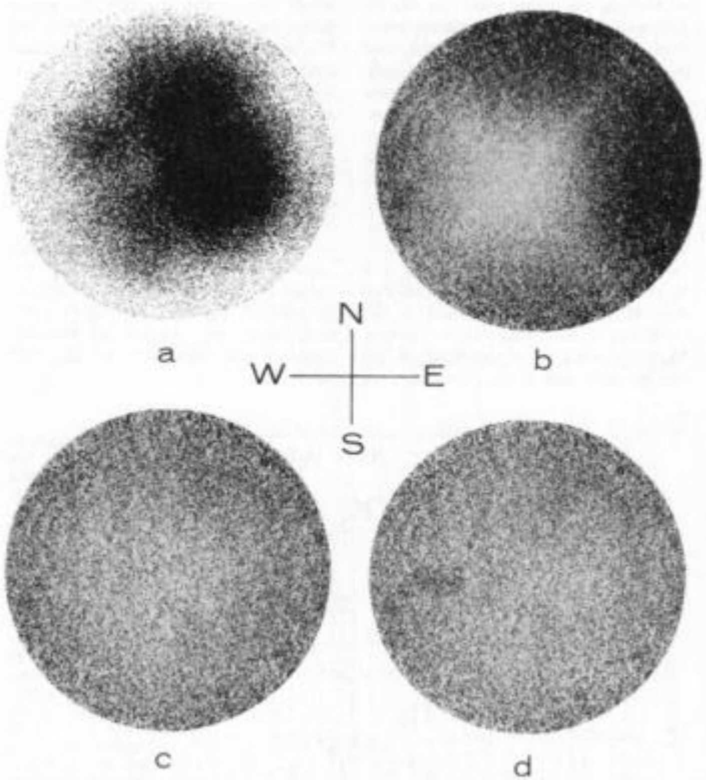

Fig. 13. Scatter plots showing the three stages in the combined analytic and visual analysis of the data and a plot with a simulated chamber. (a) Simulated "x-ray photograph" of uncorrected data. (b) Data corrected for the geometrical acceptance of the apparatus. (c) Data corrected for pyramid structure as well as geometrical acceptance. (d) Same as (c) but with simulated chamber, as in Fig. 12.

Luis Alvarez used the attenuation of muons to look for chambers in the Second Giza Pyramid → Muon Tomography

He proved that there are no chambers present.

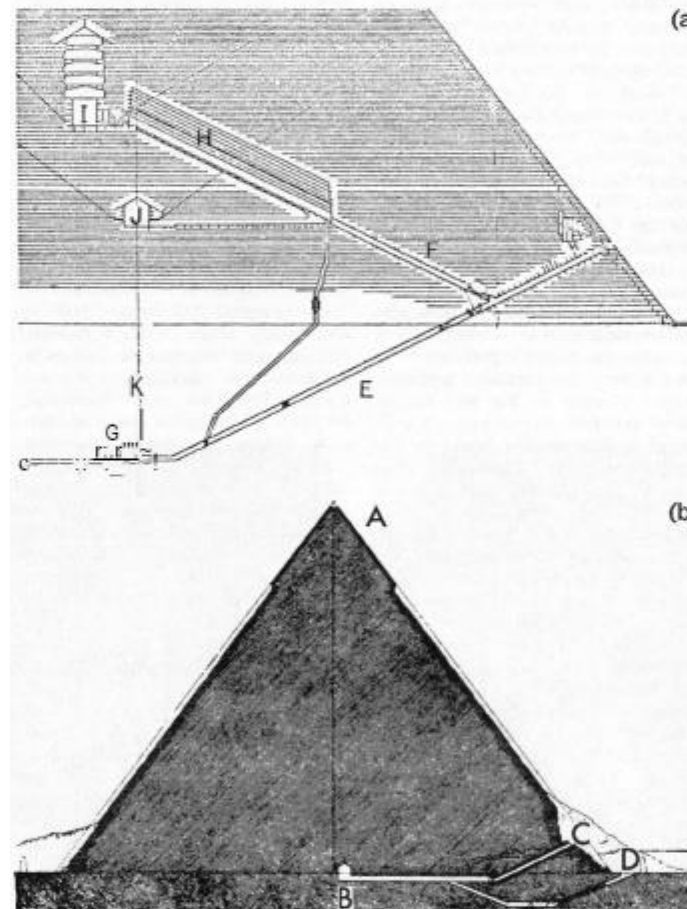

Intermezzo: Crossection

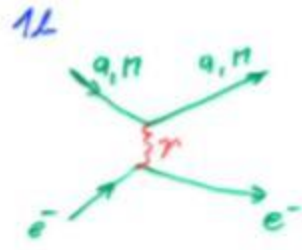

Crossection σ: Material with Atomic Mass A and density ρ contains n Atoms/cm^3

$$n[\mathrm{cm}^{-3}] = \frac{N_A[\mathrm{mol}^{-1}]\,\rho[\mathrm{g/cm}^3]}{A[\mathrm{g/mol}]} \qquad N_A = 6.022 \times 10^{23}\ \mathrm{mol}^{-1}$$

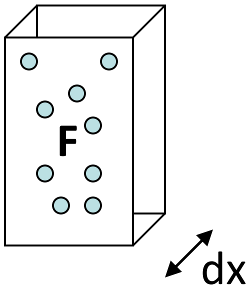

E.g. Atom (Sphere) with Radius R: Atomic Crossection $\sigma = R^2\pi$

A volume with surface F and thickness dx contains N=nFdx Atoms.
The total 'surface' of atoms in this volume is N σ.
The relative area is $p = N\sigma/F = N_A \rho\, \sigma / A\, dx$ =
Probability that an incoming particle hits an atom in dx.

What is the probability P that a particle hits an atom between distance x and x+dx ?
P = probability that the particle does NOT hit an atom in the m=x/dx material layers and that the particle DOES hit an atom in the mth layer

$$P(x)dx = (1-p)^m\,p \approx e^{-m}\,p = \exp\left(-\frac{N_A\rho\sigma}{A}x\right)\frac{N_A\rho\sigma}{A}dx = \frac{1}{\lambda}\exp\left(-\frac{x}{\lambda}\right)dx \qquad \lambda = \frac{A}{N_A\rho\sigma}$$

Mean free path $= \int_0^\infty x P(x)dx = \int_0^\infty \frac{x}{\lambda} e^{-\frac{x}{\lambda}}dx = \lambda$

Average number of collisions/cm $= \frac{1}{\lambda} = \frac{N_A\rho\sigma}{A}$

Intermezzo: Differential Crossection

Differential Crossection: $\frac{d\sigma(E,E')}{dE'}$

→ **Crossection for an incoming particle of energy E to lose an energy between E' and E'+dE'**

Total Crossection: $\sigma(E) = \int \frac{d\sigma(E,E')}{dE'} dE'$

Probability P(E) that an incoming particle of Energy E loses an energy between E' and E'+dE' in a collision:

$$P(E,E')dE' = \frac{1}{\sigma(E)} \frac{d\sigma(E,E')}{dE'} dE'$$

Average number of collisions/cm causing an energy loss between E' and E'+dE' $= \frac{N_A \rho}{A} \frac{d\sigma(E,E')}{dE'}$

Average energy loss/cm: $\frac{dE}{dx} = -\frac{N_A \rho}{A} \int E' \frac{d\sigma(E,E')}{dE'} dE'$

Fluctuation of Energy Loss

Up to now we have calculated the average energy loss. The energy loss is however a statistical process and will therefore fluctuate from event to event.

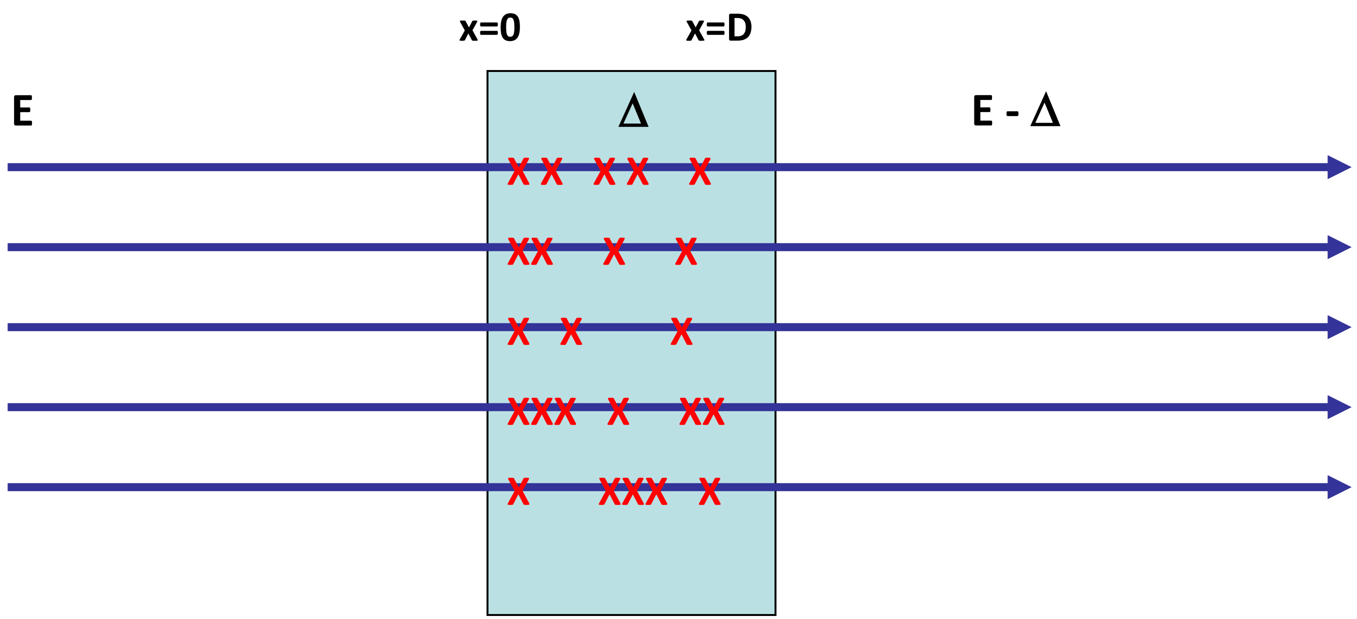

P(Δ) = ? Probability that a particle loses an energy Δ when traversing a material of thickness D

We have see earlier that the probability of an interaction ocuring between distance x and x+dx is exponentially distributed

$$P(x)dx = \frac{1}{\lambda}\exp\left(-\frac{x}{\lambda}\right)dx \qquad \lambda = \frac{A}{N_A \rho \sigma}$$

Probability for n Interactions in D

We first calculate the probability to find n interactions in D, knowing that the probability to find a distance x between two interactions is P(x)dx = 1/ λ exp(-x/λ) dx   with $\lambda = A/ N_A \rho \sigma$

Probability to have no interaction between 0 und D:

$$P(x > D) = \int_D^\infty P(x_1)dx_1 = e^{-\frac{D}{\lambda}}$$

Probability to have one interaction at x_1 and no other interaction:

$$P(x_1, x_2 > D) = \int_D^\infty P(x_1)P(x_2 - x_1)dx_2 = \frac{1}{\lambda}e^{-\frac{D}{\lambda}}$$

Probability to have one interaction independently of x_1:

$$\int_0^D P(x_1, x_2 > D) = \frac{D}{\lambda}e^{-\frac{D}{\lambda}}$$

Probability to have the first interaction at x_1, the second at x_2 .... the n^{th} a
x_n and no other interaction:

$$P(x_1, x_2 ... x_n > D) = \int_D^\infty P(x_1)P(x_2 - x_1)...P(x_n - x_{n-1})dx_n = \frac{1}{\lambda^n}e^{-\frac{D}{\lambda}}$$

Probability for n interactions independently of $x_1, x_2 ... x_n$

$$\int_0^D \int_0^{x_{n-1}} \int_0^{x_{n-1}} ... \int_0^{x_1} P(x_1, x_2 ..., x_n > D)dx_1 ... dx_{n-1} = \frac{1}{n!}\left(\frac{D}{\lambda}\right)^n e^{-\frac{D}{\lambda}}$$

Probability for n Interactions in D

For an interaction with a mean free path of λ , the probability for n interactions on a distance D is given by

$$P(n) = \frac{1}{n!}\left(\frac{D}{\lambda}\right)^n e^{-\frac{D}{\lambda}} = \frac{\overline{n}^n}{n!}e^{-\overline{n}} \qquad \overline{n} = \frac{D}{\lambda} \qquad \lambda = \frac{A}{N_A \rho \sigma}$$

→Poisson Distribution !

<u>If the distance between interactions is exponentially distributed with an mean free path of λ→ the number of interactions on a distance D is Poisson distributed with an average of n̄=D/λ.</u>

How do we find the energy loss distribution ?
If f(E) is the probability to lose the energy E' in an interaction, the probability p(E) to lose an energy E over the distance D ?

$$f(E) = \frac{1}{\sigma}\frac{d\sigma}{dE}$$

$$p(E) = P(1)f(E) + P(2)\int_0^E f(E-E')f(E')dE' + P(3)\int_0^E\int_0^{E'} f(E-E'-E'')f(E'')f(E')dE''dE' + \ldots$$

$$F(s) = \mathcal{L}\left[f(E)\right] = \int_0^\infty f(E)e^{-sE}dE$$

$$\mathcal{L}\left[p(E)\right] = P(1)F(s)+P(2)F(s)^2+P(3)F(s)^3+\ldots = \sum_{n=1}^{\infty} P(n)F(s)^n = \sum_{n=1}^{\infty}\frac{\overline{n}^n F^n}{n!}e^{-\overline{n}} = e^{\overline{n}(F(s)-1)}-1 \approx e^{\overline{n}(F(s)-1)}$$

$$p(E) = \mathcal{L}^{-1}\left[e^{\overline{n}(F(s)-1)}\right] = \frac{1}{2\pi i}\int_{\sigma-i\infty}^{\sigma+i\infty} e^{\overline{n}(F(s)-1)+sE}ds$$

Fluctuations of the Energy Loss

Probability f(E) for loosing energy between E' and E'+dE' in a single interaction is given by the differential crossection dσ (E,E')/dE'/ σ(E) which is given by the Rutherford crossection at large energy transfers

dσ (E,E')/dE'/ σ(E)

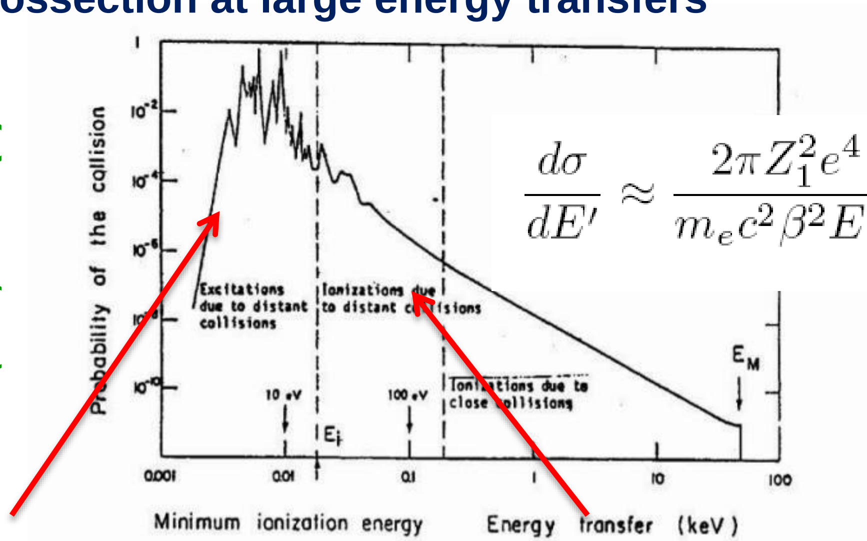

$$\frac{d\sigma}{dE'} \approx \frac{2\pi Z_1^2 e^4}{m_e c^2 \beta^2 E'^2}$$

Excitation and ionization

Scattering on free electrons

$$p(x) = \frac{1}{2\pi i}\int_{c-i\infty}^{c+i\infty} \exp(s\log s + xs)\,ds. = \frac{1}{\pi}\int_0^{\infty} \exp(-t\log t - xt)\sin(\pi t)\,dt.$$

$$x = \frac{E}{\overline{n}\epsilon} + C_\gamma - 1 - \ln\overline{n} \qquad \overline{n} = \frac{N_A \rho Z_2 k D}{A\epsilon}$$

$$\ln\epsilon = \ln\frac{I^2}{E_{max}} + 2\beta^2$$

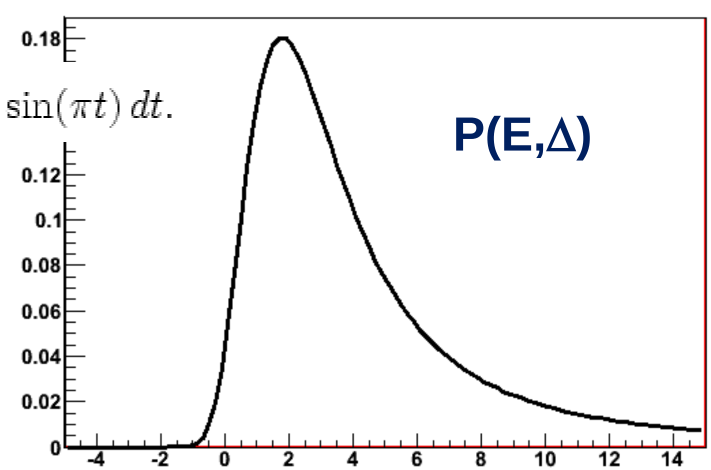

Landau Distribution

P(Δ): Probability for energy loss Δ in matter of thickness D.

Landau distribution is very asymmetric.

Average and most probable energy loss must be distinguished !

Measured Energy Loss is usually smaller that the real energy loss:

3 GeV Pion: E'_{max} = 450MeV → A 450 MeV Electron usually leaves the detector.

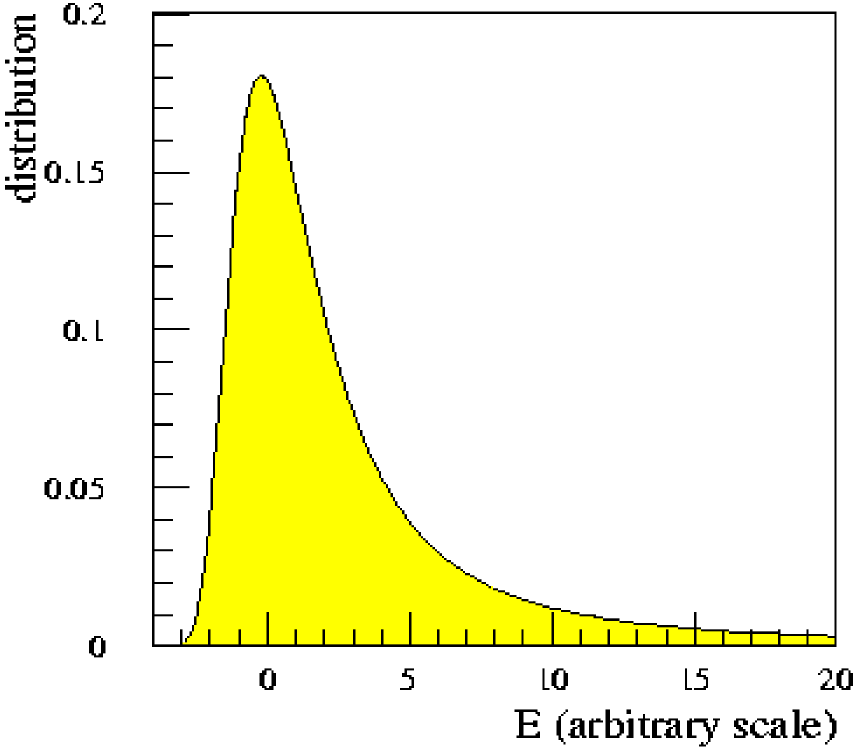

Landau Distribution

LANDAU DISTRIBUTION OF ENERGY LOSS:

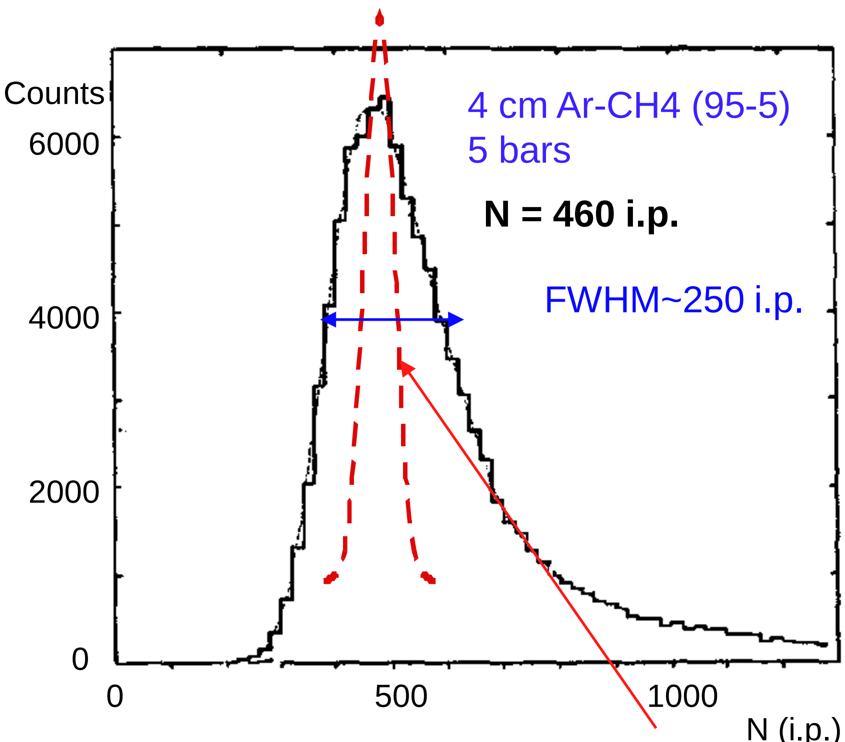

For a Gaussian distribution: **σ_N ~ 21 i.p.**
FWHM ~ 50 i.p.

PARTICLE IDENTIFICATION
Requires statistical analysis of hundreds of samples

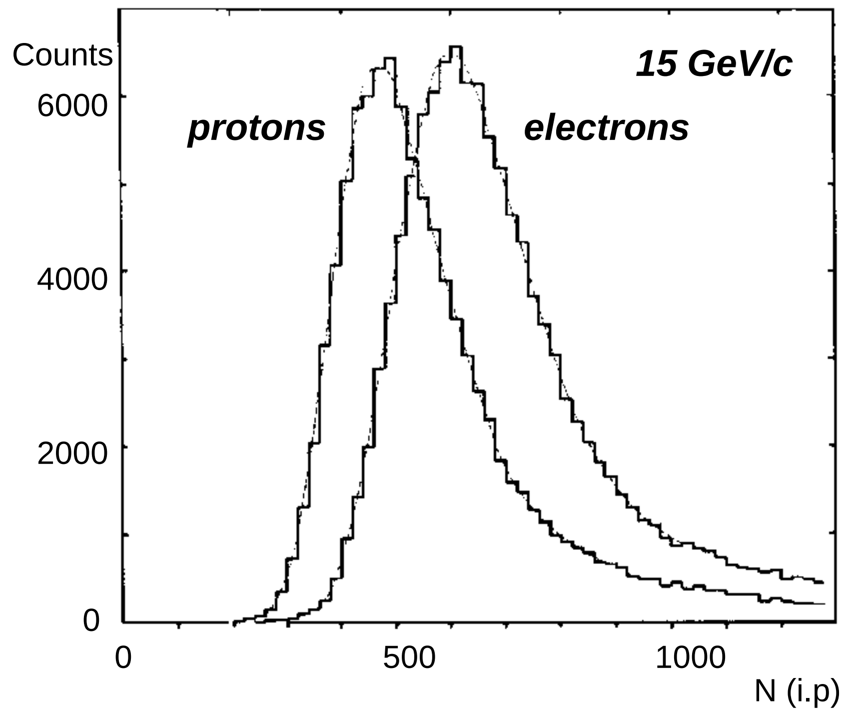

I. Lehraus et al, Phys. Scripta 23(1981)727

Particle Identification

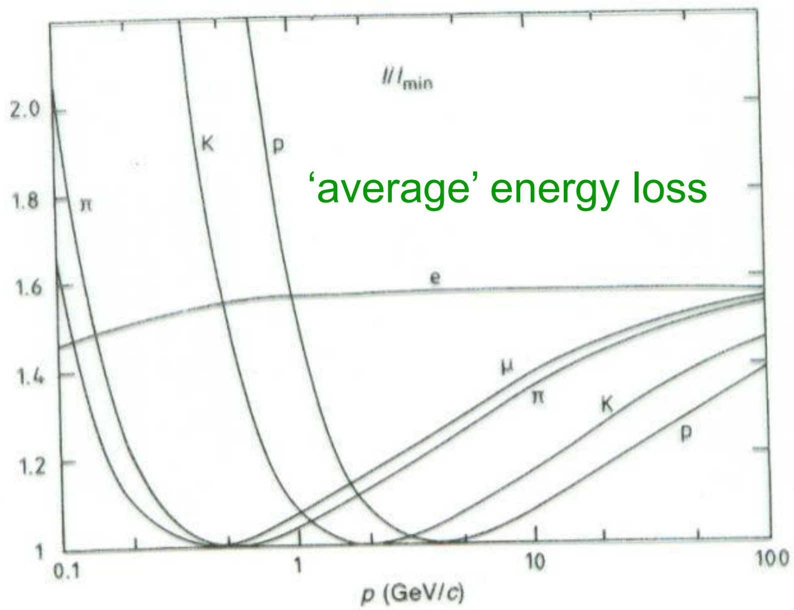

Measured energy loss

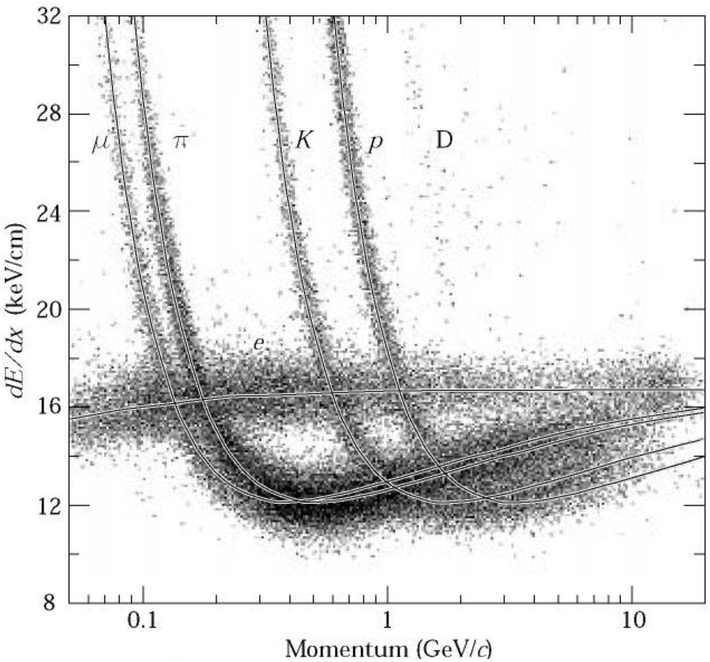

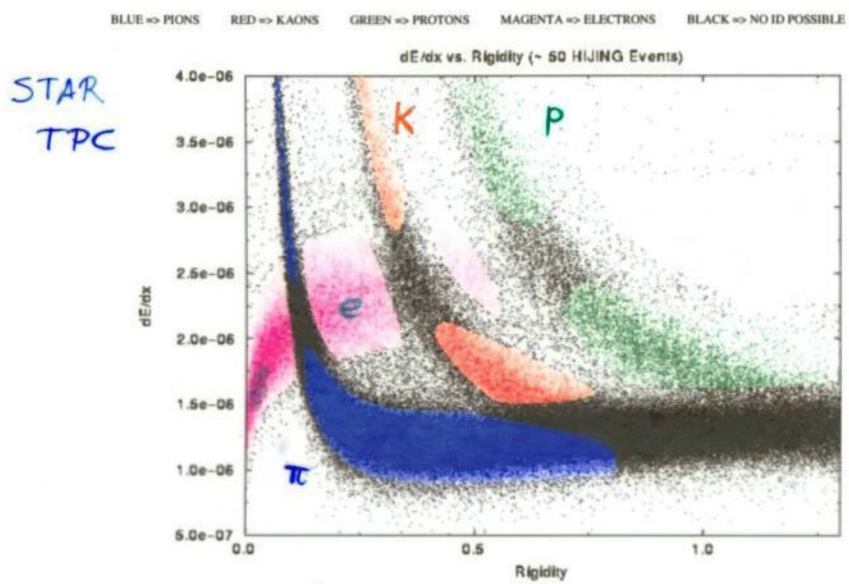

In certain momentum ranges, particles can be identified by measuring the energy loss.

Bremsstrahlung

A charged particle of mass M and charge $q=Z_1e$ is deflected by a nucleus of charge Ze which is partially 'shielded' by the electrons. During this deflection the charge is 'accelerated' and it therefore radiated → Bremsstrahlung.

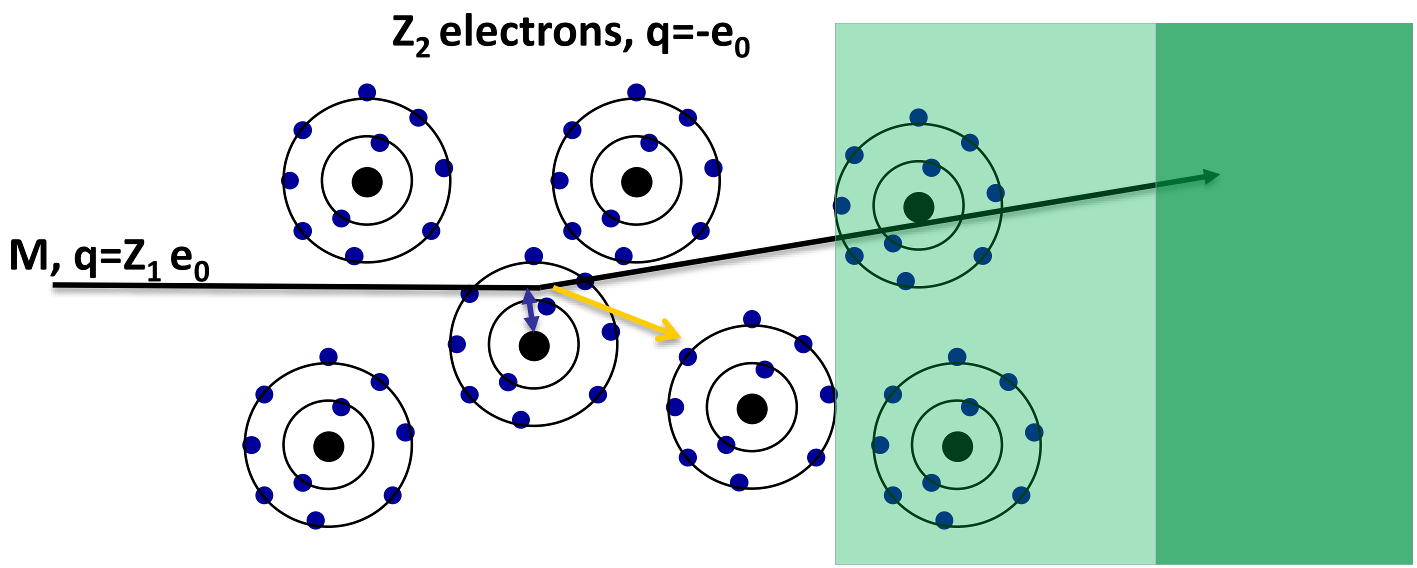

Bremsstrahlung, Classical

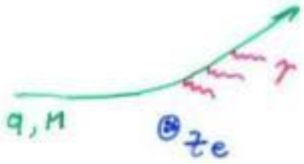

$q = Z_1 \cdot e$

$$\frac{d\sigma}{d\Omega} = \left(\frac{2 Z_1 Z_2 e^2}{4\pi\varepsilon_0\, p \cdot v}\right)^2 \frac{1}{(2\sin\frac{\theta}{2})^4} \qquad p = Mv\gamma$$

"Rutherford Scattering"

Written in Terms of Momentum Transfer $Q^2 = 2p^2(1-\cos\theta)$

$$\frac{d\sigma}{dQ} = 8\pi\left(\frac{Z_1 Z_2 e^2}{4\pi\varepsilon_0 \beta c}\right)^2 \cdot \frac{1}{Q^3}$$

$Q = |\vec{p} - \vec{p}\,'|$

→ From Maxwell's Eq (Jackson)

$$\lim_{\omega \to 0} \frac{dI}{d\omega} \sim \frac{2}{3\pi} \frac{Z_1^2 e^2}{M^2 c^3} \frac{1}{4\pi\varepsilon_0} Q^2$$ Radiated Energy between $\omega, \omega + d\omega$

$$\frac{dE}{dx} = \frac{N_A \rho}{A} \cdot \int_0^{\omega_{max}} d\omega \int_{Q_{min}}^{Q_{max}} dQ \frac{dI}{d\omega} \cdot \frac{d\sigma}{dQ}, \quad \omega_{max} = \frac{E}{\hbar}$$

$$\frac{dE}{dx} = \frac{N_A \rho}{A} \cdot \frac{16}{3} \alpha \cdot Z^2 \cdot \left(\frac{Z_1^2 e^2}{4\pi\varepsilon_0 M c^2}\right)^2 \cdot E \cdot \ln \frac{Q_{max}}{Q_{min}}$$

$$\alpha = \frac{e^2}{4\pi\varepsilon_0 \hbar c} \sim \frac{1}{137}$$

A charged particle of mass M and charge $q=Z_1e$ is deflected by a nucleus of Charge Ze.

Because of the acceleration the particle radiated EM waves → energy loss.

Coulomb-Scattering (Rutherford Scattering) describes the deflection of the particle.

Maxwell's Equations describe the radiated energy for a given momentum transfer.

→ dE/dx

Bremsstrahlung, QM

2b Bremsstrahlung QM.

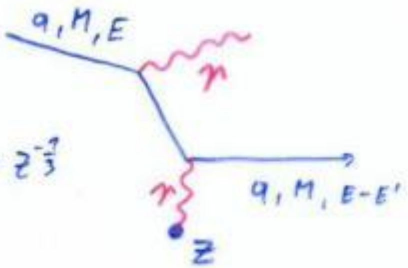

$q = Z_1 e, \quad E + Mc^2 \gg 137\, Mc^2 Z^{-\frac{1}{3}}$

→ highly Relativistic:

$$\frac{d\sigma(E,E')}{dE'} = 4\alpha Z^2 Z_1^4 \left(\frac{1}{4\pi\varepsilon_0}\frac{e^2}{Mc^2}\right)^2 \frac{1}{E'} F(E,E')$$

$$F(E,E') = \left[1 + \left(1-\frac{E'}{E+Mc^2}\right)^2 - \frac{2}{3}\left(1-\frac{E'}{E+Mc^2}\right)\right] \ln 183 Z^{-\frac{1}{3}} + \frac{1}{9}\left(1-\frac{E'}{E+Mc^2}\right)$$

$$\frac{dE}{dx} = -\frac{N_A \rho}{A}\int_0^E E' \frac{d\sigma}{dE'} dE' \approx 4\alpha Z^2 Z_1^4 \left(\frac{1}{4\pi\varepsilon_0}\frac{e^2}{Mc^2}\right)^2 E \left[\ln 183 Z^{-\frac{1}{3}} + \frac{1}{18}\right]$$

$$\underline{\underline{\frac{dE}{dx} = -\frac{N_A \rho}{A} 4\alpha Z^2 Z_1^4 \left(\frac{1}{4\pi\varepsilon_0}\frac{e^2}{Mc^2}\right)^2 E \ln\left(183 Z^{-\frac{1}{3}}\right)}}$$

$$E(x) = E_0 e^{-\frac{x}{X_0}} \qquad X_0 = \frac{A}{4\alpha N_A \rho Z^2 \left(\frac{1}{4\pi\varepsilon_0}\frac{e^2}{Mc^2}\right)^2 \ln 183 Z^{-\frac{1}{3}}}$$

X_0 ... Radiation length

Proportional to Z^2/A of the Material.

Proportional to Z_1^4 of the incoming particle.

Proportional to ρ of the material.

Proportional $1/M^2$ of the incoming particle.

Proportional to the Energy of the Incoming particle →

$E(x)=\mathrm{Exp}(-x/X_0)$ – 'Radiation Length'

$X_0 \propto M^2 A/ (\rho\, Z_1^4\, Z^2)$

X_0: Distance where the Energy E_0 of the incoming particle decreases $E_0 \mathrm{Exp}(-1)=0.37 E_0$.

Critical Energy

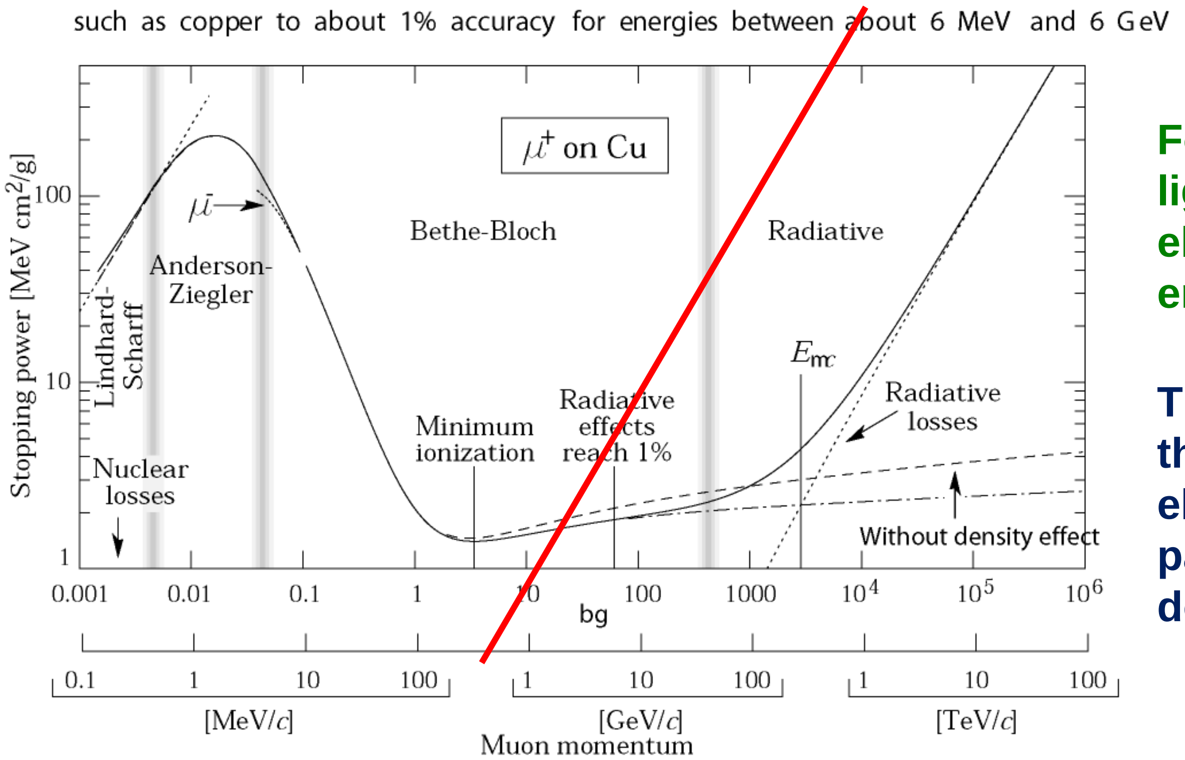

Electron Momentum 5 50 500 MeV/c

For the muon, the second lightest particle after the electron, the critical energy is at 400GeV.

The EM Bremsstrahlung is therefore only relevant for electrons at energies of past and present detectors.

Critical Energy: If dE/dx (Ionization) = dE/dx (Bremsstrahlung)

Myon in Copper: p ≈ 400GeV
Electron in Copper: p ≈ 20MeV

Pair Production, QM

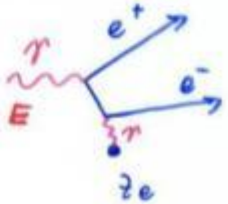

γ + Nucl. → $e^+ + e^-$ + Nucl

The Diagram is very similar to Bremsstrahlung

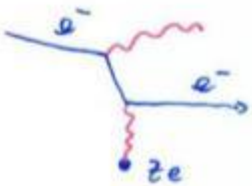

e^- + Nucl → γ + e^- + Nucl

'Crossing Symmetry: bring particle to the other side and make it the anti particle' → 'some' correction ...

$$\frac{d\sigma(E,E')}{dE'} = 4\alpha Z^2 r_e^2 \frac{1}{E}\cdot G(E,E') \qquad E \gg 137 m_e c^2 Z^{-\frac{1}{3}}$$

$$G(E,E') = \left[\left(\frac{E'+m_ec^2}{E}\right)^2 + \left(1-\frac{E'+m_ec^2}{E}\right)^2 + \frac{2}{3}\frac{E'+m_ec^2}{E}\left(1-\frac{E'+m_ec^2}{E}\right)\ln Z^{-\frac{1}{3}} - \frac{1}{9}\frac{E'+m_ec^2}{E}\left(1-\frac{E'+m_ec^2}{E}\right)\right]$$

$$\sigma = \int_0^{E-2m_ec^2} \frac{d\sigma}{dE'}dE' = 4\alpha Z^2 r_e^2 \cdot \frac{7}{9}\ln 183 Z^{-\frac{1}{3}}$$

$$P(x) = \frac{1}{\lambda}e^{-\frac{x}{\lambda}} \qquad \lambda = \frac{A}{\rho N_A \sigma} = \frac{9}{7}X_0$$

↳ Probability that Photon converts to e^+e^- after a distance x.

For $E\gamma \gg m_ec^2 = 0.5$MeV : $\lambda = 9/7X_0$

Average distance a high energy photon has to travel before it converts into an $e^+ e^-$ pair is equal to 9/7 of the distance that a high energy electron has to travel before reducing it's energy from E_0 to E_0*Exp(-1) by photon radiation.

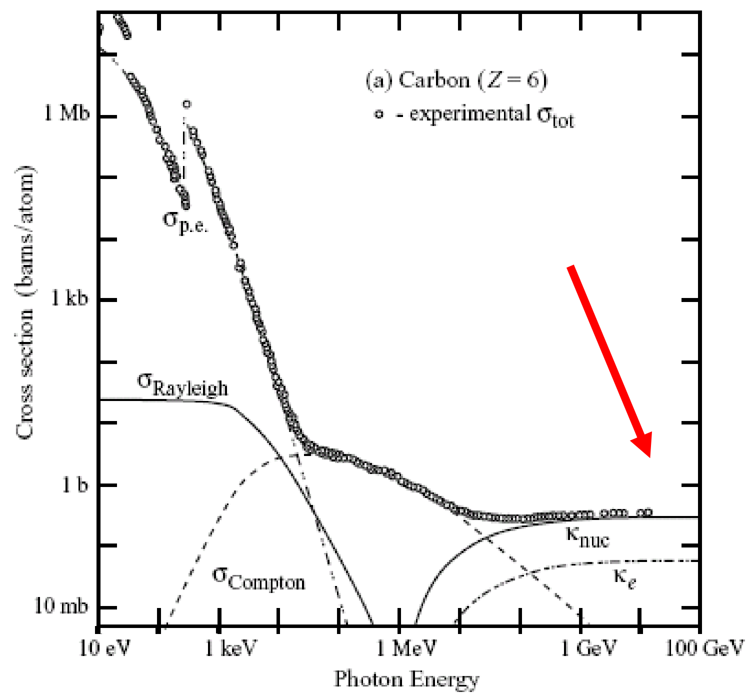

Bremsstrahlung + Pair Production → EM Shower

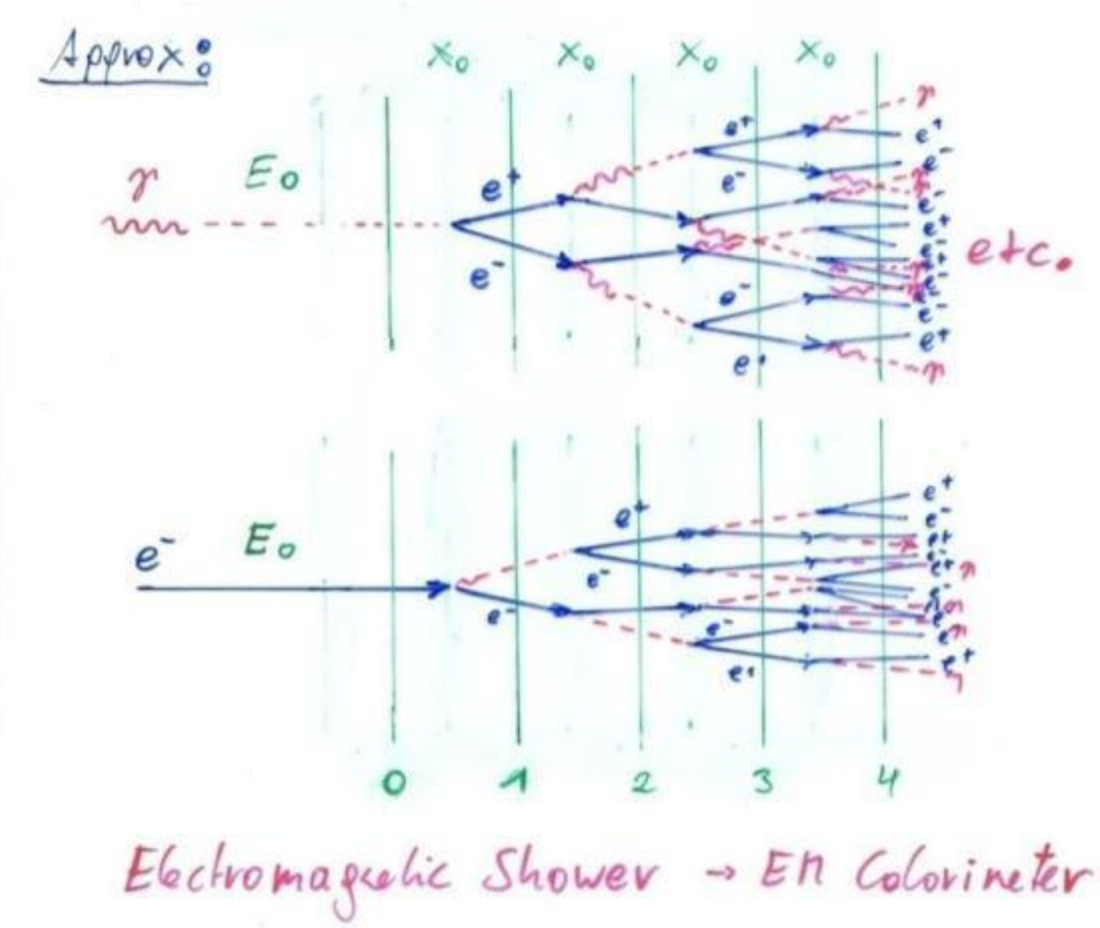

Multiple Scattering

Statistical (quite complex) analysis of multiple collisions gives:

Probability that a particle is defected by an angle θ after travelling a distance x in the material is given by a Gaussian distribution with sigma of:

$$\Theta_0 = \frac{0.0136}{\beta c p[\mathrm{GeV/c}]} Z_1 \sqrt{\frac{x}{X_0}}$$

X_0 ... Radiation length of the material
Z_1 ... Charge of the particle
p ... Momentum of the particle

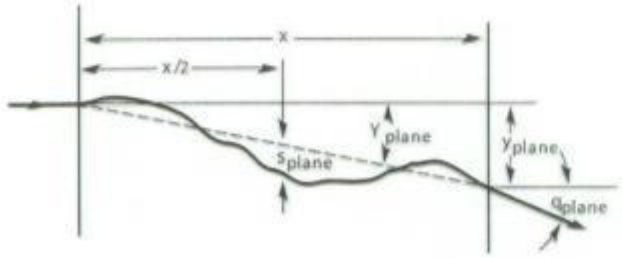

Multiple Scattering

Magnetic Spectrometer: A charged particle describes a circle in a magnetic field:

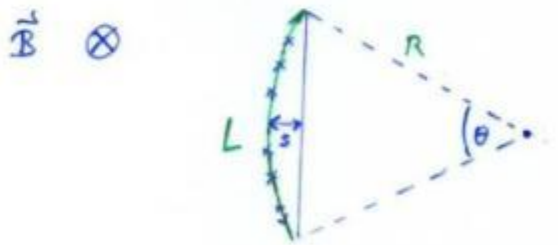

$$p = q \cdot R \cdot B$$

$$p\left[\frac{GeV}{c}\right] = 0.3\, R[m]\, B[T]$$

$$L = R \cdot \theta$$

$$s = R\left(1 - \cos\frac{\theta}{2}\right) \sim R\frac{\theta^2}{8} = \frac{L^2}{8R} \rightarrow R = \frac{L^2}{8s}$$

$$\Delta p = 0.3\, B\, \Delta R = 0.3\, B\, \frac{L^2}{8s^2}\, \Delta s$$

$$\Delta s = \frac{\sigma_x}{\sqrt{N}}$$ σ_x ... point resolution, N ... Measurement Points

$$\boxed{\frac{\Delta p}{p} = \frac{\Delta s}{s} = \frac{\sigma_x[m]}{\sqrt{N}} \cdot \frac{3.3 \cdot 8\, p\left[\frac{GeV}{c}\right]}{B[T] \cdot L^2[m^2]}}$$

E.g.: $p = 10\,\frac{GeV}{c}$, $B = 1T$, $L = 1m$, $\sigma = 200\mu m$, $N = 25$

$$\frac{\Delta p}{p} = 0.01 \rightarrow 1\%$$

Limit → Multiple Scattering

Multiple Scattering

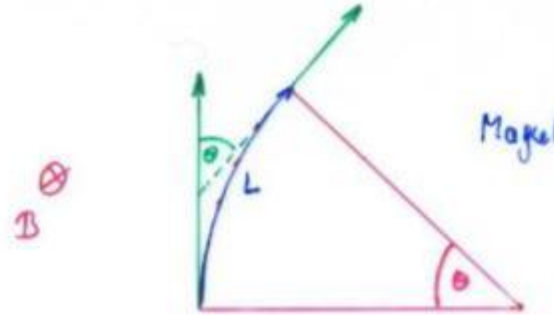

Magnetic Deflection

$$p\left[\frac{\mathrm{GeV}}{c}\right] = 0.3\, R[\mathrm{m}]\, B[\mathrm{T}]$$

$$\theta = \frac{L}{R} = \frac{L}{p} \cdot 0.3\, B$$

$$\frac{\Delta p}{p} = \frac{\Delta\theta}{\theta} = \frac{\theta_0}{\theta} \sim \frac{0.05}{\beta B[\mathrm{T}] L[\mathrm{m}]} \cdot \sqrt{\frac{L}{X_0}}$$

→ Independent of p

$$\left.\frac{\Delta p}{p}\right|_{tot} = \sqrt{\left(\left.\frac{\Delta p}{p}\right|_{sag}\right)^2 + \left(\left.\frac{\Delta p}{p}\right|_{ms}\right)^2}$$

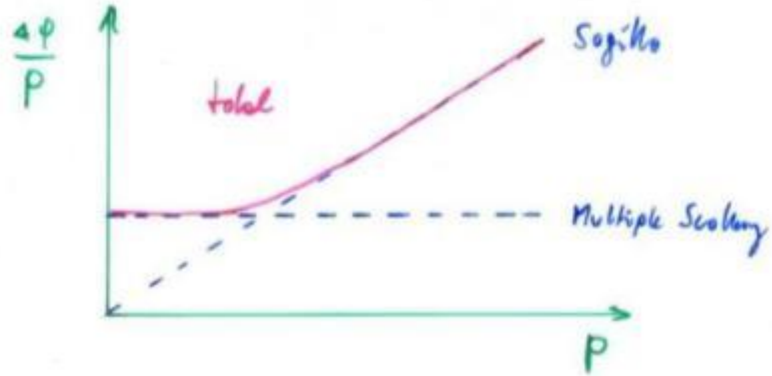

Multiple Scattering

ATLAS Muon Spectrometer:
N=3, sig=50um, P=1TeV,
L=5m, B=0.4T

Δp/p ~ 8% for the most energetic muons at LHC

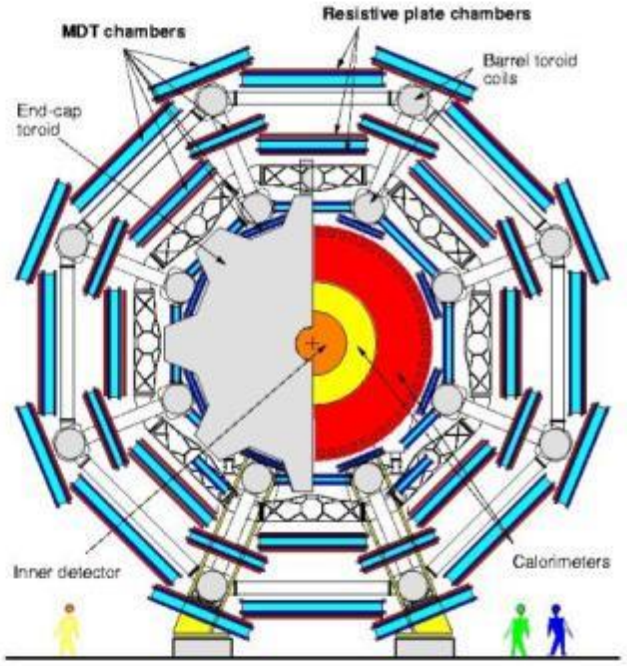

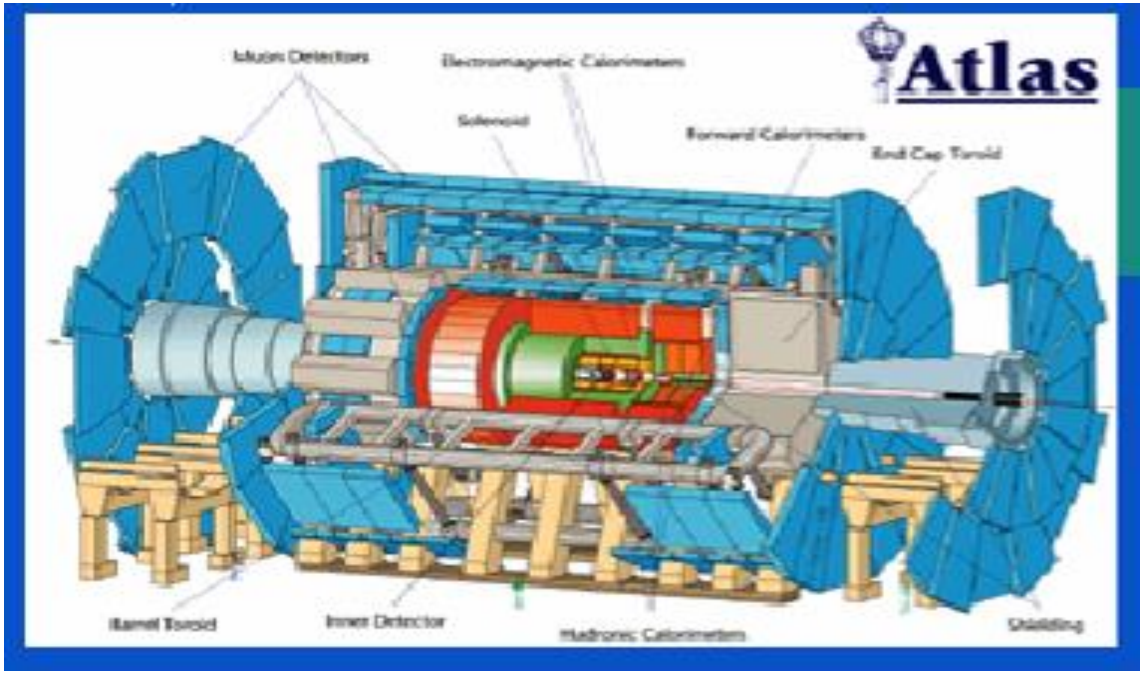

Cherenkov Radiation

If we describe the passage of a charged particle through material of dielectric permittivity ♏ (using Maxwell’s equations) the differential energy crossection is >0 if the velocity of the particle is larger than the velocity of light in the medium is

$$\frac{d\sigma}{dE} = \frac{\alpha}{\beta^2\pi}\,\frac{A}{N_A\rho Z_2\hbar c}\left(\beta^2 - \frac{1}{\epsilon_1}\right) \quad \rightarrow \quad \frac{N_A\rho Z_2}{A}\,\frac{d\sigma}{d\omega}\,\frac{d\omega}{dE} = \frac{\alpha}{c}\left(1 - \frac{1}{\beta^2 n^2}\right) \qquad n = \sqrt{\epsilon_1} \qquad E = \hbar\omega$$

$$\frac{dE}{dx\,d\omega}\,\frac{1}{\hbar} = \frac{\alpha}{c}\left(1 - \frac{1}{\beta^2 n^2}\right) \quad \rightarrow \quad \frac{dN}{dx\,d\lambda} = \frac{2\pi\alpha}{\lambda^2}\left(1 - \frac{1}{\beta^2 n^2}\right) \qquad \omega = \frac{2\pi c}{\lambda}$$

N is the number of Cherenkov Photons emitted per cm of material. The expression is in addition proportional to Z_1^2 of the incoming particle.

The radiation is emitted at the characteristic angle ❑$_c$, that is related to the refractive index n and the particle velocity by

$$\cos\Theta_c = \frac{1}{n\beta}$$

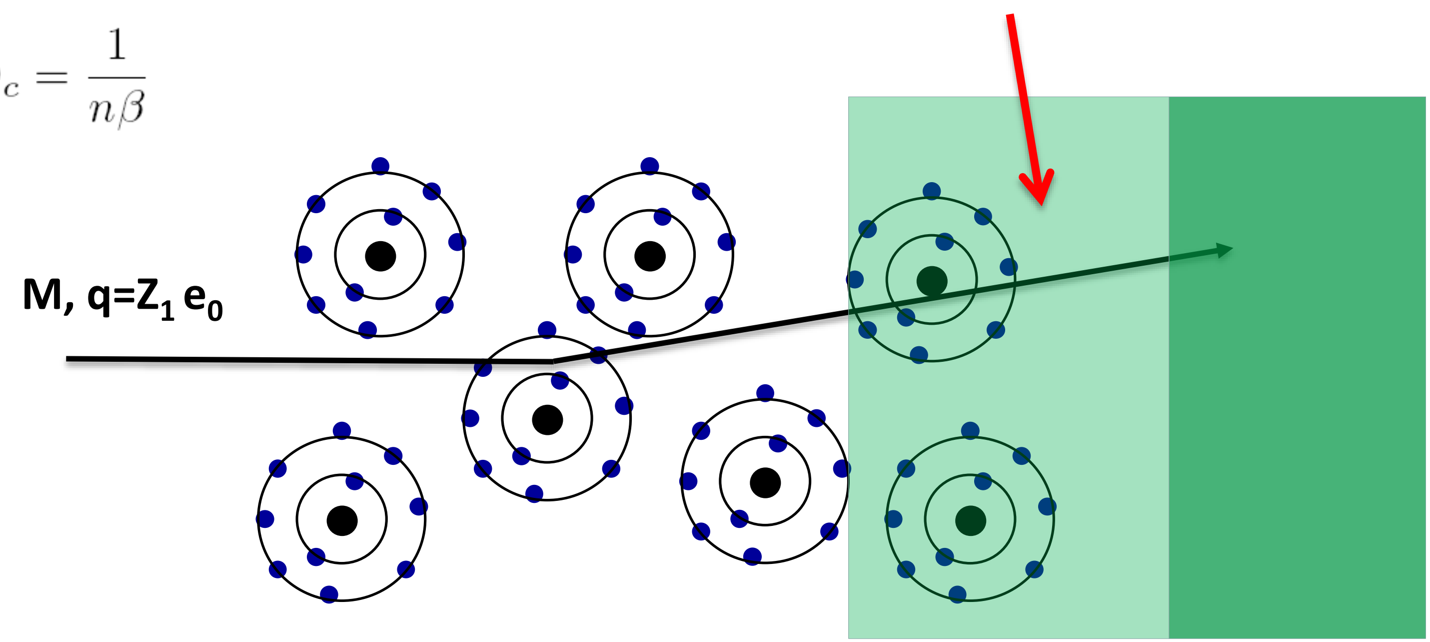

Cherenkov Radiation

with velocity $\beta \geq \beta_{thr} = \frac{1}{n}$ n: refractive index

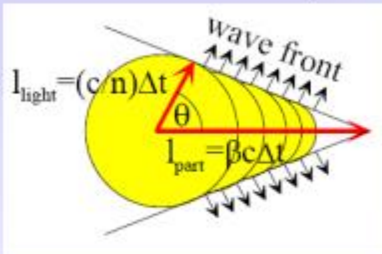

$$\boxed{\cos\theta_C = \frac{1}{n\beta} \quad \text{with } n = n(\lambda) \geq 1}$$

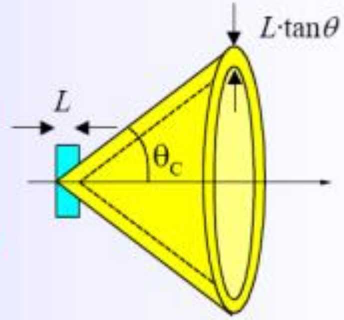

- $\beta_{thr} = \frac{1}{n} \rightarrow \theta_C \approx 0$ Cherenkov threshold
- $\theta_{max} = \arccos\frac{1}{n}$ 'saturated' angle (β=1)

If the velocity of a charged particle is larger than the velocity of light in the medium $v > \frac{c}{n}$ (n... Refractive Index of material) it emits 'Cerenkov' radiation at a characteristic angle of $\cos\theta_c = \frac{1}{n\beta}$ ($\beta = \frac{v}{c}$)

Material	n-1	β threshold	γ threshold
solid Sodium	3.22	0.24	1.029
lead glass	0.67	0.60	1.25
water	0.33	0.75	1.52
silica aerogel	0.025-0.075	0.93-0.976	2.7 - 4.6
air	$2.93\cdot10^{-4}$	0.9997	41.2
He	$3.3\cdot10^{-5}$	0.99997	123

$$\frac{dN}{dx} \sim 2\pi\alpha z_1^2 \left(1 - \frac{1}{\beta^2 n^2}\right)\frac{\lambda_2 - \lambda_1}{\lambda_2 \cdot \lambda_1}$$

= Number of emitted Photons/length with λ between λ_1 and λ

With $\lambda_1 = 400\,nm$ $\lambda_2 = 700\,nm$

$$\frac{dN}{dx} = 490\left(1 - \frac{1}{\beta^2 n^2}\right)\left[\frac{1}{cm}\right]$$

Ring Imaging Cherenkov Detector (RICH)

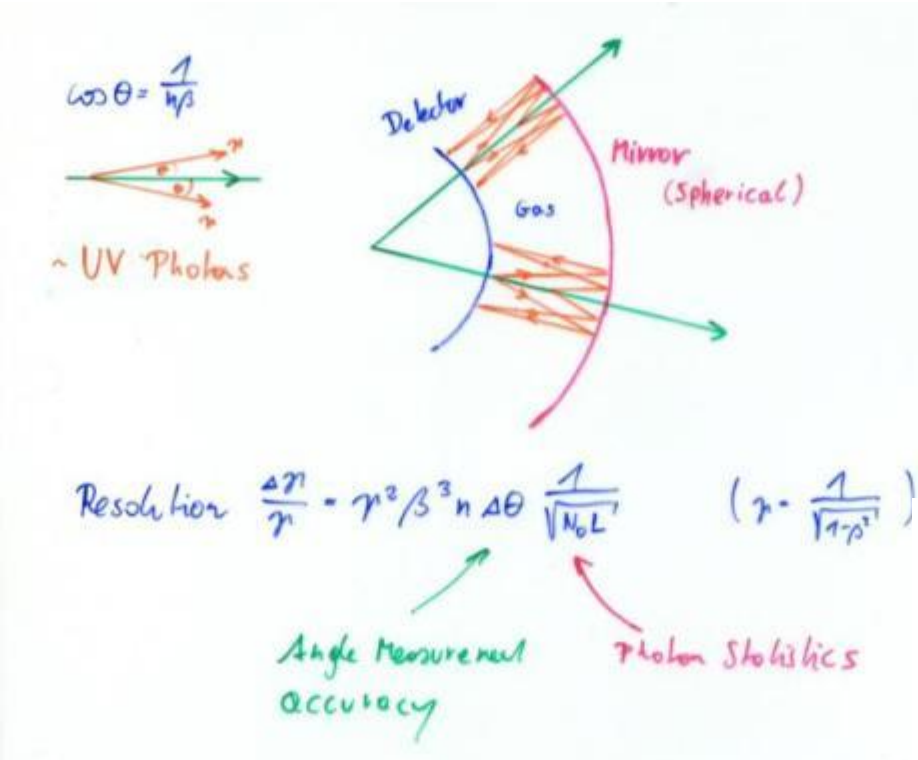

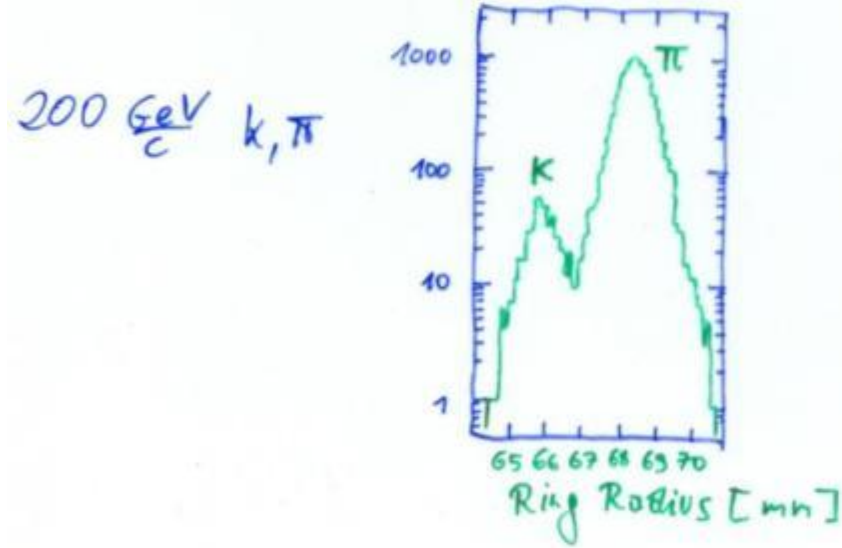

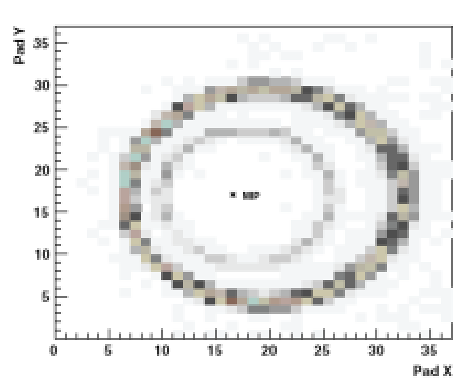

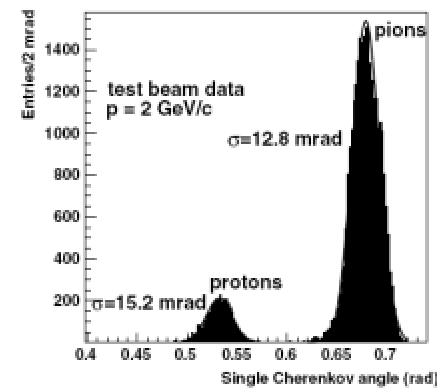

medium	n	θ_{max} (deg.)	N_{ph} (eV^{-1} cm^{-1})
air*	1.000283	1.36	0.208
isobutane*	1.00127	2.89	0.941
water	1.33	41.2	160.8
quartz	1.46	46.7	196.4

There are only 'a few' photons per event →one needs highly sensitive photon detectors to measure the rings !

LHCb RICH

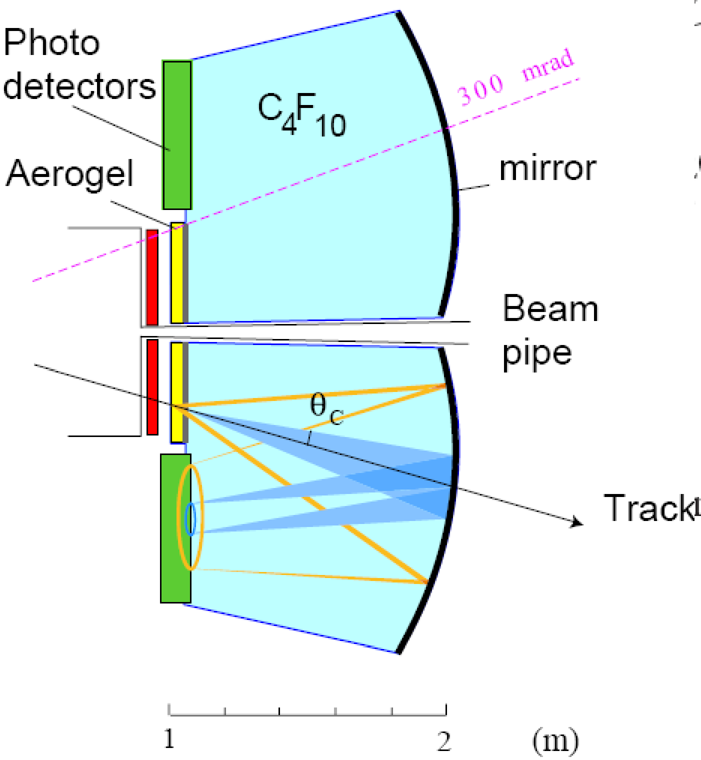
Photo detectors
C_4F_{10}
300 mrad
mirror
Aerogel
Beam pipe
θ_C
Track
1
2
(m)

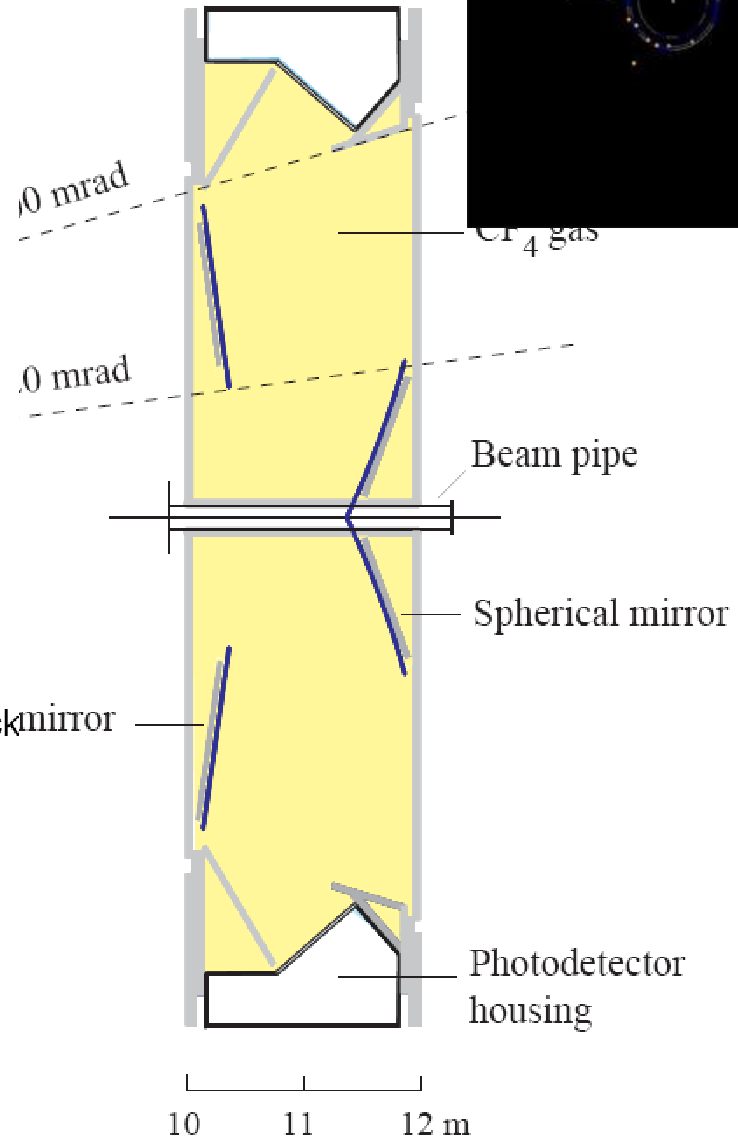
Beam pipe
Spherical mirror
mirror
Photodetector housing
10
11
12 m

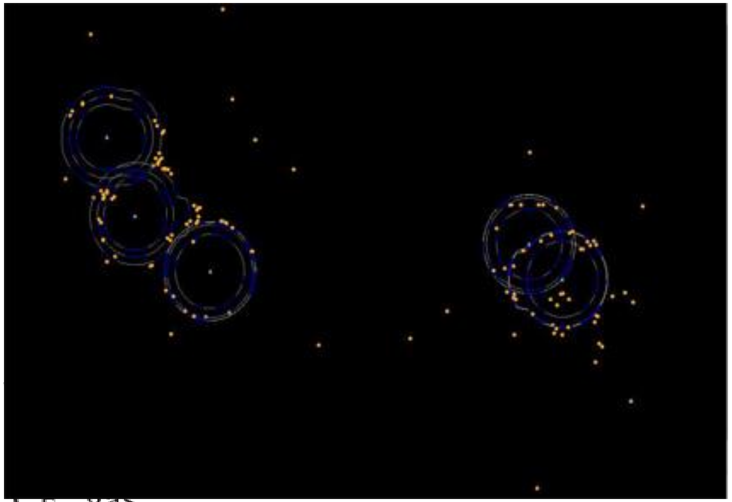

Transition Radiation

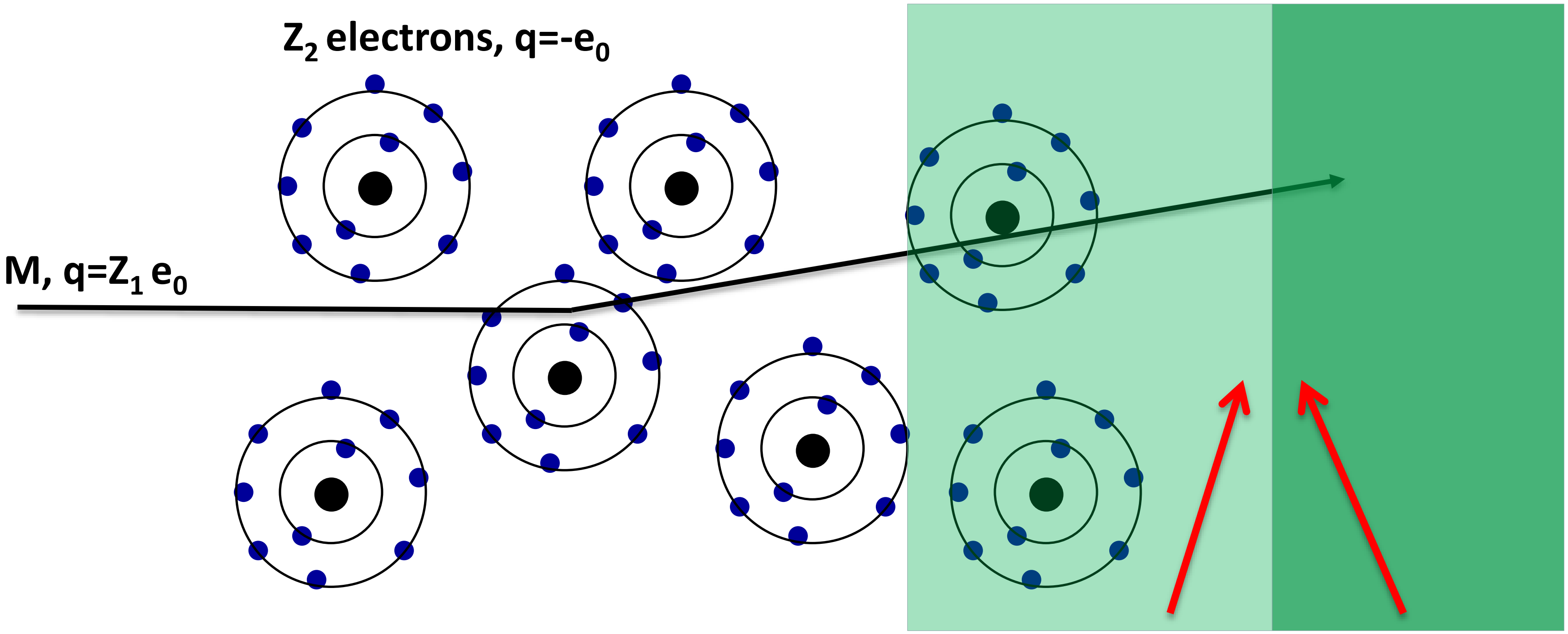

When the particle crosses the boundary between two media, there is a probability of the order of 1% to produced and X ray photon, called <u>Transition radiation</u>.

Transition Radiation

Radiation (~ keV) emitted by ultra-relativistic Particles when they traverse the boarder of 2 materials of different Dielectric Permittivity $(\varepsilon_1, \varepsilon_2)$

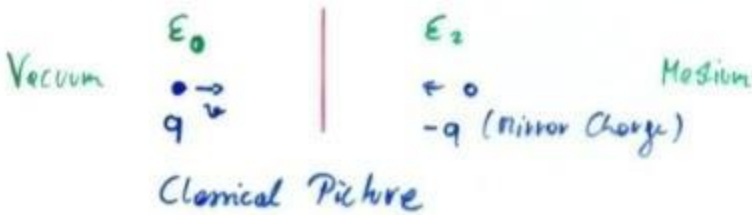

$q = Z_1 e$

$I = \frac{1}{3} \alpha Z_1^2 (\hbar \omega_p) \gamma$ … Radiated Energy per Transition

$\hbar\omega_p$ …. plasma Frequency of the Medium

…. ~ 20 eV for Styrene

About half the Energy is radiated between

$0.1\, \hbar\omega_p \gamma < \hbar\omega < \hbar\omega_p\gamma$

E.g. $\gamma = 1000$ 2-20 keV X-Rays

$N_\gamma \sim \frac{2}{3} \alpha Z_1^2 \sim 5 \cdot 10^{-3} \cdot Z_1^2$

γ - Dependence from hardening rather than N_γ

Emission Angle ~ $\frac{1}{\gamma}$

The Number of Photons can be increased by placing many foils of material.

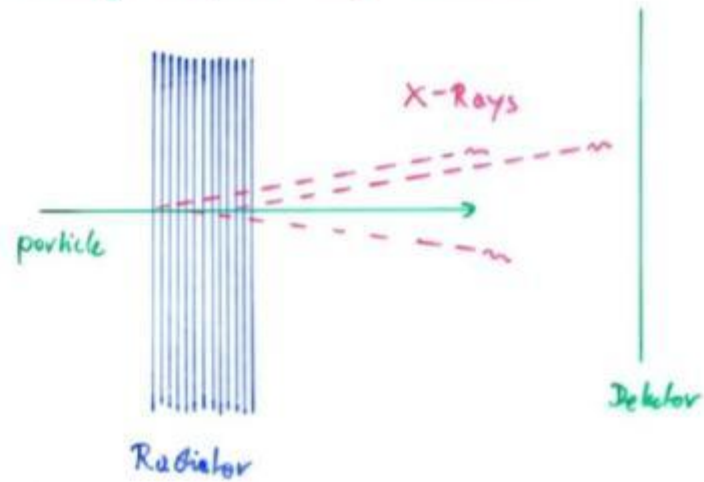

Electromagnetic Interaction of Particles with Matter

Ionization and Excitation:

Charged particles traversing material are exciting and ionizing the atoms.

The average energy loss of the incoming particle by this process is to a good approximation described by the Bethe Bloch formula.

The energy loss fluctuation is well approximated by the Landau distribution.

Multiple Scattering and Bremsstrahlung:

The incoming particles are scattering off the atomic nuclei which are partially shielded by the atomic electrons.

Measuring the particle momentum by deflection of the particle trajectory in the magnetic field, this scattering imposes a lower limit on the momentum resolution of the spectrometer.

The deflection of the particle on the nucleus results in an acceleration that causes emission of Bremsstrahlungs-Photons. These photons in turn produced e+e- pairs in the vicinity of the nucleus, which causes an EM cascade. This effect depends on the 2nd power of the particle mass, so it is only relevant for electrons.

Electromagnetic Interaction of Particles with Matter

Cherenkov Radiation:

If a particle propagates in a material with a velocity larger than the speed of light in this material, Cherenkov radiation is emitted at a characteristic angle that depends on the particle velocity and the refractive index of the material.

Transition Radiation:

If a charged particle is crossing the boundary between two materials of different dielectric permittivity, there is a certain probability for emission of an X-ray photon.

→ The strong interaction of an incoming particle with matter is a process which is important for Hadron calorimetry and will be discussed later.

Hadronic Calorimetry

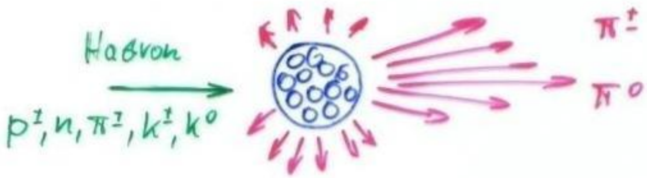

Strong Interaction

Approximate Energy Distribution

~50%	~20%	~30%
π^+, π^- $\quad \pi^0 \to \gamma\gamma$	Nuclear Excitation	Slow Nucleons
π^+, π^- $\quad \pi^+, \pi^-, \pi^0 \to \gamma\gamma$	5-30 MeV	
Hadron kaskade	p, n, γ	

$\pi^0 \to \gamma\gamma \to$ Electromagnetic Component

In Hadronic Cascades the Longitudinal Shower is given by the Absorbtion Length λ_a $\quad I \sim e^{-\frac{x}{\lambda_a}}$

In typical Detector Materials λ_a is much larger than X_0

$$\lambda \sim \frac{1}{\rho} \cdot 35\, A^{\frac{1}{3}}$$

	ρ	X_0	λ
Fe	7.87	1.76 cm	~17 cm
Pb	11.35	0.56 cm	~17 cm

Energy Resolution:

- A large Fraction of the Energy 'disappears' into
  - Binding Energy of emitted Nucleons
  - $\pi \to \mu + \nu$ which are not absorbed
- π^0's Decaying into $\gamma\gamma$ start an EM Cascade ($\tau \sim 10^{-16}$s)

– Energy Resolution is worse than for EM Calorimeters

W. Riegler/CERN

Bremsstrahlung + Pair Production → EM Shower

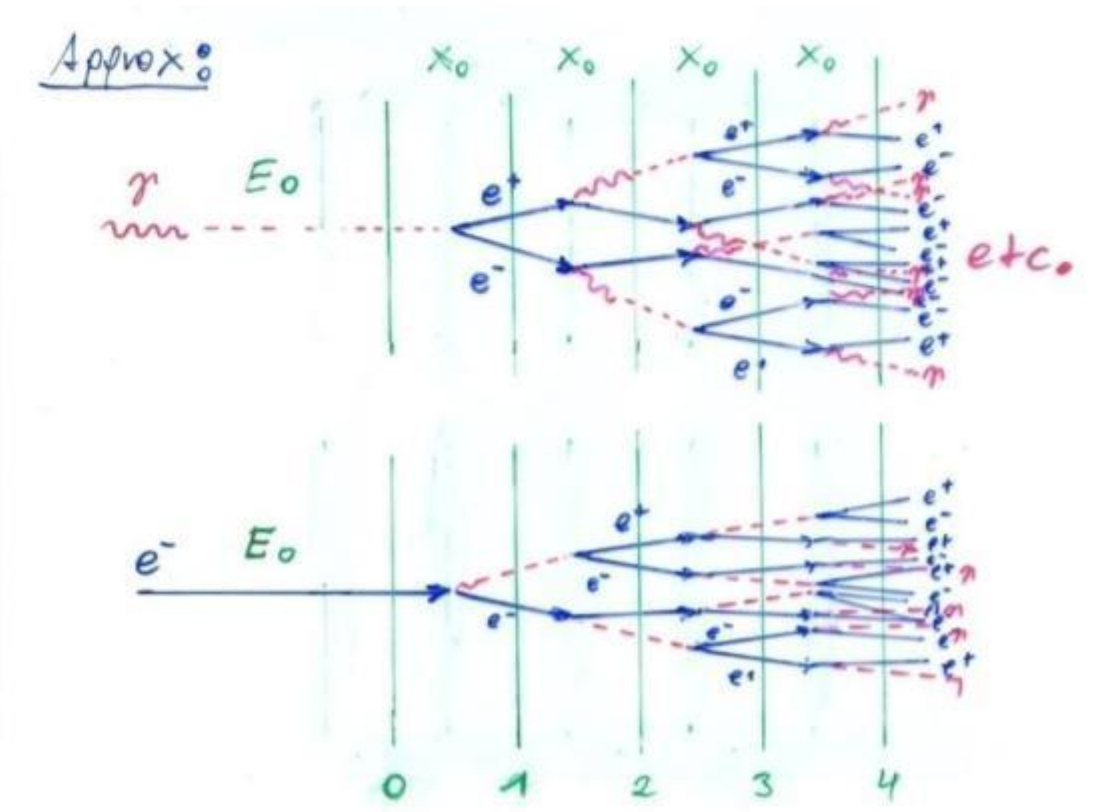

λ λ λ λ

Iron: **X_0=1.76cm**
λ=17cm

Conclusions

Knowing the basic principles of interaction of particles with matter you can understand detector performance to 20% level 'on the back of an envelope'.

In addition it crucial knowledge when you think about a new instrumentation ideas.

It is up to you to design the next generation of particle detectors !